Circuits and Systems
Mekelweg 4,
2628 CD Delft
The Netherlands
http://ens.ewi.tudelft.nl/

CAS-2014-00

M.Sc. Thesis

Offline Power Allocation and Spectrum Sensing Strategy in Energy-Harvesting Cognitive Radio Networks

Ning Pan

Abstract

Energy-harvesting cognitive radio network has emerged as a solution to increase energy and spectrum efficiency. In this thesis, we propose short-term offline optimal power allocation algorithms for multi-user energy-harvesting cognitive radio networks considering interference between secondary users. Assuming finite and rechargeable batteries for secondary users and a time-slotted operation model, an off-line optimization problem is formulated so as to maximize the network throughput during finite time-period. To that aim, the design of a power allocation and the spectrum sensing strategy is required. Together with the inherent constraints imposed by the use of energy-harvesting devices, a collision constraint is also required to limit the probability of interference with the primary user and to guarantee the quality of service. Because of the intractability of the power allocation problem in the interference channel, we spilt the optimization task for two different size cognitive radio networks: a) 2-user network, and b) multi-user network (i.e. more than 2 users). The optimal algorithms are developed for a sharing single-frequency band, and a multi-band scenario for the two-user network. We derive the optimal solution following a two-step strategy in case of a 2-user energy-harvesting CR network. A suboptimal algorithm that entails reduced computational cost and performs very close to the optimal one is also proposed for the single-band sharing scenario. In case of multi-user energy-harvesting cognitive radio networks, a SQP-based sub-optimal algorithm is derived for single-band sharing scenario. Besides, a optimal solution is proposed for a CR network applying interference cancelation techniques sharing the single band. At last, we derive the optimal power allocation strategies for the multi-user multi-band sharing scenario. Simulation results of the optimal (and suboptimal) solutions outperform those achieved by a random or priority best-user power allocation algorithms for the AND and OR fusion rules.

Offline Power Allocation and Spectrum Sensing Strategy in Energy-Harvesting Cognitive Radio Networks

THESIS

submitted in partial fulfillment of the
requirements for the degree of

MASTER OF SCIENCE

in

ELECTRICAL ENGINEERING

by

Ning Pan
born in Dongyang, China

This work was performed in:

Circuits and Systems Group
Department of Telecommunication & Electrical Engineering
Faculty of Electrical Engineering, Mathematics and Computer Science
Delft University of Technology

Delft University of Technology

DELFT UNIVERSITY OF TECHNOLOGY
DEPARTMENT OF
TELECOMMUNICATION & ELECTRICAL ENGINEERING

The undersigned hereby certify that they have read and recommend to the Faculty of Electrical Engineering, Mathematics and Computer Science for acceptance a thesis entitled **"Offline Power Allocation and Spectrum Sensing Strategy in Energy-Harvesting Cognitive Radio Networks"** by **Ning Pan** in partial fulfillment of the requirements for the degree of **Master of Science**.

Dated: 16th January, 2014

Chairman:

Prof.dr.ir. Geert Leus

Advisors:

Dr. Rocio Arroyo-Valles

Dr. ir. Sina Maleki

Committee Members:

Dr. Przemyslaw (Przemek) Pawelczak

Abstract

Energy-harvesting cognitive radio network has emerged as a solution to increase energy and spectrum efficiency. In this thesis, we propose short-term offline optimal power allocation algorithms for multi-user energy-harvesting cognitive radio networks considering interference between secondary users. Assuming finite and rechargeable batteries for secondary users and a time-slotted operation model, an off-line optimization problem is formulated so as to maximize the network throughput during finite time-period. To that aim, the design of a power allocation and the spectrum sensing strategy is required. Together with the inherent constraints imposed by the use of energy-harvesting devices, a collision constraint is also required to limit the probability of interference with the primary user and to guarantee the quality of service. Because of the intractability of the power allocation problem in the interference channel, we spilt the optimization task for two different size cognitive radio networks: a) 2-user network, and b) multi-user network (i.e. more than 2 users). The optimal algorithms are developed for a sharing single-frequency band, and a multi-band scenario for the two-user network. We derive the optimal solution following a two-step strategy in case of a 2-user energy-harvesting CR network. A suboptimal algorithm that entails reduced computational cost and performs very close to the optimal one is also proposed for the single-band sharing scenario. In case of multi-user energy-harvesting cognitive radio networks, a SQP-based sub-optimal algorithm is derived for single-band sharing scenario. Besides, a optimal solution is proposed for a CR network applying interference cancelation techniques sharing the single band. At last, we derive the optimal power allocation strategies for the multi-user multi-band sharing scenario. Simulation results of the optimal (and suboptimal) solutions outperform those achieved by a random or priority best-user power allocation algorithms for the AND and OR fusion rules.

Acknowledgments

I would like to express my deep gratitude to Dr. ir. Sina Maleki, Dr. Rocio Arroyo-Valles, and Prof.dr.ir. Geert Leus, my research supervisors, for their patient guidance, enthusiastic encouragement and useful critiques of this master thesis. I am extremely grateful to my daily supervisors, Sina and Rocio, for their valuable comments and scholarly inputs throughout the research work. Special thanks to Sina. His brilliant ideas, encyclopedic information and positive attitude inspired me to construct the problem and solve it. I owe a very important debt to Rocio, for the efforts patiently checking and correcting all the mathematical analysis and writing mistakes and the academic assistance during the total work progress. Words cannot address all the help and support they gave me, it is a fortune to be their student. My heartfelt appreciation also goes to Geert, for offering me the opportunity to work in the CAS group and introducing the topics and knowledge in signal processing. Without his insightful suggestions and support, this thesis paper would not be materialized.

I would also like to thank Dr. Przemyslaw (Przemek) Pawelczak, for being my committee member and offering me constructive comments. My particular thanks are also goes to Dr. Andrea Simonetto, for spending efforts and time assisting me to solve optimization problem in the multi-user scenario. I would also like to extend my thanks to Ms Minaksie Ramsoekh and Ing. Antoon Frehe, for the logistical help and technical assistance during the work progress.

My warmest thanks also go to all the friends and academic staffs who have offered their sincere help during my two-year Master project. They stimulate me to greater efforts in studying and chasing my life targets.

Finally, I wish to thank my parents particularly, for their dedication, spritual support, and encouragement throughout my undergraduate studies that provided the foundation for this work.

Ning Pan
Delft, The Netherlands
16th January, 2014

Contents

List of Figures

Energy-harvesting cognitive radios: state-of-the art and problem statement

1

This Master thesis focuses on energy-harvesting cognitive radio (CR) networks. In this chapter, we introduce the background information about energy-harvesting CR networks, the related work in the field, and the problem statement. The objectives, the outline of the presentation as well as the main contributions are also described.

1.1 Introduction to cognitive radios and energy harvesting techniques

In this section, we give an overview of cognitive radio and energy harvesting techniques. First, an introduction and a description of CR networks are presented. Later, the energy harvesting techniques that can be applied to CR devices in order to prolong their lifetime are stated.

1.1.1 Cognitive radio networks

In most countries, radio users that provide different services are licensed to specific frequency bands by government regulators such as the Federal Communications Commission (FCC).

Fig. 1.1 shows the frequency allocation of the radio spectrum in the United States. We can observe that the radio spectrum is almost fully occupied by the different types of radio users. On the one hand, the telecommunication data volume of different applications increases explosively [1], which calls for more frequency spectrum resources. On the other hand, the usage rate of the licensed spectrum is very low [2]. Fig. 1.2 shows the spectrum occupancy rate averaged over seven locations reported by Shared Spectrum Company and IIT Wireless Interference Lab. It shows that the spectrum occupancy is always almost under 25 percent for any frequency band [3]. Thus, a more efficient spectrum sharing strategy is urgently needed.

Since CRs were first introduced by Mitola [4] in 1999, there has been an increasing interest in CRs in order to solve the spectrum scarcity problem. In CR networks, there are two classes of users with different spectrum utilization priorities, as it is shown in Fig. 1.3: a) primary users (PU) with certificated licenses which can access the spectrum with no restriction, and b) CR users (also called secondary users, SU) which gain spectrum access after sensing the activity of the PU.

Depending on how secondary users share the spectrum with the PU, three schemes can be identified (see Fig. 1.4): a) *interweave*, where SUs identify spectrum holes by performing periodic spectrum sensing and employ the empty frequency bands while avoiding harmful interference to the PUs; b) *underlay*, where SUs always transmit data under the maximum allowable interference to the PU; c) *overlay*, where SUs cooperate with the PUs while transmitting their own signal [5]. In this thesis, we consider interweave CR networks. As it was

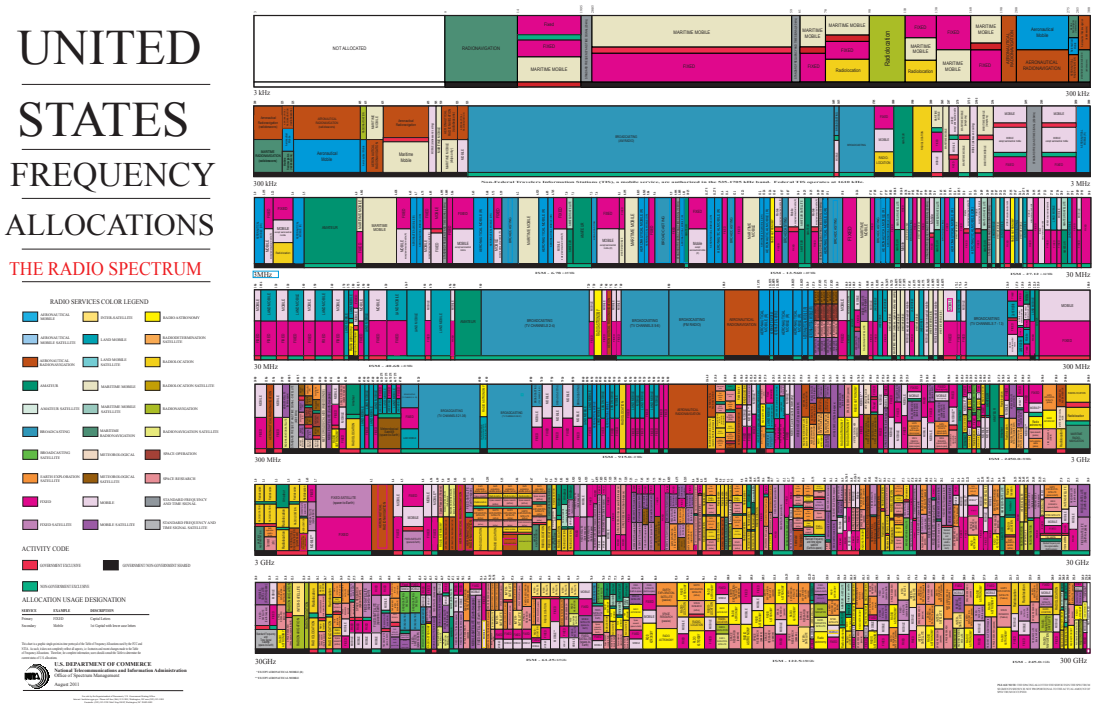

Figure 1.1: United States frequency allocations chart. Radio spectrum in 2011 (FCC)

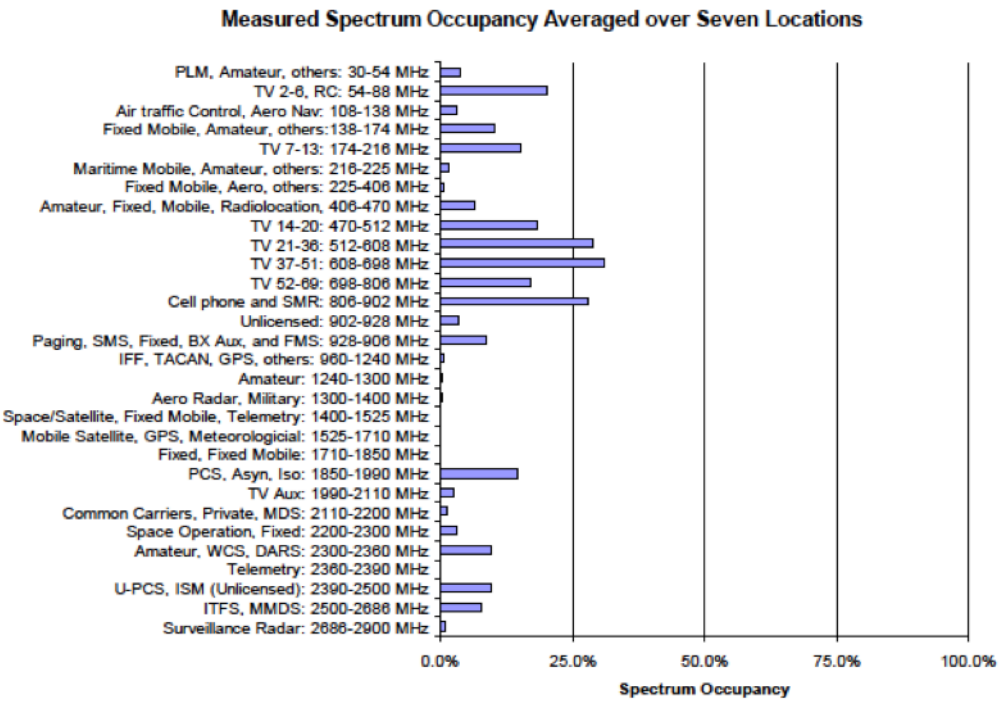

Figure 1.2: Bar graph of the spectrum occupancy averaged over seven locations [3]

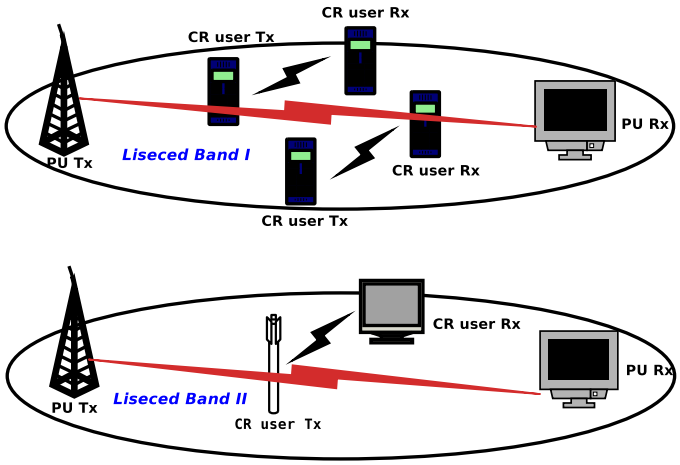

Figure 1.3: Cognitive radio architecture

aforementioned, this scheme avoids the interference with the PUs by only allowing secondary users to access the spectrum holes. The use of interweave CRs enhances spectrum efficiency because of the opportunistic access of cognitive devices to the underutilized spectrum which is licensed to primary users [6]. The major task in interweave CR networks is to detect the PU activity with allowable error. This task becomes more difficult when the PU activity is highly dynamic and the distance between the PUs and SUs increases (in this case, the PU signal is very weak at the CR user) [5].

We use cooperative spectrum sensing in order to improve spectrum sensing performance in CR networks. Previous studies [7–9] have reported that reliability of spectrum sensing in CR networks can be improved by applying cooperative spectrum sensing techniques. The work in [7] shows that the detection time decreases by allowing SUs cooperating and operating in the same band. The hidden terminal problem occurs when SUs are shadowed in severe multi-path fading or inside buildings with high penetration loss while a PU is active in the neighborhood area, which is a great challenge when implementing spectrum sensing. The authors of [8] state that the use of cooperative spectrum sensing can solve this hidden terminal problem successfully.

In this work, we consider a CR network where the SUs perform cooperative sensing by first performing local spectrum sensing. Then, SUs transmit the sensing results to a fusion center (FC) that is in charge of determining the presence or absence of the PU. Here, the FC is an information-sharing center for the SUs. The FC collects the individual sensing information from every SU and makes a global decision based on the collected results and following a fusion rule in order to allow SUs to access the idle spectrum band [10]. Fusion strategies can be divided into three types: a) hard fusion decision, b) soft fusion decision, and c) quantized (softened hard) fusion. In the hard fusion decision scheme, users forward their one-bit decision regarding the existence of the PU to the FC, and the FC makes a global decision based on a logic hard decision combing rule. In the soft fusion decision scheme, the SUs forward the entire sensing result to the FC instead of only the local decision [11]. Although the soft fusion scheme may have more precise sensing results [11], the hard fusion scheme is considered in this work due to its energy and bandwidth efficiency [9].

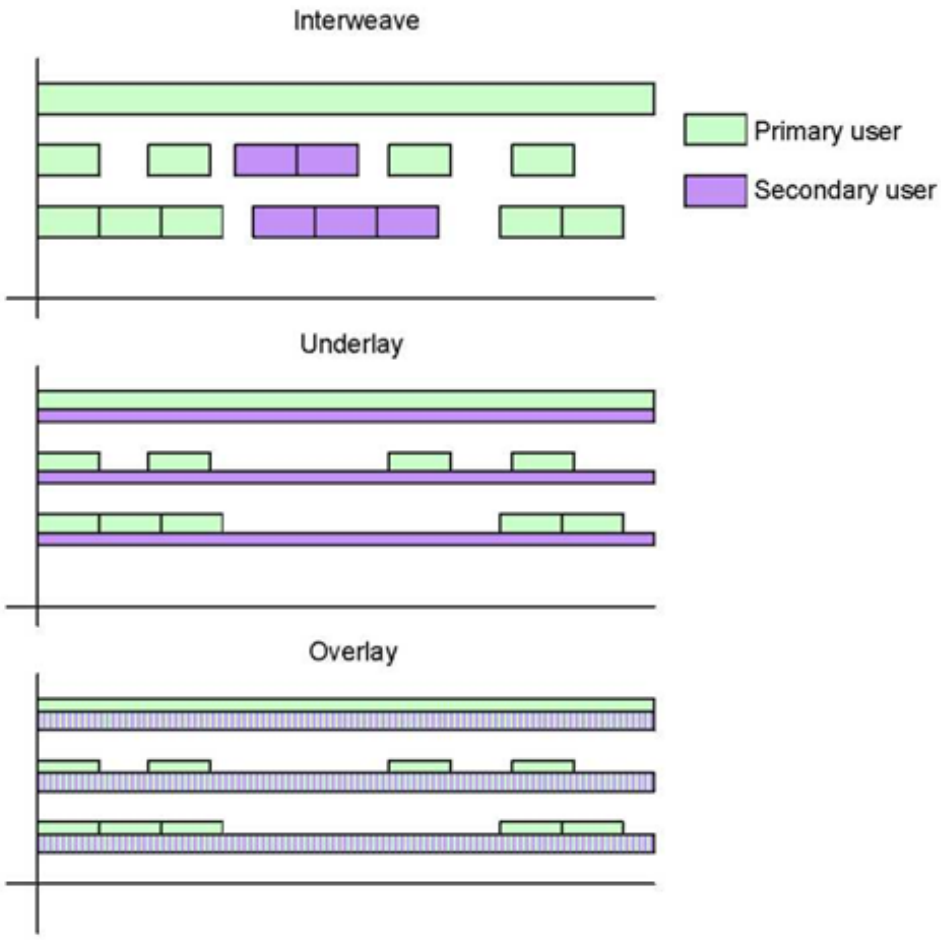

Figure 1.4: Different types of CR schemes: interweaved transmission of PU and CR signals, underlay of CR signal, and cooperative overlay of CR signal [5].

1.1.2 Energy harvesting and power management techniques

CR networks are required to run for long periods of time, often several years, without human intervention. However, CR networks are typically and widely deployed with battery-powered devices rather than wires connecting the device to the electrical power source. Thus, CR devices suffer from finite lifetime and energy shortage problem. In the past decades, researchers oriented their efforts to maximize the battery capacity (with the goal of extending the system lifetime) by using new battery materials. Nevertheless, the technologies used for improving the battery capacity have reached their ceiling, which means that the improvement achieved by the use of the newest developed batteries is not enough to extend the lifetime of the system [12]. Besides, although users can also extend the lifetime by using larger batteries, the

increase in size, weight and cost will cause other problems which need to be taken into account [13]. Even more, replacing the batteries is either impossible or expensive because the number of CR devices can be high or may be deployed in unreachable places, such as mountains or underground [14].

Apart from energy-efficient strategies, which aim at minimizing the energy consumption [15–17] or preserving it, energy harvesting also emerged as a promising technique to achieve energy efficiency. Energy-harvesting devices have the ability of capturing energy from ambient sources, such as solar, wind, thermal, etc., or other energy sources (e.g., electromagnetic energy or human movements) and then are converted into electrical energy. Thus, it allows extending the operation lifetime of CR networks without requiring battery replacement or external wired charging power.

Sources for harvesting energy can be classified into four categories: a) uncontrollable but predictable energy, which cannot be controlled but its behavior can be observed and modeled, such as solar energy, wind energy, etc.; b) uncontrollable and unpredictable energy, which cannot either be controlled or predicted, such as vibrations in an indoor environment; c) fully controllable energy, which can be produced whenever the user asks for it, such as finger-vibration energy that is harvested by piezoelectrical material devices; and d) partially controllable energy, which is controlled by designers but the resultant behavior is not fully deterministic, such as the received radio frequency (RF) source, which not only depends on the RF signals but also is influenced by the propagation environment [18]. In summary, most of the energy resources are not totally deterministic and always follow a time-dynamic behavior.

Besides, the energy-harvesting architectures can be categorized into two types, as it is shown in Fig. 1.5: a) harvest-use architecture, in which the harvested energy is immediately ready for use after being captured by the harvesting device; b) harvest-store-use architecture, where the system harvests energy whenever it is possible and stores it for future use [12].

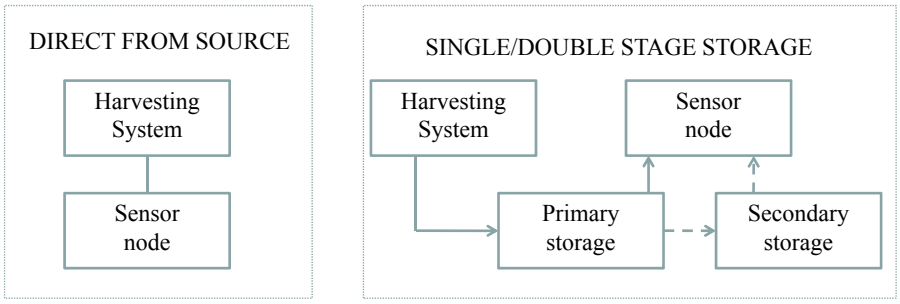

(a) Harvest-use architecture (b) Harvest-store-use architecture

Figure 1.5: Energy harvesting architechtures [12]

The choice of the energy architecture model depends on the hardware, the energy source and the working mode of the system. For instance, considering a solar energy harvesting system, it would be wise to combine the harvest-use and harvest-store-use architectures so that the harvesting device could capture the solar energy in the daytime. Thus, an amount of the energy can be powered directly to the device, and the remaining one can be stored in the system for future use.

Therefore, the power management task in energy-harvesting networks, which indicates when and how much energy should be used or stored so as to optimize the performance in order to maintain the permanent life of the system without hardware breakdown, becomes a key challenge. Different from the traditional finite battery-powered networks, the power management task in energy-harvesting networks sets limits on the maximum and minimum energy usage rate rather than on the maximum energy.

Two requirements should be satisfied to make the energy-harvesting battery-limited system operate during a long time without hardware failures [18]:

- Energy causality control
  Each device is limited to use at most the amount of currently available energy. This is a natural bound to ensure the permanent operation of the system.

- Maximum battery limit control
  As devices are battery-limited, control over the energy level should be carried out in order to assure that it never exceeds the maximum battery capacity whenever energy is harvested.

1.2 State-of-the-art

In this section, we present the state-of-the art in energy-harvesting CR networks and power allocation techniques in CR networks.

A vast amount of research has been devoted to energy harvesting in wireless networks [14, 20–23] and cognitive radio networks [24–28]. However, the performance analysis of energy harvesting in cognitive radio networks has only recently been considered in the literature. In [29], a Markov decision process (MDP) framework is used to investigate the trade-off between the sensing and access policies in a cognitive radio network with a single energy-harvesting cognitive radio with finite battery capacity. In [30], an energy-harvesting secondary user coexists with a PU and helps the PU to deliver its undelivered packets when the PU is not active. In [31], a cognitive radio optimizes the sensing duration time in order to maximize its mean data service rate when the CR and the PU harvest energy. The authors of [32] propose an optimal mode decision policy for a single cognitive radio with a non-RF energy harvester to maximize the system throughput. An optimal sensing energy algorithm and an adaptive transmission power control algorithm is also proposed. In [33], the authors maximize the spatial throughput of the secondary network and node density based on a stochastic-geometry model under outage-probability constraints for coexisting networks. The secondary users coexist with the PUs, harvest energy from the RF transmission of the nearby primary transmitters, and use all the available energy for subsequent transmission when the batteries are fully charged. The authors of [34] determine an optimal spectrum sensing policy that maximizes the expected total throughput subject to an energy-causality constraint and a collision constraint for a single-user single-band energy-harvesting CR network with an infinite battery capacity. In [35], the same authors derive an upper bound on the achievable throughput, and in [36] they design an optimal spectrum access policy in order to achieve the previous upper bound of the achievable throughput.

However, none of the previous related works have dealt with the design of a power allocation strategy in energy-harvesting multi-user cognitive radio networks. The main reason for

addressing the power allocation problem in this scenario is the following: the maximization of the achievable throughput of SUs while controlling the sensing error to protect the licensed users is a key challenge in CR networks driven by energy-harvesting devices.

The throughput of the CR network is tightly related to the transmission power, the transmission time, the environmental noise, and the probability of accessing the idle spectrum; and the probability of unexpected interference to the PU which in turn depends on the probability of successful detection [37]. On the one hand, a lower detection threshold will increase the probability of accessing the idle spectrum although it will increase the chances to interfere with the PU. This leads to solving the trade-off between the throughput maximization and the interference control by setting a proper detection threshold (e.g., maximizing the probability of accessing the idle spectrum limiting the interference with the PU). This problem has been studied in [34] considering a single user energy-harvesting CR network. On the other hand, power allocation in CR networks is an important issue in order to optimize the network performance. Among the different power allocation strategies, maximizing the network throughput by assigning the proper transmission power to SUs becomes a major challenge. However, this problem is a non-deterministic polynomial-time hard non-convex problem for the multi-user case when interference between SUs is considered [47].

The approaches to solve the power allocation optimization problem in CR networks can be classified mainly in two trends: A) Based on convex optimization techniques [38–42]. The optimization problem aimed at maximizing the throughput is solved using convex optimization techniques that consider an OFDM/FDMA-based CR network model. In the OFDM/FDMA-based CR network model, the interference between SUs can be ignored rendering the resulting power allocation problem to be a convex one. The authors of [38, 39] maximize the network sum-rate considering the primary user interference. The authors of [40] propose a two-step scheme to maximize the throughput by choosing first the optimal sub-channel, and then assigning the power to the sub-channels according to a barrier-based method. In [39], a sub-carrier and power allocation method for a joint overlay and underlay spectrum access is performed. However, the main limitation of these works is that the interference between SUs cannot be ignored in practice. B) Based on the Nash Equilibrium [43–45]. Playing a multiple user game to achieve the Nash equilibrium so as to solve the optimization problem. In [43], the weighted sum of utilities corresponding to all the users is maximized using a price-based iterative water-filling power allocation algorithm which considers the power budget of each user. The authors of [44] propose a dynamic sub-channel and power allocation scheme based on the Nash Bargaining game. In [45], the authors perform rate and power distribution among SUs to achieve the Nash equilibrium by minimizing the total transmission power and maximizing the transmission rate while satisfying a quality of service (QoS) requirement for SUs at the same time. The main challenge for algorithms playing the Nash Bargaining game is that the Nash equilibrium is not always the Pareto (global) optimal point [46]. Improvements or verifications to achieve the Pareto optimum still remain.

Nevertheless, none of these works consider CR networks where SUs are equipped with energy-harvesting devices.

1.3 Problem statement

In this section, we address the motivation of the Master thesis, the objectives of the work, and the outline of the dissertation together with the main contributions.

1.3.1 Motivation

Energy-harvesting CR networks emerged as a promising solution to improve energy and spectrum efficiency. CR networks increase the usage rate of the spectrum by accessing the spectrum holes left by the inactivity of the licensed users. Besides, the use of cooperative spectrum sensing techniques improves the CR system performance by solving the hidden terminal problem by decreasing the sensing time. Even more, the use of energy-harvesting devices can extend the CR system lifetime significantly. As it has been aforementioned, one of the remaining challenges in energy-harvesting CR networks is to find an optimal power allocation and spectrum sensing strategy, which also sets the optimal detection threshold.

Despite the great variety of the strategies proposed in the literature, there is no approach that optimally allocate the power among CR users in energy-harvesting multi-user CR networks. Although some of the recent research works previously mentioned are aimed at maximizing the throughput (as we do in this work), they direct their efforts at finding the optimal spectrum sensing or access policy, instead of tackling the power allocation problem. This is mainly due to the fact that they all (except [33]) consider a single cognitive radio network. Further, in spite of employing energy-harvesting techniques, few works [34, 36] incorporate a constraint derived from the use of energy harvesting devices in their formulation problem.

The power allocation problem in multi-user networks with channel interference is proved to be a non-convex optimization problem [47], which is more intractable than OFDM/FDMA-based networks where the power allocation problem is a convex one. In spite of solving the non-convex optimization problem by formulating the duality problem, which needs to minimize the duality gap of the optimal problem [48], or by playing a Nash Bargaining game to achieve the Nash Equilibrium which may not be the optimal solution, a power allocation algorithm which finds the global optimal or at least a local optimal solution and assigns the transmission power among CR users in energy-harvesting networks is needed. Even more, the power management task in energy-harvesting networks is even more complex compared to traditional battery-powered networks [18]. The dynamic nature of energy-harvesting CR users incurs a different design philosophy from the one concerning the energy-efficient battery-limited CRs. In order to make an efficient use of the harvested energy and make CR networks work permanently without hardware failure, some issues regarding the battery capacity and energy use should be satisfied.

Besides, two approaches can be considered for designing optimal transmission power strategies, namely, online and offline. The online approach assumes that CR users only have some statistical knowledge of the dynamics of the energy harvesting process. However, the offline approach assumes that CRs have complete knowledge about the amount and arrival time of the harvested energy. Clearly, this second approach is more idealistic, and only makes sense in the short term, although it has been recently considered in the literature trying to solve a similar problem [19, 49–51]. However, it provides analytical and intuitive solutions that can be later used to gain insight for the subsequent design of online transmission power strategies.

Moreover, the value of the detection threshold will affect the probability that CR users access the spectrum. With the decrease of the detection threshold, the probability of accurate detection is higher, while the chances to access the spectrum decreases. For that reason, when the chances to access the spectrum decreases, it is necessary to increase the transmission power when the CR user has the opportunity to transmit in order to use the harvested energy efficiently during a fixed time period. Thus, the power allocation scheme is also influenced by the detection threshold in energy-harvesting CR networks.

Based on the above discussion, in this thesis we propose offline algorithms that assign the transmission power to CRs and set the detection threshold in order to maximize the system throughput in energy-harvesting multi-user CR networks when CR users have finite batteries.

1.3.2 Objectives of the work

As stated above, the thesis is framed within the energy-harvesting CR field. The main global objective pursued in this thesis consists of

designing, for different scenarios, optimal offline power allocation schemes subject to interference constraints in order to maximize the network throughput in energy-harvesting CR networks composed of battery-limited CR users which perform cooperative spectrum sensing.

The aim is to obtain analytical results from a mathematical formulation which provide the optimal power allocation strategy and the detection threshold under an offline approach where knowledge about the amount and arrival time of the harvested energy as well as other information, such as the probability of activity of the PU or the static channel gains, are known beforehand by CR users.

The detailed objectives of the thesis can be split into specific ones, which are listed below:

- **Identify the optimization function of the problem.**
  We want to maximize the throughput of the CR network, which depends mainly on the probability of accessing the spectrum and the transmission power of CR users. Once the spectrum is sensed to be idle, CR users transmit their data according to the transmission power policy designed beforehand.

- **Determine the adequate constraints in order to limit the interference with the PU and to manage properly the energy resources considering the energy-harvesting nature of CR devices.**
  The most important task in interwave CR networks is to avoid the interference with the PU while optimizing the network performance. The interference control requirement is considered in the spectrum sensing part, so that the appropriate threshold should be set in order to limit the interference with the PU to a value below the required one while the chances to access the spectrum increase. Further, because of the dynamic nature of the energy-harvesting CR users, the CR transmitters have to adapt their transmission power at every time instant.

- **Define an appropriate system model.**
  First, we should define an appropriate energy-harvesting system model. We consider two scenarios, a single frequency band scenario and a multi-band scenario, for two types of situations: interference among users and non-interference because CR devices

apply interference cancellation techniques. We also need to define an energy model for the energy-harvesting process, which should satisfy the nature of the energy-harvesting principle.

- **Propose an optimal offline power allocation and detection threshold strategy for multi-user energy-harvesting CR networks in the different scenarios.**
  Based on the defined system model, we want to get analytical solutions using mathematical optimization tools. Thus, we optimize the transmission power and the detection threshold for the spectrum sensing in the different scenarios.

- **Evaluate the proposed strategies.**
  As a final step, the performance of the algorithms in the different scenarios should be compared and analyzed with regard to a benchmark solution.

1.3.3 Outline of the dissertation and main contributions

In this subsection, the outline of the dissertation and main contributions are presented. The dissertation of this thesis consists of three chapters.

Once exposed the relevant background information, the state-of-the-art and the problem statement, chapter 2 proposes an optimal offline power allocation and spectrum sensing algorithm for energy-harvesting CR networks in a 2-user scenario. Initially, a CR network model is defined as well as a time-slotted energy-harvesting model, which tries to reflect the dynamic nature of an energy-harvesting system.

Then, the scheme for determining the optimal transmission power of the two users as well as the detection threshold is designed to maximize the throughput of the CR users, yet limiting the probability of interfering with the primary user and adhering the energy causality and limited battery constraints. The constraint on the probability of detection ensures that the PUs are not interfered with. The energy causality constraint yields that each cognitive user transmitter is limited to use at most the amount of currently available energy; and finally, the last constraint originates from the limited battery capacity, and is necessary to assure that the energy level never exceeds the maximum battery capacity whenever energy is harvested.

A two-step strategy is implemented to solve the problem. In the first step, the optimal transmission power is considered assuming that the detection threshold is given. We solve the non-convex optimization problem by studying the objective function shape to find the global optimum. In the second step, the solution of the first step is used as input to find the optimal detection threshold. Besides, for those scenarios where computational issues are a requirement, we propose a suboptimal algorithm, which performs very close to the optimal algorithm for the one sharing frequency band scenario.

In chapter chapter 3, the problem is solved for a multiple (more than 2)-user energy harvesting CR network scenario. We split the problem into two cases: a) a single band case and b) a multi-band case. In the first scenario, all users share the band by opportunistically accessing the spectrum, so they interfere with each other. In the second scenario, the users apply an FDMA scheme (so interference can be ignored), or the access to each band is limited up to a certain number of users, so that the single frequency band-sharing algorithm can be used. A generalization of the network model is presented while the energy model remains

the same as in chapter 2. As it was done before, the CR network throughput is maximized subject to the same interference and energy constraints.

The offline transmission power algorithm for the single frequency band spectrum sharing is solved using the Sequential Quadratic Programming (SQP) method. This method shows fast convergence rate for non-linear programming problems, and the local optimum can be found efficiently. As the objective function is shown to be non-convex, it is hard to find out the global optimum without global searching in the feasible value set, so a local optimum is found.

Later, the problem is extended to the case where multiple CR users use interference cancellation techniques. In this case, the interference between CR users can be ignored. In fact, this scenario is the same as one proposed in the 2-user scenario for the multi-band case. At the end of the chapter, a multi-band scenario with multiple users is considered.

Finally, chapter 4 addresses the main results and points out further research lines.

The main contributions of the thesis is listed as below:

- **The model construction of the energy-harvesting CR networks.**
  We define the network model as a cooperative spectrum sensing CR network and also construct a time-slotted energy-harvesting model that shows the dynamic nature of the energy-harvesting process. What's more, we introduce PU interference control constraint and power management constraints that should be considered in energy-harvesting CR networks.

- **Chapter 2 derives the short-term optimal offline power allocation and detection threshold set scheme for energy-harvesting 2-user CR networks composed of battery-limited CR users performing cooperative spectrum sensing.**
  We solve the short-term offline power allocation problem for single band sharing and multi-band sharing case. In the single frequency band sharing case, we derive the optimal allocating power by comparing the vertices of the quasi-convex channel capacity function; and the best spectrum sensing strategy is set by a through-search process for the detection threshold. Besides, in the multi-band sharing case, the optimal power allocation algorithm is achieved by assigning power to SUs solving a convex optimization problem and a through-search for detection threshold. A sub-optimal solution is also proposed to reduce computation time. And a benchmark solution named as random power allocation scheme is constructed in the end.

- **Chapter 3 proposes the short-term offline optimal/ sub-optimal power allocation schemes for energy harvesting multi-user CR networks in different scenarios.**
  Firstly, an SQP-based sub-optimal power allocation algorithm is derived for the single-band sharing case. And we show its advantages over the benchmark solution in different channel environments. We also investigate the power allocation problem in energy-harvesting CR networks using interference control techniques and also in the multi-band scenario and give their optimal solution.

- **Apply the offline power allocation algorithms to a realistic scenario: solar energy harvesting.**
  We apply the power allocation algorithms to a solar energy harvesting CR network

case. And the simulation results show that the optimal/ sub-optimal power allocation algorithms improve the network output significantly in different settings.

Power allocation and detection threshold set for 2-user energy harvesting CR networks

2

In this chapter, we consider a 2-user energy-harvesting CR network that aims at using the spectrum holes left by a PU. We aim at solving the offline optimization problem by allocating the optimal power and setting the best threshold for SUs in a short-term time period. As we consider a short-term period, the energy-harvesting behavior can be predicted beforehand. One typical example that may happen in practice is the solar-energy harvesting system. The solar-energy harvesting rate mainly depends on the weather conditions, the collectors' surface and the mounted angle [52]. Once the CR system is deployed and the weather conditions are known (or can be predicted) during a certain time period, it is possible to model the solar-harvesting behavior beforehand. In particular, the CRs perform spectrum sensing by employing energy detectors, which use the optimal detection threshold, in order to determine the presence or absence of the primary user in the bands. A local hard decision is then made at each cognitive radio for each band, and sent to the fusion center (FC), which makes the final decision based on the AND or the OR fusion rule. If the spectrum is deemed to be idle, then the CRs start to transmit data following the predetermined optimal power allocation strategy carried out in the previous offline step. We only consider a scenario where at most two available bands are accessed at the same time. Then, two spectrum access strategies are considered. a) In the first scenario, the cognitive users share one or the two available frequency bands, so that channel interference should be taken into account. b) In the second one, each CR is assigned to a different band, and thus, there is no cross channel interference between cognitive users. In case only one channel is deemed to be available at a specific time instant, the channel shall be assigned to the CR user with the best channel quality.

2.1 System model

In this section, we construct the energy-harvesting CR network model and energy model together with the considered constraints.

2.1.1 Network model

We consider a cognitive radio network composed of $S = 2$ secondary users (SUs) (each user includes a transmitter and a receiver) which opportunistically use the frequency bands licensed to a PU, as it is shown in Fig. 2.1 [19]. To that aim, SUs should sense the spectrum, i.e., detect the licensed users, and identify the free spectrum holes in order to use efficiently the scarce frequency resources.

Hence, sensing for the primary user detection can be formulated as a binary hypothesis

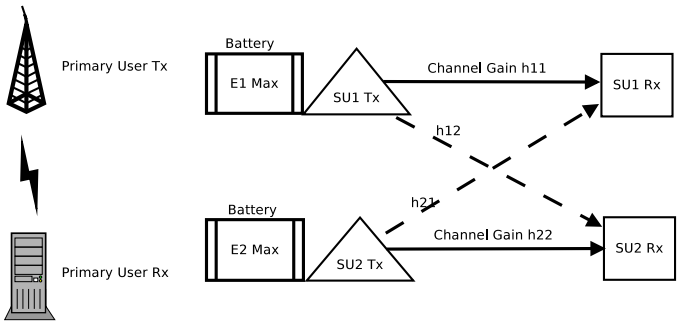

Figure 2.1: Network Model

problem

$$\begin{aligned} \mathcal{H}_0 &: \mathbf{y} = \mathbf{w} \\ \mathcal{H}_1 &: \mathbf{y} = \mathbf{x} + \mathbf{w} \end{aligned} \tag{2.1}$$

where $\mathbf{y}$ is the received signal vector at the SU, $\mathbf{x}$ is the signal vector transmitted by the PU, and $\mathbf{w}$ is the noise vector. $\mathcal{H}_0$ and $\mathcal{H}_1$ denote the hypothesis of the absence and the presence, respectively, of the PU signal in a band of interest. To decide whether $\mathbf{y}$ was generated under hypothesis $\mathcal{H}_0$ or $\mathcal{H}_1$, every SU should form a test statistic $T(\mathbf{y})$ from the received data $\mathbf{y}$, and compare it with a predetermined threshold ε,

$$T(\mathbf{y}) \underset{\mathcal{H}_0}{\overset{\mathcal{H}_1}{\gtrless}} \varepsilon. \tag{2.2}$$

The local detection technique that we consider in this paper is the Neyman-Pearson energy detector, which detects the signal of the PU based on the sensed energy, i.e., $T(\mathbf{y}) = \|\mathbf{y}\|^2 = \sum_{k=1}^{N_s} |y_i|^2$, where N_s denotes the number of collected samples ($N_s < \tau_s f_s$, where f_s is the sampling frequency and τ_s the sensing time [53]). Also, we assume that the signal transmitted by the primary user, $\mathbf{x}$, and the noise, $\mathbf{w}$, are i.i.d. zero-mean circularly symmetric complex Gaussians with variance σ_x^2 and σ_w^2, respectively, which can be written as $\mathbf{x} \sim \mathcal{N}(\mathbf{0}, \sigma_{\mathbf{x}}^{\mathbf{2}}\mathbf{I})$ and $\mathbf{w} \sim \mathcal{N}(\mathbf{0}, \sigma_{\mathbf{w}}^{\mathbf{2}}\mathbf{I})$, where $\mathbf{I}$ is the identity matrix. Then, $T(\mathbf{y})$ follows a Chi-square distribution with $2N_s$ degrees of freedom under hypothesis $\mathcal{H}_0$ and $\mathcal{H}_1$ [54]:

$$\mathcal{H}_0 : \frac{T(\mathbf{y})}{\sigma_w^2/2} \sim \chi^2_{2N_s} \tag{2.3a}$$

$$\mathcal{H}_1 : \frac{T(\mathbf{y})}{(\sigma_x^2 + \sigma_w^2)/2} \sim \chi^2_{2N_s}. \tag{2.3b}$$

To evaluate the detection performance of the cognitive radios, the probabilities of detection and false alarm are used, which are defined as

$$\mathcal{P}_{\mathrm{d}}(\varepsilon) = \mathcal{P}(\mathcal{H}_1 \mid \mathcal{H}_1) = \mathcal{P}(T(\mathbf{y}) \geq \varepsilon | \mathcal{H}_1) \tag{2.4a}$$

$$\mathcal{P}_{\mathrm{fa}}(\varepsilon) = \mathcal{P}(\mathcal{H}_1 \mid \mathcal{H}_0) = \mathcal{P}(T(\mathbf{y}) \geq \varepsilon | \mathcal{H}_0), \tag{2.4b}$$

where ε is the detection threshold. For the energy detector, the local probabilities of detection, $\mathcal{P}_{\mathrm{d}}$, and false alarm, $\mathcal{P}_{\mathrm{fa}}$, are computed as

$$\mathcal{P}_{\mathrm{d}}\left(\varepsilon\right) = 1 - F_{2N_s}^{2}\left(\frac{\varepsilon}{\left(\sigma_x^2 + \sigma_w^2\right)/2}\right), \tag{2.5a}$$

$$\mathcal{P}_{\mathrm{fa}}\left(\varepsilon\right) = 1 - F_{2N_s}^{2}\left(\frac{\varepsilon}{\sigma_w^2/2}\right), \tag{2.5b}$$

where F is the cumulative distribution function of the Chi-square distribution with $2N_s$ degrees of freedom.

In a centralized cooperative sensing scheme, a fusion center (FC) is responsible for receiving and combining the local decisions of all the secondary users in order to make a common decision about the presence or absence of the PU. Later it diffuses the common decision back to the SUs. In a two-user cognitive radio network, two different rules (AND and OR) can be used for combining the hard decisions. In the AND rule, the FC decides that the PU is present if the two SUs detect the signal, i.e., $\sum_{s=0}^{S=1} T^{(s)} = 2$. If the OR rule is considered, the FC decides the presence of the PU if any of the two SUs reports signal detection, i.e., $\sum_{s=0}^{S=1} T^{(s)} \geq 1$. Hence, the global probability of detection, Q_{D}, and the global probability of false alarm, Q_{FA}, for the two aforementioned fusion rules can be computed based on the local probabilities of detection and false alarm of the two SUs, $\mathcal{P}_{\mathrm{d},j}$ and $\mathcal{P}_{\mathrm{fa},j}(j \in \{1,2\})$, as [8]:

$$\begin{aligned}
Q_{\mathrm{D,OR}} &= \left(1 - \mathcal{P}_{\mathrm{d},1}\right)\mathcal{P}_{\mathrm{d},2} + \left(1 - \mathcal{P}_{\mathrm{d},2}\right)\mathcal{P}_{\mathrm{d},1} + \mathcal{P}_{\mathrm{d},1}\mathcal{P}_{\mathrm{d},2} \\
Q_{\mathrm{D,AND}} &= \mathcal{P}_{\mathrm{d},1}\mathcal{P}_{\mathrm{d},2}, \qquad (2.6) \\
Q_{\mathrm{FA,OR}} &= \left(1 - \mathcal{P}_{\mathrm{fa},1}\right)\mathcal{P}_{\mathrm{fa},2} + \left(1 - \mathcal{P}_{\mathrm{fa},2}\right)\mathcal{P}_{\mathrm{fa},1} + \mathcal{P}_{\mathrm{fa},1}\mathcal{P}_{\mathrm{fa},2} \\
Q_{\mathrm{FA,AND}} &= \mathcal{P}_{\mathrm{fa},1}\mathcal{P}_{\mathrm{fa},2}. \qquad (2.7)
\end{aligned}$$

Without loss of generality, we assume that the detection threshold and the received SNR of the PU are the same at every time instant for the two SUs, and thus, they have identical $\mathcal{P}_{\mathrm{d}}\left(\varepsilon\right)$ and $\mathcal{P}_{\mathrm{fa}}\left(\varepsilon\right)$.

Because our aim is designing an offline optimization scheme, we need to know how many chances SUs may have to access the spectrum during the short-term time period. Defining $\pi_1 = \mathcal{P}\left(\mathcal{H}_1\right)$ and $\pi_0 = \mathcal{P}\left(\mathcal{H}_0\right)$ $(\pi_1 + \pi_0 = 1)$ as the probability that the PU is present or absent in the spectrum, respectively, the probability that a SU accesses the spectrum (denoted by $\mathcal{P}(\mathcal{A})$) can be expressed in terms of Q_{D} and Q_{FA} as

$$\begin{aligned}
\mathcal{P}(\mathcal{A}) &= \mathcal{P}(\mathcal{A}|\mathcal{H}_1)\mathcal{P}\left(\mathcal{H}_1\right) + \mathcal{P}(\mathcal{A}|\mathcal{H}_0)\mathcal{P}\left(\mathcal{H}_0\right) \\
&= \left(1 - Q_{\mathrm{D}}\right)\pi_1 + \left(1 - Q_{\mathrm{FA}}\right)\pi_0. \qquad (2.8)
\end{aligned}$$

Besides, we consider an energy-harvesting scenario. SUs harvest energy independently and store it in a rechargeable finite battery with $E_{j,\max}$ denoting the maximum battery capacity for SU j. Further, we assume a continuous traffic model where the SU transmitters always have data to transmit to their corresponding receivers [1]. Denoting x_j as the transmitted signals at SU j; y_j as the received signals at secondary receiver j; n_j as the noise received by

[1] The analysis can be also extended to a more general traffic model in which SU have intermittent traffic.

SU receivers; and h_{jk} ($j, k \in \{1, 2\}$) as the channel coefficients (see Fig. 2.1), where h_{jk} for $j = k$ are the channel gains and h_{jk} for $j \neq k$ are the interference coefficients, the channel output in a two-user scenario is represented by

$$y_1 = h_{11}x_1 + h_{21}x_2 + n_1; y_2 = h_{22}x_2 + h_{12}x_1 + n_2. \tag{2.9}$$

2.1.2 Interference control constraint

Cognitive radios will inevitably create interference to the primary users and therefore, the quality of service (QoS) of the system will be degraded. In order to reduce the impact on the primary user performance and assure a stable and efficient transmission environment, the interference should be controlled. This is achieved by limiting the interference that the PU may have to a certain value. To that aim, the detection performance of the system is lower-bounded by α, a pre-specified detection design parameter,

$$Q_{\mathrm{D}} \geq \alpha, \tag{2.10}$$

or alternatively, the maximum probability of collision should be $1 - \alpha$.

2.1.3 Energy model and power management constraints

As mentioned above, cognitive radios are considered in an energy-harvesting scenario. Assuming a time-slotted model of duration τ [55], the energy-harvesting and energy-consumption processes for user $j \in \{1, 2\}$ are shown in Fig. 2.2.

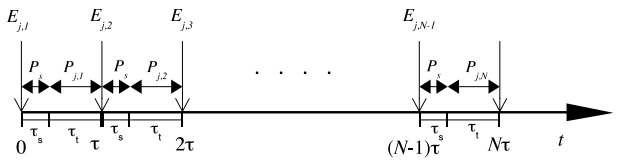

Figure 2.2: Energy-harvesting and energy-consumption models for user $j \in \{1, 2\}$.

The energy consumed by a SU may include the energy spent for sensing the channel, reporting the sensing result, the data transmission, the energy leakage caused by the device, the inefficient energy harvesting, etc. [24]. Usually, the main sources of energy consumption are the sensing and transmitting processes, being the energy consumption due to the other tasks negligible [56] [57].

At the beginning of time slot i, SU j harvests a random amount of energy, $E_{j,i} \geq 0$, which is immediately available in the same time slot. To avoid collisions with the PU, user j senses the spectrum during τ_s (consuming a constant sensing power P_{s}), and reports the sensing result to a FC. If the spectrum is free, then the users can access to the channel and transmit data during the remaining time of the slot, $\tau_t = \tau - \tau_s$, consuming a transmission power $P_{j,i}$ [34]. As it was mentioned above, we are solving a short-term optimization problem. It means we can model and predict the current working environment of the system. Thus,

the harvested energy can be predicted, i.e., we can know the harvested energy packages $E_{j,i}$ beforehand. This scheme assumes that both, secondary transmitters and receivers are synchronized with the slot structure of the primary network.

Different from the scenarios where cognitive radios are battery-operated, several considerations need to be taken into account in an energy-harvesting scenario [18]. These considerations come from the dynamic nature of the energy-harvesting process, so that dynamic power management plays a key role. Specifically, two constraints should be considered [19].

a) The *energy causality constraint*, which is due to the random harvested energy. It is based on the idea that the total energy consumption should not exceed the maximum amount of current available energy, and can be expressed as

$$\sum_{k=1}^{i} \mathcal{P}\left(\mathcal{A}\right) P_{j,k}\tau_t + iP_{\mathrm{s}}\tau_s \leq \sum_{k=1}^{i} E_{j,k}, \tag{2.11}$$

where $i = 1, 2, \cdots, N$ denotes the current time slot. At every time slot, the Implicitly, the transmission power is assumed to be constant during each time slot. Clearly, more accurate expressions for the energy causality constraint can be defined if the leakage from the battery or the inefficiency in storing energy is taken into account [**?**], but as it was aforementioned, we neglect them. Note that the consumed energy up to time slot i, $\sum_{k=1}^{i} \mathcal{P}\left(\mathcal{A}\right) P_{j,k}\tau_t$, is computed as a statistical average value for each user.

b) *The overflow constraint*, which comes from the fact that the battery size is finite. Physically, overflow can happen when the battery capacity is not enough to store the newest harvested energy package. However, in most cases overflow is not desirable because it would lose capacity in the sense that the excess of energy could have been consumed previously to the overflow situation [49, 50], and further overflow of energy can harm the radio electronics. See Section 2.4 at the end of the chapter for a discussion about this constraint. Therefore, it is necessary to assure that the battery level never exceeds the maximum battery capacity whenever energy is harvested, which can be expressed as

$$\sum_{k=1}^{i+1} E_{j,k} - \sum_{k=1}^{i} \mathcal{P}\left(\mathcal{A}\right) P_{j,k}\tau_t - iP_{\mathrm{s}}\tau_s \leq E_{j,\max}. \tag{2.12}$$

Thus, the interference constraint (2.10) together with the two power management constraints (2.11) - (2.12) are accounted for in the offline optimization problem presented in the next section. Clearly, more accurate expressions for the transmission power can be considered using statistical models in more dynamic decision frameworks. This would lead to a nondeterministic computation of the energy consumption, which is out of the scope of this work.

2.2 Optimal power allocation for a single-frequency-band scenario

In this scenario, the two secondary transmitters share the spectrum with the primary network, and both of them opportunistically access and share the primary user spectrum (a single-frequency band) when the primary user is deemed to be absent. We formulate the underlying problem in order to set the appropriate detection threshold and optimally allocate

the available power between the SUs under the interference and power management constraints. The optimal power allocation and detection threshold will be viewed as the solution of a constrained optimization problem, which is dealt in the next subsections.

2.2.1 Problem formulation

The objective function is defined as the total throughput of the cognitive radio network over a time period $T = N\tau$. Let $C_{j,i}$ denote the channel capacity of SU j at time slot i. The throughput of the cognitive radio network at time slot i can be expressed as

$$R_i = (C_{1,i} + C_{2,i})\,\tau_t. \tag{2.13}$$

As the two SUs share a common communication medium, interference between them should be considered (look at Fig. 2.1). Assuming that the noise received at both SUs is additive white Gaussian noise (AWGN) with variance $N_{0,j}$, the channel capacity at time slot i for both users is computed as follows

$$\begin{aligned} C_{1,i} &= W\log_2\left(1 + \frac{|h_{11}|^2 P_{1,i}}{|h_{21}|^2 P_{2,i} + N_{0,1}}\right) \\ C_{2,i} &= W\log_2\left(1 + \frac{|h_{22}|^2 P_{2,i}}{|h_{12}|^2 P_{1,i} + N_{0,2}}\right), \end{aligned} \tag{2.14}$$

where W is the spectrum bandwidth (a single-frequency band in this scenario), and h_{jk} are the channel coefficients between the j-th cognitive transmitter and the k-th cognitive receiver, which are assumed to be constant.

Thus, the total throughput at time T is

$$R_T = \sum_{i=1}^{N} (\pi_0 \mathcal{P}\left(\mathcal{A}|\mathcal{H}_0, \varepsilon_i\right) \mathcal{P}\left(\mathcal{S}|\mathcal{H}_0\right) R_i + \pi_1 \mathcal{P}\left(\mathcal{A}|\mathcal{H}_1, \varepsilon_i\right) \mathcal{P}\left(\mathcal{S}|\mathcal{H}_1\right) R_i), \tag{2.15}$$

where $\mathcal{P}\left(\mathcal{S}|\mathcal{H}_p\right)$, $p = \{0, 1\}$ is the probability that a SU can successfully transmit the data to its receiver when the spectrum is idle or occupied, respectively. In case of a successful detection of a spectrum hole, $\mathcal{P}\left(\mathcal{S}|\mathcal{H}_0\right) \to 1$ because that frequency band is completely free for being used by the SU. On the other hand, in case of miss detection of the PU, $\mathcal{P}\left(\mathcal{S}|\mathcal{H}_1\right) \to 0$ since the bandwidth is completely occupied by the PU [9]. Hence, the second term in (2.15) is negligible, and the total throughput function can be simplified as

$$R_T = \sum_{i=1}^{N} \pi_0 \mathcal{P}\left(\mathcal{A}|\mathcal{H}_0, \varepsilon_i\right) R_i. \tag{2.16}$$

The transmission power and the detection threshold at every time slot are the optimization (design) variables, namely $\varepsilon_i, P_{j,i}$. And the conditions presented in the previous section, (2.10) - (2.12), are imposed as constraints. Thus, based on the above discussions, the optimization problem for finding the optimal transmission power and the detection threshold at every time instant i can be formulated as

$$\underset{\varepsilon_i, P_{j,i}}{\text{maximize}} \quad R_T \tag{2.17a}$$

$$\text{subject to} \quad P_{j,i} \geq 0 \quad j \in \{1,2\}, i = 1,2,\cdots,N \tag{2.17b}$$

$$(2.10), (2.11), (2.12) \tag{2.17c}$$

Note that the power constraint (2.17b) should be always satisfied since obtaining a negative transmission power is meaningless.

2.2.2 Offline solution

Based on the assumption that at time instant i there is no prior knowledge about the harvested energy and the transmission power at time instants $n > i$, the optimization problem has to be solved in an iterative way. In this section, we propose the optimal solution for the problem stated in (2.17), which aims at maximizing the total throughput during a short-term period T by designing the power allocation and the detection threshold strategy that should be used at every time slot i. Remind that we are using an offline approach for solving the optimization problem, i.e., we optimize the power and detection threshold that should be used at any time slot i from an initial time slot 0. In order to reduce the computational complexity, a suboptimal solution is also proposed.

2.2.2.1 Optimal power allocation algorithm

By exploring the structure of (2.16), three different terms can be identified in the total throughput. a) $\mathcal{P}(\mathcal{A}|\mathcal{H}_0)$, which is related to the detection threshold ε_i; b) R_i (2.13, 2.14), which depends on the channel and the transmission powers $P_{j,i}$; and c) π_0, which is determined by the primary user activity (and it is assumed to be constant). Further, ε_i influences not only $\mathcal{P}(\mathcal{A}|\mathcal{H}_0)$, but also the energy constraints (2.11) and (2.12), which in turn will influence the range of feasible values of the transmission powers $P_{j,i}$, and consequently, R_i.

For that reason, we propose to solve the optimization problem in two steps. In the first step, we assume that the detection threshold ε_i is known at time slot i and we aim at allocating the SUs transmission powers $P_{j,i}$ by maximizing the throughput. In a second step, the optimal detection threshold is determined using the transmission power result achieved in the first step.

Energy constraints (2.11) and (2.12) should be taken into account in the first step. However, since the interference control constraint (2.10) only affects the detection threshold ε_i, it can be neglected. Therefore, this optimization problem can be expressed as

$$\underset{P_{j,i}}{\text{maximize}} \quad (C_{1,i} + C_{2,i})\,\tau_t \tag{2.18a}$$

$$\text{subject to} \quad P_{j,i} \geq 0 \quad j \in \{1,2\}; i,k = 1,2,\cdots,N \tag{2.18b}$$

$$\sum_{k=1}^{i} E_{j,k} - \sum_{k=1}^{i-1} \mathcal{P}\left(\mathcal{A}|\varepsilon_k\right) P_{j,k}\tau_t - iP_s\tau_s - \mathcal{P}\left(\mathcal{A}|\varepsilon_i\right) P_{j,i}\tau_t \geq 0 \tag{2.18c}$$

$$\sum_{k=1}^{i+1} E_{j,k} - \sum_{k=1}^{i-1} \mathcal{P}\left(\mathcal{A}|\varepsilon_k\right) P_{j,k}\tau_t - iP_s\tau_s - \mathcal{P}\left(\mathcal{A}|\varepsilon_i\right) P_{j,i}\tau_t \leq E_{j,\max} \tag{2.18d}$$

Note that τ_t is constant. From (2.18c) and (2.18d), a lower and upper bound of $P_{j,i}$ can be derived. Let us denote $c_i\left(P_{j,i}\right) = \left(1+\frac{P_{1,i}}{\alpha_i P_{2,i}+N_1}\right)\left(1+\frac{P_{2,i}}{\beta_i P_{1,i}+N_2}\right)$, where $N_j = N_{0,j}/\left|h_{jj}\right|^2$ denotes the normalized background noise power, and $\alpha = \left|h_{21}/h_{11}\right|^2$ and $\beta = \left|h_{12}/h_{22}\right|^2$ are the normalized crosstalk coefficients from transmitter 1 (or 2) to receiver 2 (or 1), respectively. Thus, the previous problem can be reduced to

$$\begin{aligned}
\underset{P_{j,i}}{\text{maximize}} \quad & W\log_2\left[c_i\left(P_{j,i}\right)\right] && \text{(2.19a)}\\
\text{subject to} \quad & P_{j,i} \geq 0, \quad j \in \left\{1,2\right\}; i = 1,2,\cdots,N && \text{(2.19b)}\\
& P_{j,i} \leq U_{j,i} && \text{(2.19c)}\\
& P_{j,i} \geq L_{j,i} && \text{(2.19d)}
\end{aligned}$$

where the upper and lower bounds for the transmission powers are given by $U_{j,i} = \frac{\sum_{k=1}^{i} E_{j,k} - \sum_{k=1}^{i-1} \mathcal{P}(\mathcal{A}|\varepsilon_k) P_{j,k}\tau_t - iP_s\tau_s}{\mathcal{P}(\mathcal{A}|\varepsilon_i)\tau_t}$, and $L_{j,i} = \frac{\sum_{k=1}^{i+1} E_{j,k} - \sum_{k=1}^{i-1} \mathcal{P}(\mathcal{A}|\varepsilon_k) P_{j,k}\tau_t - iP_s\tau_s - E_{j,\max}}{\mathcal{P}(\mathcal{A}|\varepsilon_i)\tau_t}$, respectively.

Note that (2.19) is only feasible if the upper bound $U_{j,i}$ is positive and bigger than or equal to lower bound $L_{j,i}$ (i.e., $U_{j,i} \geq L_{j,i}$). If $U_{j,i} < 0$ or $U_{j,i} < L_{j,i}$, then $P_{j,i}$ is not meaningful and there will not be a feasible solution. In order to satisfy the condition $U_{j,i} \geq L_{j,i}$, the condition $E_{j,\max} \geq E_{j,i}$ should be satisfied for every SU j and every time slot i. If the condition $U_{j,i} \geq 0$ is not satisfied, it means that the residual energy is not enough to provide energy to transmit or perform spectrum sensing. Thus, we set the transmission power to be zero in this case.

As the spectrum bandwidth W is constant, and taking into account that $\log_2(z)$ is a monotonic increasing function of z, the optimization problem (2.19) is equivalent to

$$\begin{aligned}
\underset{P_{j,i}}{\text{maximize}} \quad & \left(1+\frac{P_{1,i}}{\alpha_i P_{2,i}+N_1}\right)\left(1+\frac{P_{2,i}}{\beta_i P_{1,i}+N_2}\right) && \text{(2.20a)}\\
\text{subject to} \quad & \text{(2.19b), (2.19c), (2.19d)} && \text{(2.20b)}
\end{aligned}$$

The optimization problem formulated in (2.20) is not convex. However, its objective function $c_i\left(P_{j,i}\right)$ is quasi-convex on its domain [47]. Fig. 2.3 represents the objective function for different values of the transmission power and the parameters.

It can be seen that, independently of the channel parameters, the objective function always achieves the largest value at the vertices. Therefore, the maximum value of (2.20a) is attained at the vertices, i.e.,

$$c_{i,\max} = \max\{c_i\left({L_1}^+, {L_2}^+\right), c_i\left({L_1}^+, U_2\right), c_i\left(U_1, {L_2}^+\right), c_i\left(U_1, U_2\right)\}, \tag{2.21}$$

where $(z)^+ = \max\{z, 0\}$, for any z. Then, the optimal transmission powers, denoted as $P^*_{j,i}$, correspond to those transmission power values which contribute to attain the largest value of the objective function c_i.

In the second step, we solve the optimal detection threshold ε_i at every time slot i using the solution of the first step. Initially, we analyze the impact of the detection threshold ε_i

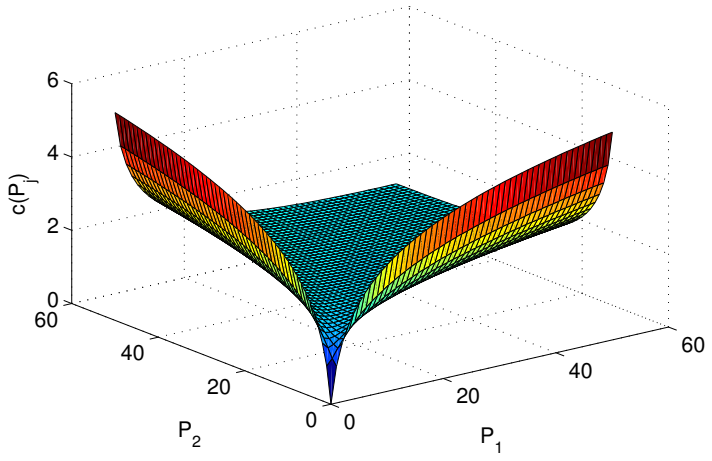

(a)

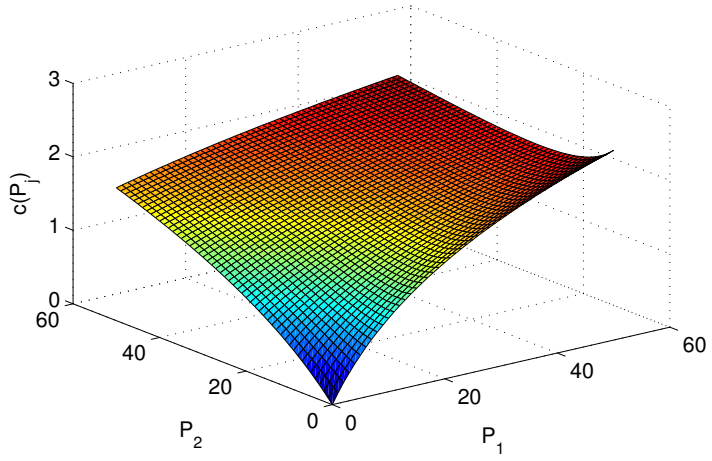

(b)

Figure 2.3: Objective function of the optimization problem (2.20), $c(P_j)$, for (a) $N_1 = N_2 = 1$ and $\alpha = \beta = 1$, and (b) $N_1 = 20$, $N_2 = 10$, $\alpha = 0.1$, and $\beta = 1$.

on both, $\mathcal{P}\left(\mathcal{A}|\mathcal{H}_0, \varepsilon_i\right)$ and the SU capacity R_i, which are the terms appearing in the total throughput R_T, given by (2.16).

The maximum value of $\mathcal{P}\left(\mathcal{A}|\mathcal{H}_0, \varepsilon_i\right) = 1 - Q_{\mathrm{FA}}(\varepsilon_i)$ is achieved when the detection threshold ε_i is maximal. However, the higher the detection threshold value is, the lower Q_{FA} and Q_{D} are. Hence, as Q_{D} decreases with an increase of ε_i, (2.10) states an upper bound for ε_i, denoted as ε_0,

$$\varepsilon_i \leq {Q_D}^{-1}\left(\alpha\right) = \varepsilon_0. \tag{2.22}$$

Specifically, for the AND and OR fusion rules, the upper bound for the detection threshold can be expressed as

$$\varepsilon_{0,\mathrm{AND}} = \frac{\sigma_x^2 + \sigma_w^2}{2} F_{2N_s}^{-1}\left(1 - \sqrt{\alpha}\right) \tag{2.23a}$$

$$\varepsilon_{0,\mathrm{OR}} = \frac{\sigma_x^2 + \sigma_w^2}{2} F_{2N_s}^{-1}\left(\sqrt{1-\alpha}\right). \tag{2.23b}$$

On the other hand, the opposite effect is observed in R_i. Remark that $\mathcal{P}(\mathcal{A})$ is a monotonic increasing function of the detection threshold ε when the energy detector is applied. According to (2.5), when the threshold ε increases, the local probabilities of detection and false alarm ($\mathcal{P}_{\mathrm{d}}$ and $\mathcal{P}_{\mathrm{fa}}$) decrease, as well as the global probabilities of detection and false alarm, Q_{D} and Q_{FA} (see (2.6) and (2.7)). Yet $\mathcal{P}(\mathcal{A}|\mathcal{H}_0)$ increases with a decrease of Q_{D} and Q_{FA} (2.8). A larger value of ε_i increases $\mathcal{P}(\mathcal{A})$. However, the upper and lower bounds of the transmission powers ($U_{j,i}$ and $L_{j,i}$, respectively) decrease, in the same way as the range of possible values for the optimal transmission values do.Therefore, the channel capacity C_j decreases. An intuitive explanation for this may be the following. When the chances to access the channel increase, the optimal solution may tend to assign less power during each access for a given finite harvested energy (in a short time period), which results in fewer channel capacity for a successful transmission.

In short, the election of the optimal detection threshold states a trade-off between maximizing $\mathcal{P}(\mathcal{A}|\mathcal{H}_0, \varepsilon_i)$ and the throughput R_i. Further, the influence of ε_i on the total throughput R_T does not obey a monotonic rule. To get some intuition about the curve shape, Fig. 2.4 shows the total throughput for Q_{D} varying from 0.01 to 0.99 and two SNRs values: $-10, -5$ dB.

As it was aforementioned, parameter α establishes an upper bound for the value of the detection threshold, and influences the achievable throughput. Fig. 2.4 shows a concave behavior, whose mathematical closed-form expression is still left to be proved in future work. Further, the particular shape of the curve depends on the considered SNR value. Therefore, we solve the problem by performing a bounded exhaustive search over the detection threshold. Setting an appropriate step size for Q_{D}, the optimal value ε_i^* corresponds to the one that maximizes the throughput for the optimal $P_{j,i}$ obtained after solving (2.19).

The algorithm to jointly optimize the detection threshold and the power allocation for the SUs is shown in Algorithm 1. $Q_{\mathrm{D,max}}$ denotes the maximum probability of detection (which ideally is 1), P is the length of the set of values Q_{D}, and ΔQ_{D} is the step size to search for the optimal detection threshold when the transmission powers are unfeasible.

2.2.2.2 Suboptimal power allocation algorithm

To overcome the computational cost of searching for the optimal detection threshold, we present a suboptimal approach, which operates under less demanding, conditions. Instead of performing a bounded exhaustive search over ε_i, we set its initial value to the one corresponding to the interference constraint boundary (i.e., (2.23a) or (2.23b)). The related algorithm is summarized in Algorithm 2.

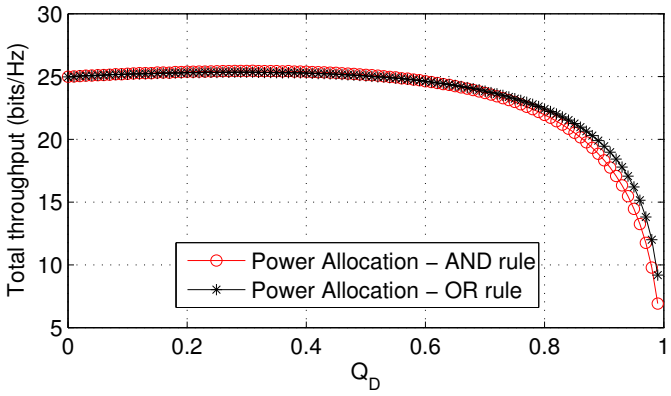

(a)

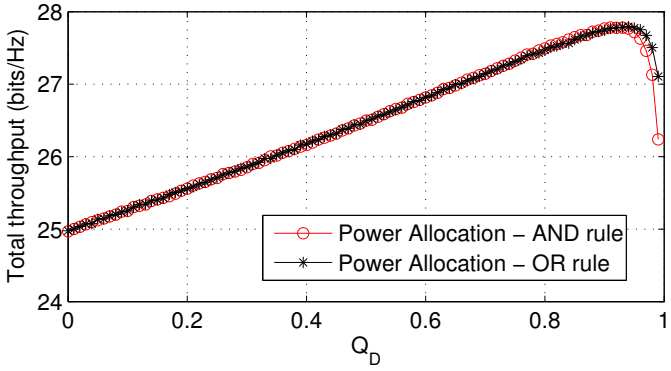

(b)

Figure 2.4: Total throughput versus Q_{D} for (a) $SNR = -10$ dB, and (b) $SNR = -5$ dB.

2.2.2.3 Random power allocation algorithm

Finally, we introduce a simplified version of the suboptimal approach as a benchmark for the performance evaluation. In this benchmark algorithm, we select the transmission powers $P_{j,i}$ from the real set which is uniformly distributed in the interval $({L_{j,i}}^{+}, U_{j,i})$. As it can be expected, the assigned powers might not be the optimal ones, however, they satisfy the power management constraints. Similar to the suboptimal approach, we consider the detection threshold value such that $Q_{\mathrm{D}} = \alpha$. The benchmark algorithm is summarized in Algorithm 3.

2.2.3 Simulation results

In this subsection, we present some simulation results in order to compare the performance of the proposed algorithms (the optimal and suboptimal strategies) with the benchmark algorithm for the AND and OR fusion rules. Results are also compared with an approach that we call as the priority best-channel power allocation algorithm. In this strategy, the free frequency band is assigned to the SU with the best channel gain. In case the channel gains of

Algorithm 1 Optimal power allocation and detection threshold

Require: $E_{j,\max} \geq E_{j,i}$, for $j = 1, 2$ and $i = 1, 2, \cdots, N$

Initialize $Q_{\mathrm{D},0} = \alpha$; $Q_{\mathrm{D},\max} = 0.99$

for $p = 1, 2, \cdots, P$; $P = \frac{Q_{\mathrm{D},\max} - \alpha}{\Delta Q_{\mathrm{D}}}$ **do**

  $Q_{\mathrm{D},p} = Q_{\mathrm{D},0} + (p-1)\,\Delta Q_{\mathrm{D}}$

  for $i = 1$ to N **do**

    $\varepsilon_i \leftarrow \varepsilon_0$, $\varepsilon_0 = Q_{\mathrm{D},p}^{-1}$.

    For $j = 1, 2$ do

    $L_{j,i} \leftarrow \frac{\sum_{k=1}^{i+1} E_{j,k} - \sum_{k=1}^{i-1} \mathcal{P}(\mathcal{A}|\varepsilon_k) P_{j,k} \tau_t - i P_{\mathrm{s}} \tau_s - E_{j,\max}}{\mathcal{P}(\mathcal{A}|\varepsilon_i)\tau_t}$

    $U_{j,i} \leftarrow \frac{\sum_{k=1}^{i} E_{j,k} - \sum_{k=1}^{i-1} \mathcal{P}(\mathcal{A}|\varepsilon_k) P_{j,k} \tau_t - i P_{\mathrm{s}} \tau_s}{\mathcal{P}(\mathcal{A}|\varepsilon_i)\tau_t}$

    if $U_{j,i} \geq 0$ **then**

      $\left\{P_{1,i,p}, P_{2,i,p}\right\} = \arg\max c_i,$

      where $\left\{P_{1,i,p}, P_{2,i,p}\right\} \in \left\{ \begin{matrix} \left\{L_{1,i}^{+}, L_{2,i}^{+}\right\} \\ \left\{U_{1,i}, L_{2,i}^{+}\right\} \\ \left\{U_{1,i}, U_{2,i}\right\} \\ \left\{L_{1,i}^{+}, U_{2,i}\right\} \end{matrix} \right\}$

    else

      $P_{j,i,p} = 0$

    end if

  end for

  $\left\{P_{1,p}, P_{2,p}\right\} = \left\{ \begin{matrix} P_{1,1,p} & P_{2,1,p} \\ P_{1,2,p} & P_{2,2,p} \\ \cdots & \cdots \\ P_{1,N,p} & P_{2,N,p} \end{matrix} \right\}$

end for

Choose $\left\{P_1, P_2\right\} = \arg\max R_T$; where $\left\{P_1, P_2\right\} \in \left\{P_{1,p}, P_{2,p}\right\}$.

Algorithm 2 Suboptimal power allocation and detection threshold

Require: $E_{j,\max} \geq E_{j,i}$, for $j = 1, 2$ and $i = 1, 2, \cdots, N$

Initialize $\varepsilon_0 = Q_{\mathrm{D}}^{-1}(\alpha)$; $\Delta\varepsilon$

for $i = 1$ to N **do**

  $\varepsilon_i \leftarrow \varepsilon_0$

  For $j = 1, 2$ do

  $L_{j,i} \leftarrow \frac{\sum_{k=1}^{i+1} E_{j,k} - \sum_{k=1}^{i-1} \mathcal{P}(\mathcal{A}|\varepsilon_k) P_{j,k} \tau_t - i P_{\mathrm{s}} \tau_s - E_{j,\max}}{\mathcal{P}(\mathcal{A}|\varepsilon_i)\tau_t}$

  $U_{j,i} \leftarrow \frac{\sum_{k=1}^{i} E_{j,k} - \sum_{k=1}^{i-1} \mathcal{P}(\mathcal{A}|\varepsilon_k) P_{j,k} \tau_t - i P_{\mathrm{s}} \tau_s}{\mathcal{P}(\mathcal{A}|\varepsilon_i)\tau_t}$

  if $U_{j,i} \geq 0$ **then**

    $\left\{P_{1,i,p}, P_{2,i,p}\right\} = \arg\max c_i,$

    where $\left\{P_{1,i,p}, P_{2,i,p}\right\} \in \left\{ \begin{matrix} \left\{L_{1,i}^{+}, L_{2,i}^{+}\right\} \\ \left\{U_{1,i}, L_{2,i}^{+}\right\} \\ \left\{U_{1,i}, U_{2,i}\right\} \\ \left\{L_{1,i}^{+}, U_{2,i}\right\} \end{matrix} \right\}$

  else

    $P_{j,i,p} = 0$

  end if

end for

both users are identical, the spectrum is assigned with equal probability to one of them. We denoted this approach as *priority*.

Secondary users are equipped with a heliomote harvesting system which uses a solar panel and Nickel Metal Hydride (NiMH) batteries, whose capacity is 2500mAh, i.e. 3 Joules [13]. The recharge cycle is 1000. The maximum harvesting rate can vary from 190 mJ/s to 240 mJ/s from 12:30 pm to 3:00 pm if the 4-4.0-100 solar panel is used [58].

Algorithm 3 Random power allocation and detection threshold

Require: $E_{j,\max} \geq E_{j,i}$, for $j = 1, 2$ and $i = 1, 2, \cdots, N$

Initialize $\varepsilon_0 = Q_{\mathrm{D}}^{-1}(\alpha)$; $\Delta\varepsilon$

for $i = 1$ to N **do**

  $\varepsilon_i \leftarrow \varepsilon_0$

  For $j = 1, 2$ do

  $L_{j,i} \leftarrow \frac{\sum_{k=1}^{i+1} E_{j,k} - \sum_{k=1}^{i-1} \mathcal{P}(\mathcal{A}|\varepsilon_k) P_{j,k} \tau_t - i P_{\mathrm{s}} \tau_s - E_{j,\max}}{\mathcal{P}(\mathcal{A}|\varepsilon_i)\tau_t}$

  $U_{j,i} \leftarrow \frac{\sum_{k=1}^{i} E_{j,k} - \sum_{k=1}^{i-1} \mathcal{P}(\mathcal{A}|\varepsilon_k) P_{j,k} \tau_t - i P_{\mathrm{s}} \tau_s}{\mathcal{P}(\mathcal{A}|\varepsilon_i) \cdot \tau_t}$

  if $U_{j,i} \geq 0$ **then**

    $P_{j,i} \leftarrow P_{j,i,random} \in \mathbb{U}\left(L_{j,i}^{+}, U_{j,i}\right)$;

  else

    $P_{j,i,random} = 0$

    return to Step 4

  end if

end for

The primary user sends a complex QPSK signal with variance $\sigma_x^2 = 1$. The probability of the PU activity is known by the cognitive radios and, unless stated otherwise, a low probability of the PU to be present is considered, $\pi_1 = 0.2$ (and $\pi_0 = 0.8$), so that SUs may access the spectrum. In practice, estimates of π_1 and π_0 can be obtained via spectrum measurements. The SNR of the PU signal measured at both SUs is the same and varies in the interval [-20,30] dB. The spectrum bandwidth is $W = 6$ KHz, and the sampling frequency $f_s = 12$ KHz. AWGN noise is added to the channel (with noise power $N_{0,1} = N_{0,2} = 1$ mW). The channel gain coefficients are set to $h_{11} = h_{22} = -10$ dB and the interference coefficients to $h_{12} = h_{21} = -20$ dB. The detection design parameter α is set to 0.9 and the sensing power to $P_s = 0.12$ mW. The time slot duration is $\tau = 100$ ms, where $\tau_s = 10$ ms and $\tau_t = 90$ ms, and a total period time $T = 10$ s is considered. The battery capacities are finite and identical for both SUs, $E_{1,\max} = E_{2,\max} = 3$ J. Further, each SU harvest energy independently according to the system described before, so that the $E_{j,i}$ varies uniformly from 19 mJ to 24 mJ. Results are averaged over 200 simulation runs.

Fig. 2.5 illustrates the total throughput of the cognitive network for different values of the primary user SNR. Both, the optimal and suboptimal power allocation policies, always perform better than the benchmark and the priority algorithm for a given fusion rule. By far, the worst performance corresponds to the priority approach, independently of the fusion rule. Optimal and suboptimal approaches obtain almost a similar performance. For SNR values larger than -7 dB, the performance of the optimal algorithm for the AND and OR rule is identical, and differences with their corresponding suboptimal algorithm are minimal. For lower SNR values, the OR rule performs slight better than the AND rule, and there are no differences between the optimal and suboptimal algorithms. Also, remark that differences between optimal and suboptimal algorithms reduces with regard to the random power allocation approach for low SNR values.

Fig. 2.6 shows the allocated transmission power to both SUs when the $SNR = 0$ dB for the AND and OR rules. Although the random power allocation algorithm sometimes assigns a higher transmission power, the optimal and suboptimal algorithms using a lower transmission power achieve a better performance, as the total throughput also depends on the detection threshold. Further, it can be confirmed that the priority approach only assigns transmission power to one of the users.

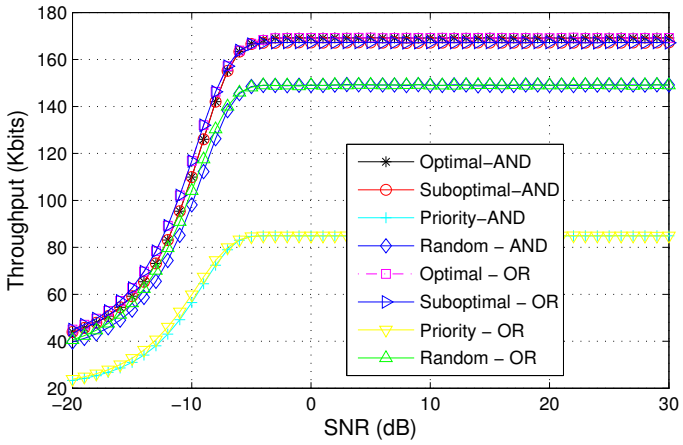

Figure 2.5: Throughput of the SUs versus the SNR of the PU.

2.2.3.1 Severe change in the energy harvesting rate

In the previous scenario, energy was harvested from a single source (solar panels). In practice, different energy sources can be combined in the device (e.g., solar, wind, vibrations [13]), so that the harvested energy (and consequently, the harvesting rate) may vary severely. This is the scenario considered in this subsection. To that aim, we consider that the harvested energy at each time instant, $E_{j,i}$, varies between [0,100] mJ. The other parameters remain the same as in the previous scenario.

Fig. 2.7 depicts the SU throughput for different values of SNR. Given a fusion rule, the optimal and suboptimal algorithms also outperform the benchmark and the priority algorithm. As it was expected, the worst performance corresponds to the priority approach. For SNR values larger than -5 dB and independently of the fusion rule, the optimal approach improves slightly the suboptimal one. Remark that there is a significant difference between the performance achieved by the AND rule and that achieved by the OR rule. If the SNR decreases, differences in performance between the algorithms following both fusion rules tend to reduce, although the algorithms under the AND rule perform still better. As it happened in the previous scenario, under low SNR scenarios, there is no difference between the optimal and suboptimal algorithms. Note also that an increase in the throughput is observed compared to the previous scenario since the harvested energy may be greater. Fig. 2.8 shows the allocated transmission power to both SUs when the $SNR = 0$ dB and under the AND fusion rule. In this case, there are no huge differences in the manner of (sub) optimal policies assigning the transmission power to the users.

2.2.3.2 Different channel environments

Next, the optimal power allocation under different channel environments is analyzed.

- *Asymmetric channel gains*
  In this first setup, we assume that the channel gain for the first SU is larger than for the second SU, while the interference coefficients are the same for both users. Specifically,

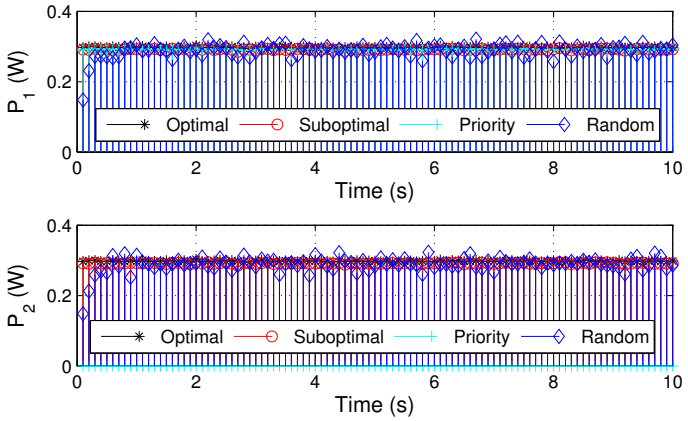

(a)

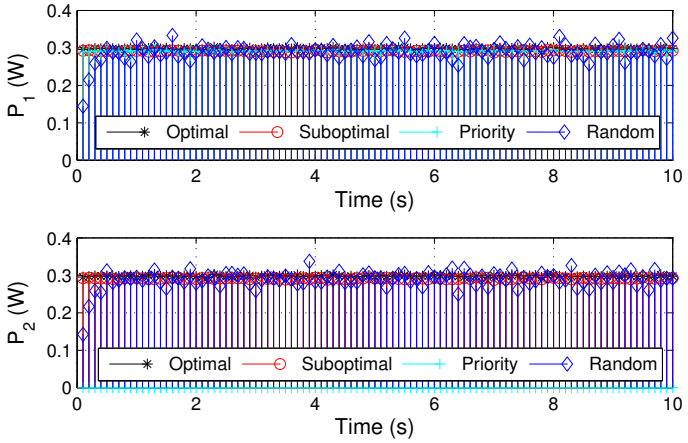

(b)

Figure 2.6: Allocated transmission power to the SUs for all the algorithms for SNR=0 dB using (a) AND, and (b) OR fusion rule.

$h_{11} = 0$ dB, $h_{22} = -20$ dB, $h_{12} = \ h_{21} = -20$ dB. The remaining parameters are the same as in the initial scenario.

Regarding the throughput (see Fig. 2.9), the optimal and suboptimal algorithms perform evenly for both fusion rules. In this case, the worst behavior corresponds to the random approach. This can be explained by looking at the transmission power allocation under the AND rule in Fig. 2.10. The optimal and suboptimal policies allocate all the transmission power to the first SU because the channel gain is larger. However, the random policy still assigns power to both users, which is not efficient. Remind that assigning a high transmission power to SUs is not enough to maximize the total throughput since the detection threshold should be jointly optimized with the transmission powers. Further, the optimal approach becomes the priority one, since all the transmission power is assigned to the user with the best channel gain.

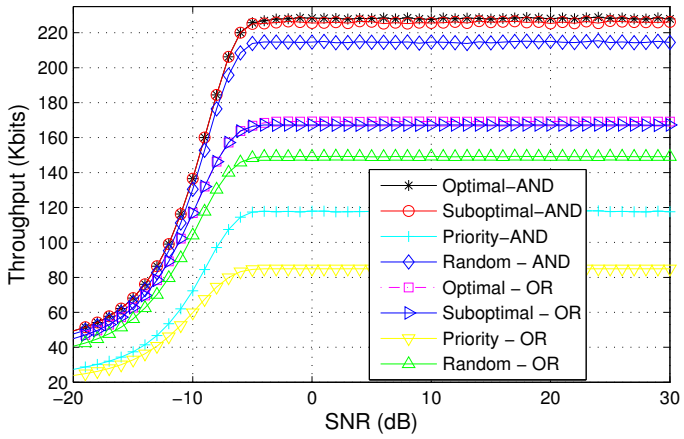

Figure 2.7: Throughput of the SUs versus the SNR of the PU under severe changes in the energy harvested rate.

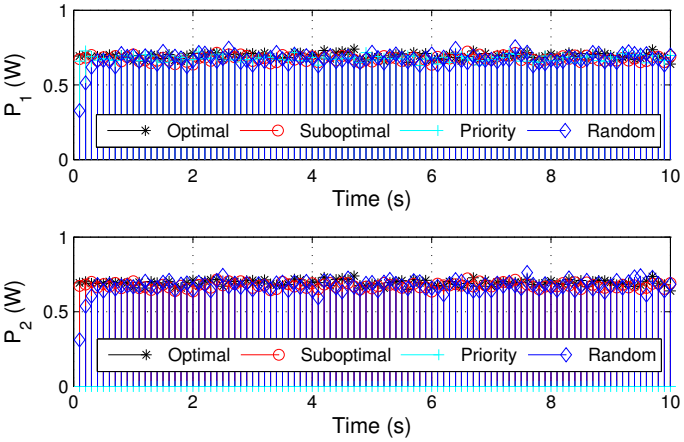

Figure 2.8: Allocated transmission power to the SUs for all the algorithms when SNR=0 dB under severe changes in the energy harvested rate under the AND fusion rule.

- *Asymmetric interference channel*
  In the second case, channel gains are the same for both SUs; but the interference coefficients differ: $h_{11} = h_{22} = -10$ dB, $h_{12} = -15$ dB, $h_{21} = -5$ dB for $i = 1, 2, \cdots, N$.

  In Fig. 2.11, where the throughput versus the SNR is depicted, the better performance of the optimal and suboptimal algorithms with regard to the benchmark and the priority algorithms is clearly observed. Even the priority approach works better than the random one. Besides, for low SNR values, the OR rule gets a slightly better performance than the AND rule, while their behavior is identical for high SNR values. Differences between the optimal and suboptimal algorithms are negligible. On the other hand, the (sub) optimal transmission power allocation, which is shown in Fig. 2.12 for the AND rule, follows a TDMA scheme as all the available transmission power is allocated alternatively to only one user at every time slot. The priority and the random policies

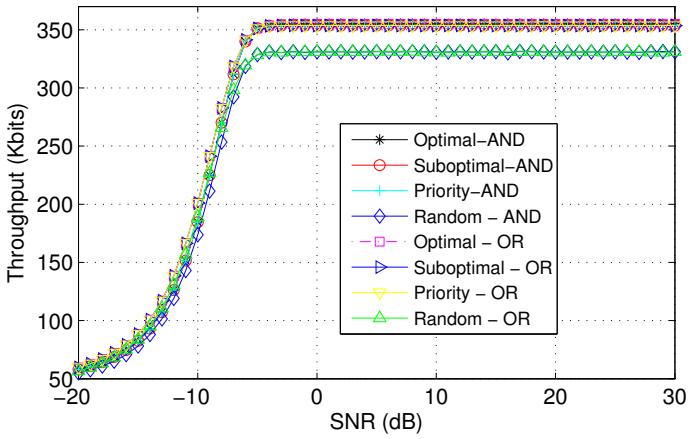

Figure 2.9: Throughput of the SUs versus the SNR of the PU for asymmetric channel gains.

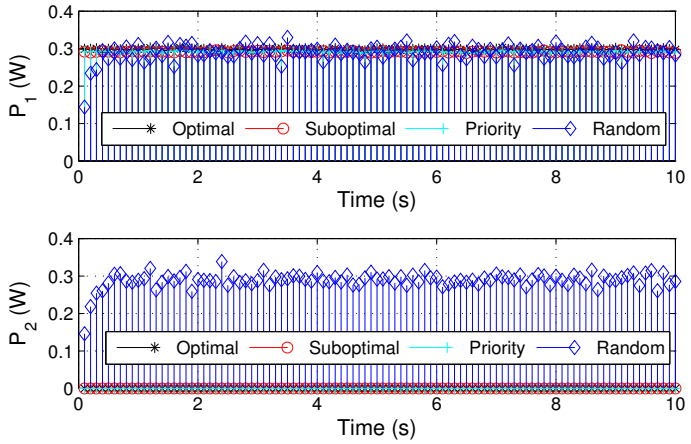

Figure 2.10: Allocated transmission power to the SUs for all the algorithms for asymmetric channel gains when SNR=0 dB under the AND fusion rule.

allocate power to one or both SUs, respectively, at every time slot. In both cases, the allocated power is approximately half of the transmission power assigned to the optimal and suboptimal approaches.

- *Strong symmetric interference channel*
  Finally, we consider a scenario with a strong interference, where the interference coefficients are even greater than the channel gain coefficients, i.e., $h_{11} = h_{22} = -10$ dB, $h_{12} = h_{21} = 0$ dB.

  In this scenario, performance results are similar to those that were obtained in the previous scenario, except for the benchmark algorithm. The total throughput achieved by the random power allocation policy is close to zero (see Fig. 2.13), while the allocated transmission powers (see Fig. 2.14) follow a similar trend to that observed in the previous scenario. Analyzing the similarities between both scenarios, at least one of the

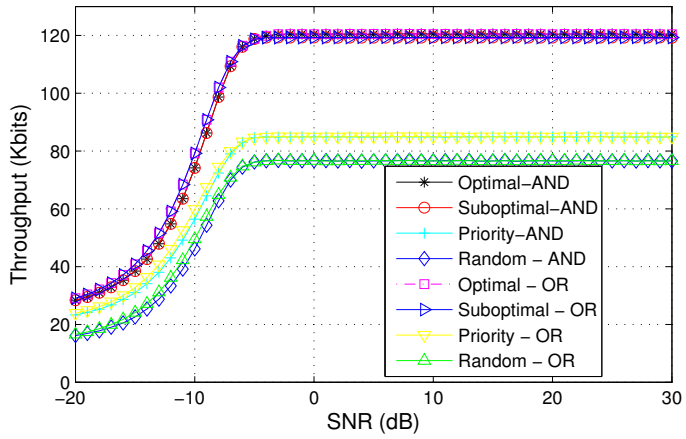

Figure 2.11: Throughput of the SUs versus the SNR of the PU for asymmetric interference coefficients.

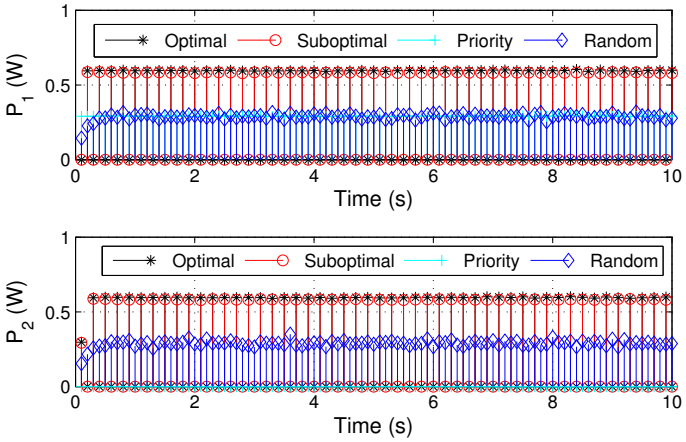

Figure 2.12: Allocated transmitted power to the SUs for all the algorithms for asymmetric interference coefficients when SNR=0 dB under the AND fusion rule.

interference coefficients is larger than the channel gain. Hence, under these channel conditions, the advantage of using the optimal or suboptimal schemes is remarkable.

2.2.3.3 Influence of other parameters

In this subsection, the influence of other parameters over the proposed algorithms, such as the sensing time τ_s, or the probability of the PU being absent in the spectrum π_0, is explored.

- *Influence of the sensing time*
  In this scenario, the sensing time τ_s varies from 0.1 ms to 100 ms with step size 0.1 ms. Remind that 100 ms is the duration of the time slot τ. Fig. 2.15 illustrates the throughput for two different values of the SNR: -10 dB and 0 dB under the AND and OR fusion rules. The other parameters remain the same as those set in the initial scenario.

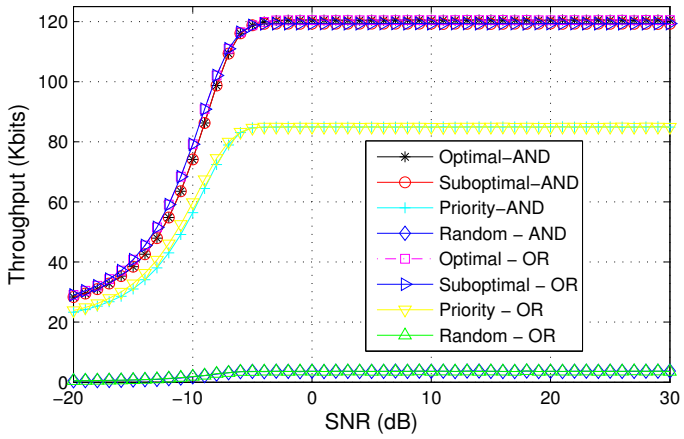

Figure 2.13: Throughput of the SUs versus the SNR of the PU for a strong symmetric interference channel.

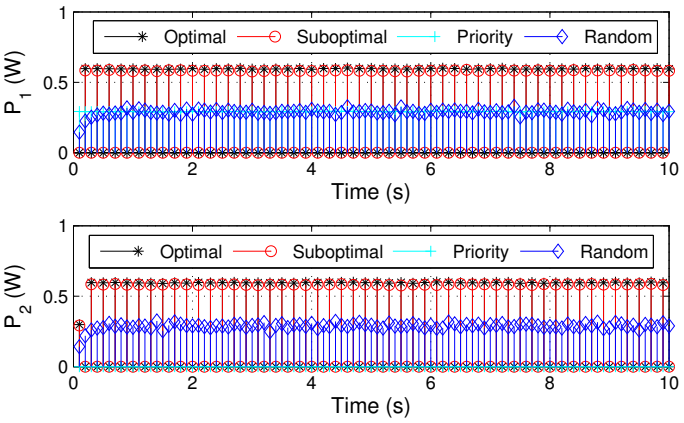

Figure 2.14: Allocated transmitted power to the SUs for the all the algorithms for a strong symmetric interference channel when SNR=0 dB under the AND fusion rule.

It can be observed that the throughput curve varies with the sensing time τ_s as a concave function. For this reason, the performance of the optimal algorithm could be improved if the sensing time is included as a parameter to be optimized (so the optimal τ_s that maximizes the throughput is taken into account). Further, as the optimal τ_s depends on the SNR value, it would be necessary to measure or estimate the SNR at the SU at every time slot in order to always consider the optimal value.

- *Influence of the probability of idle spectrum*

Finally, the influence of the probability of idle spectrum (i.e., the probability that the PU is absent) over the throughput is analyzed. To that aim, π_0 varies from 0 to 1 with step size 0.05, and results are explored for two values of the SNR: -10 dB, and 0 dB for the AND and OR fusion rules (see Fig. 2.16).

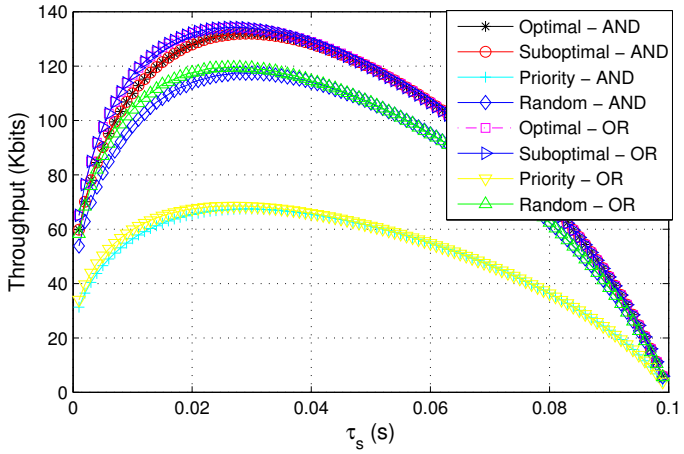

(a)

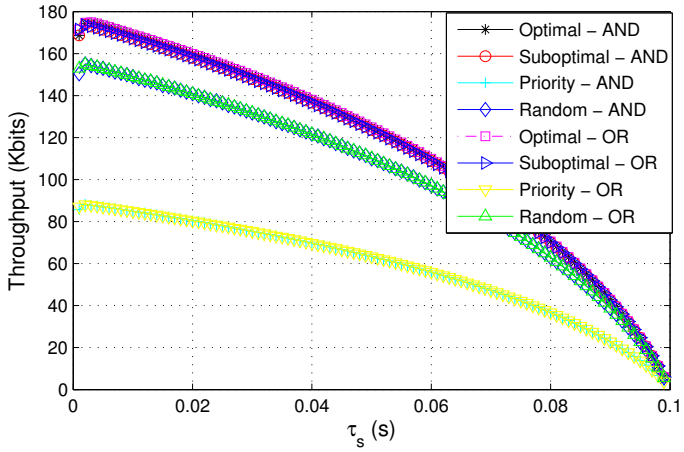

(b)

Figure 2.15: Influence of the sensing time τ_s over the throughput for (a) SNR= -10 dB, and (b) SNR= 0 dB.

As expected, the higher the probability of the PU being absent is, the larger the throughput is, since the SUs can take advantage of the free spectrum and transmit data. Also, and depending on the SNR value and the fusion strategy, results differ. For instance, for low SNR (Fig. 2.16(a)), the OR fusion rule performs slightly better than the AND rule, while differences tend to disappear when the SNR increases (Fig. 2.16(b)). In the last case, the performance of the optimal and suboptimal algorithms converge when $\pi_0 = 1$, while for a lower SNR value, the performance of both is the same even for low values of π_0.

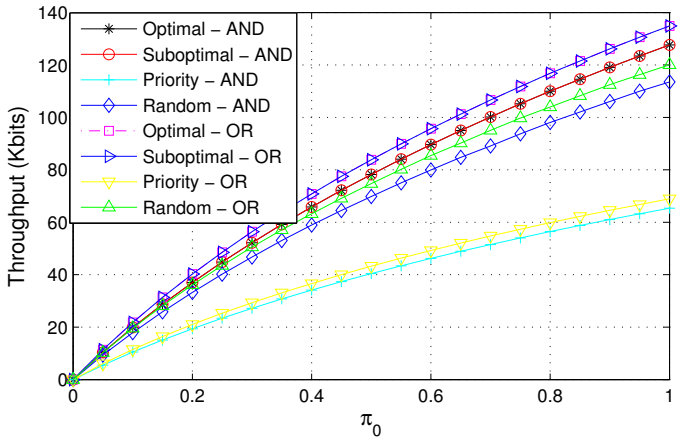

(a)

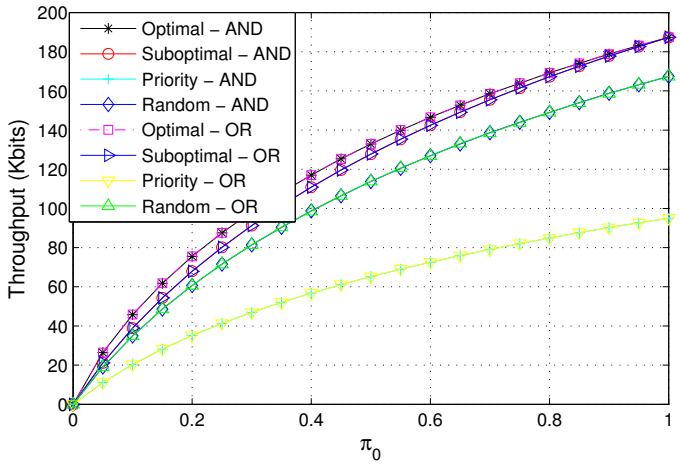

(b)

Figure 2.16: Influence of π_0 over the throughput for (a) SNR= -10 dB, and (b) SNR= 0 dB.

2.3 Optimal power allocation for a multi-frequency-band scenario

In this section we consider a two-user multi-band cognitive radio network, i.e., the two SUs want to gain opportunistic access to a wide-band spectrum consists of 2 sub-bands that is licensed to the PU. The same system model presented before is also considered here. However, some details need to be specified. Each cognitive radio employs a multi-band energy detector to look for empty bands in the spectrum. We only consider a scenario where at most two available bands are accessed at the same time. Two spectrum access strategies are analyzed and compared. a) In the first case, the empty channels are assigned so as to each cognitive radio can access at most one band at each time instant. This way, in case more than two channels are deemed to be empty at a specific time instant, the two best channels in terms of gain are assigned individually to the SUs. Therefore, each SU can access the spectrum with no cross channel interference from the other user. Further, in case that at a

specific time instant, only one channel is deemed to be empty, the channel is assigned to the SU with the best channel gain, and if the channel gains are identical, the channel is assigned with equal probability to one of the SUs. b) In the second case, both SUs share the empty bands, so channel interference should be taken into account. This context is similar to the single-frequency band scenario described in Section 2.2. We also assume that the SUs can adapt their transmission bandwidth according to the bandwidth of the available channels. Therefore, the available bandwidth can be different for each SU. However, as shall be shown later, such a bandwidth difference has no effect on the proposed optimal algorithm. Note that although the channel is frequency-selective between the PU and SUs in such a multi-band scenario, for mathematical simplicity, we assume that both SUs experience the same SNR from the PU in each band. However, the extension of the proposed method to a more general one that considers different SNRs is straightforward.

2.3.1 Optimal power allocation in a multi-band non-sharing frequency bands scenario

In this first scenario, we consider a multi-band case where each cognitive user is assigned to at most one band that is deemed to be empty. As in the previous scenario, we aim at jointly allocating the transmission powers and setting the detection thresholds in order to maximize the total throughput of the cognitive network. To properly formulate the problem, the objective function, the variables to be optimized and the constraints to be satisfied need to be identified. The optimization variables and the constraints are the same as in the single-frequency band scenario: ε_i and $P_{j,i}$ for $j \in \{1,2\}$ and $i = 1, 2, ...N$ as optimization variables, and conditions (2.10)- (2.12) are the constraints. Denoting W_j as the spectrum bandwidth accessed by SU j, and $C_{j,i}$ as the channel capacity for user j at time slot i, the objective function to be optimized is the total throughput of the whole frequency band W, which is denoted as R_T^{wb},

$$R_T^{\text{wb}} = \sum_{i=1}^{N} \pi_0 \mathcal{P}\left(\mathcal{A}|\mathcal{H}_0, \varepsilon_i\right) \tau_t \left(W_1 C_{1,i}^{\text{wb}} + W_2 C_{2,i}^{\text{wb}}\right). \tag{2.24}$$

Since τ_t and π_0 are assumed to be constant, and $\mathcal{P}\left(\mathcal{A}|\mathcal{H}_0, \varepsilon_i\right) = 1 - Q_{\text{FA}}\left(\varepsilon_i\right)$, given by (2.7) and (2.5b) when the energy detector is considered, only the channel capacity needs to be specified.

As SUs do not interfere with each other (i.e., interference coefficients h_{12} and h_{21} are disregarded), and assuming that the noise received at both SUs is AWGN with variance $N_{0,j}$, the channel capacity $C_{j,i}$ at time slot i is given by

$$C_{j,i}^{\text{wb}} = W_j \log_2 \left(1 + \frac{|h_{jj}|^2 P_{j,i}}{N_{0,j}}\right). \tag{2.25}$$

In case only one SU accesses the spectrum at a specific time slot, then the channel gain corresponding to the non-transmittting SU shall be set to zero in (2.24)-(2.25) in that time slot.

Taking into account all the components for the optimization problem, the optimal detection threshold and transmission power allocation at each time slot is obtained by solving the following constrained maximization problem:

$$\begin{aligned} \underset{\varepsilon_i, P_{j,i}}{\text{maximize}} \quad & R_T^{\text{wb}} && \text{(2.26a)} \\ \text{subject to} \quad & P_{j,i} \geq 0 \quad j \in \{1,2\}, i = 1, 2, \cdots, N && \text{(2.26b)} \\ & \text{(2.10), (2.11), (2.12)} && \text{(2.26c)} \end{aligned}$$

Following a similar procedure to that exposed for the single-frequency band scenario, we initially assume that the detection threshold ε_i is known, and we aim at optimally allocating the user transmission powers by maximizing the term $\left(W_1 C_{1,i}^{\text{wb}} + W_2 C_{2,i}^{\text{wb}}\right)$. Thus, the power allocation problem can be stated as

$$\begin{aligned} \underset{P_{j,i}}{\text{maximize}} \quad & \sum_{i=1}^{N} \left(W_1 C_{1,i}^{\text{wb}} + W_2 C_{2,i}^{\text{wb}}\right) && \text{(2.27a)} \\ \text{subject to} \quad & P_{j,i} \geq 0 \quad j \in \{1,2\}, i = 1, 2, \cdots, N && \text{(2.27b)} \\ & \text{(2.11), (2.12)} && \text{(2.27c)} \end{aligned}$$

Considering the fact that the SUs have independent energy budget and harvesting processes, and the channel capacity is completely independent from the other SU transmission power, power allocation can be performed independently at each SU. Therefore, the optimization problem (2.27) for a given ε_i at time slot i can be reduced to

$$\begin{aligned} \underset{P_{j,i}}{\text{maximize}} \quad & \log_2\left(1 + \frac{|h_{jj}|^2 P_{j,i}}{N_{0,j}}\right) && \text{(2.28a)} \\ \text{subject to} \quad & P_{j,i} \geq 0 \quad j \in \{1,2\}, i = 1, 2, \cdots, N && \text{(2.28b)} \\ & \text{(2.11), (2.12)} && \text{(2.28c)} \end{aligned}$$

The objective function in problem (2.28) is concave in its domain and the constraints are convex [59]. Therefore, the optimization problem in (2.28) is a convex one and has a unique optimal solution. We solve the problem using the Lagrange dual function. Let $\eta_i \geq 0$, $\lambda_i \geq 0$, and $\mu_i \geq 0$ denote the Lagrange multipliers associated with the constraints in (2.28b), (2.11), (2.12), respectively. The Lagrangian function of problem (2.28) is

$$\begin{aligned} \mathcal{L}_{j,i} = \log_2\left(1 + \frac{|h_{jj,i}|^2 P_{j,i}}{N_{0,j}}\right) + \eta_i P_{j,i} - \lambda_i \left(-\sum_{k=1}^{i} E_{j,k} + \sum_{k=1}^{i} \mathcal{P}\left(\mathcal{A}|\varepsilon_k\right) P_{j,k}\tau_t + i P_{\text{s}}\tau_s\right) \\ - \mu_i \left(\sum_{k=1}^{i+1} E_{j,k} - \sum_{k=1}^{i} \mathcal{P}\left(\mathcal{A}|\varepsilon_k\right) P_{j,k}\tau_t - i P_{\text{s}}\tau_s - E_{j,\max}\right). \end{aligned} \quad \text{(2.29)}$$

And the complementary slackness conditions are

$$\lambda_i \left(-\sum_{k=1}^{i} E_{j,k} + \sum_{k=1}^{i} \mathcal{P}\left(\mathcal{A}|\varepsilon_k\right) P_{j,k}\tau_t + iP_{\mathrm{s}}\tau_s \right) = 0 \tag{2.30a}$$

$$\mu_i \left(\sum_{k=1}^{i+1} E_{j,k} - \sum_{k=1}^{i} \mathcal{P}\left(\mathcal{A}|\varepsilon_k\right) P_{j,k}\tau_t - iP_{\mathrm{s}}\tau_s - E_{j,\max} \right) = 0 \tag{2.30b}$$

$$\eta_i P_{j,i} = 0. \tag{2.30c}$$

Noting that we are willing to assign transmission powers to the users, i.e., $P_{j,i} > 0$, $\eta_i = 0$ to make (2.30c) hold. Applying the Karush-Kuhn-Tucker (KKT) conditions to the Lagrangian function (2.29), the optimal transmission powers ${P_{j,i}}^*$ must satisfy the following conditions

$$\nabla \mathcal{L}_{j,i}\left({P_{j,i}}^*\right) = \frac{1}{\ln 2\left(N_{j,i} + {P_{j,i}}^*\right)} - \lambda_i \mathcal{P}\left(\mathcal{A}|\varepsilon_i\right)\tau_t + \mu_i \mathcal{P}\left(\mathcal{A}|\varepsilon_i\right)\tau_t = 0; \tag{2.31a}$$

$$-\sum_{k=1}^{i} E_{j,k} + \sum_{k=1}^{i} \mathcal{P}\left(\mathcal{A}|\varepsilon_k\right) P_{j,k}\tau_t + iP_{\mathrm{s}}\tau_s \leq 0 \tag{2.31b}$$

$$\sum_{k=1}^{i+1} E_{j,k} - \sum_{k=1}^{i} \mathcal{P}\left(\mathcal{A}|\varepsilon_k\right) P_{j,k}\tau_t - iP_{\mathrm{s}}\tau_s - E_{j,\max} \leq 0 \tag{2.31c}$$

$$P_{j,i} > 0, \tag{2.31d}$$

where $N_j = \frac{N_{0,j}}{|h_{jj}|^2}$ is the normalized background noise power.

From (2.31a), the optimal transmission power is given by

$$P_{j,i}^* = \left(V_{j,i} - N_{j,i}\right)^+, \tag{2.32}$$

where $V_{j,i} = \frac{1}{\ln 2\mathcal{P}(\mathcal{A}|\varepsilon_i)\tau_t(\lambda_i - \mu_i)}$. Note that the optimal policy to assign the transmission power is a time-dynamic water-filling strategy where $V_{j,i}$ represents the power water level at time slot i for SU j.

Considering the slackness conditions (2.30a) and (2.30b), and in oder to $V_{j,i}$ have physical meaning (i.e., $\lambda_i > \mu_i$ so that the power water level $V_{j,i}$ is positive), the optimal transmission power solution only exists in the following two cases:

- a) $\lambda_i > 0$ and $\mu_i = 0$
  As $\mu_i = 0$, the term that is multiplying μ_i in (2.30b) is different from zero, so KKT condition (2.31c) is strictly lower than 0, which means that the battery capacity is large enough. Given that $\lambda_i > 0$, the term $\left(\sum_{k=1}^{i} \mathcal{P}\left(\mathcal{A}|\varepsilon_k\right) P_{j,k}\tau_t + iP_{\mathrm{s}}\tau_s - \sum_{k=1}^{i} E_{j,k}\right)$ should be zero in order to satisfy slackness condition (2.30a). Thus, the optimal transmission power is

  $$P_{j,i} = U_{j,i}, \tag{2.33}$$

  where $U_{j,i} = \frac{\sum_{k=1}^{i} E_{j,k} - \sum_{k=1}^{i-1} \mathcal{P}(\mathcal{A}|\varepsilon_k) P_{j,k}\tau_t - iP_s\tau_s}{\mathcal{P}(\mathcal{A}|\varepsilon_i)\tau_t}$. Note that $U_{j,i}$ has the same expression that the upper bound found in constraint (2.19c) in Section 2.2.2.

- b) $\lambda_i > \mu_i > 0$

  If both Lagrange multipliers, μ_i and λ_i, are positive, then λ_i should be larger than μ_i to have (2.32) feasible meaning. To make slackness conditions (2.30a) and (2.30b) hold, the equality $\sum_{k=1}^{i} \mathcal{P}\left(\mathcal{A}|\varepsilon_k\right) P_{j,k}\tau_t + iP_{\mathrm{s}}\tau_s - \sum_{k=1}^{i} E_{j,k} = \sum_{k=1}^{i} \mathcal{P}\left(\mathcal{A}|\varepsilon_k\right) P_{j,k}\tau_t + iP_{\mathrm{s}}\tau_s + E_{j,\max} - \sum_{k=1}^{i+1} E_{j,k} = 0$ should be satisfied. This implies that $E_{j,\max} = E_{j,i+1}$, i.e., the energy harvested at time slot $i+1$ should be equal to the maximum battery capacity. In this case, the optimal transmission power can be also calculated using (2.33).

In case that (2.31b) does not hold (i.e., $U_{j,i} < 0$), $\mathcal{P}\left(\mathcal{A}\right)$ should be decreased by choosing a lower ε_i. Also, the harvested energy should not be larger than the battery capacity, as it happened for the single-frequency band case.

Following the same procedure, the next step consists of performing the optimization of the detection threshold ε_i. As it was mentioned in Section 2.2.2.1, $\mathcal{P}(\mathcal{A})$ and $\mathcal{P}(\mathcal{A}|\mathcal{H}_0)$ both increase with the increase of ε_i, but the optimal transmitting power $U_{j,i}^{+}$ (2.33) decreases as well as the total throughput. The same trade-off between maximizing $\mathcal{P}\left(\mathcal{A}|\mathcal{H}_0, \varepsilon_i\right)$ and $C_{j,i}^{\mathrm{wb}}$ appears. Again, we solve the problem by performing a bounded exhaustive search over the parameter ε_i, so that the optimal value ε_i^* corresponds to the one that maximizes the throughput for the optimal $P_{j,i}$ obtained after solving (2.28).

The related algorithm is summarized in Algorithm 4.

Algorithm 4 Optimal power allocation and detection threshold for a multi-band non-sharing frequencies scenario

Require: $E_{j,\max} \geq E_{j,i}$, for $j = 1, 2$ and $i = 1, 2, \cdots, N$

Initialize $Q_{\mathrm{D},0} = \alpha$; $Q_{\mathrm{D},\max} = 0.99$

for $p = 1, 2, \cdots, P$; $P = \frac{Q_{\mathrm{D},\max} - \alpha}{\Delta Q_{\mathrm{D}}}$ **do**

  $Q_{\mathrm{D},p} = Q_{\mathrm{D},0} + (p-1)\,\Delta Q_{\mathrm{D}}$

  for $i = 1$ to N **do**

    $\varepsilon_i \leftarrow \varepsilon_0$, $\varepsilon_0 = Q_{\mathrm{D},p}^{-1}$

    For $j = 1, 2$ do

    $U_{j,i} \leftarrow \frac{\sum_{k=1}^{i} E_{j,k} - \sum_{k=1}^{i-1} \mathcal{P}(\mathcal{A}|\varepsilon_i) P_{j,k}\tau_t - iP_{\mathrm{s}}\tau_s}{\mathcal{P}(\mathcal{A}|\varepsilon_i)\tau_i}$

    if $U_{j,i} \geq 0$ **then**

      $P_{j,i,p} = U_{j,i}$

    else

      $P_{j,i,p} = 0$

    end if

  end for

  $\left\{P_{1,p}, P_{2,p}\right\} = \begin{Bmatrix} P_{1,1,p} & P_{2,1,p} \\ P_{1,2,p} & P_{2,2,p} \\ \cdots & \cdots \\ P_{1,N,p} & P_{2,N,p} \end{Bmatrix}$

end for

Choose $\left\{P_1, P_2\right\} = \arg\max R_T$, $\left\{P_1, P_2\right\} \in \left\{P_{1,p}, P_{2,p}\right\}$.

2.3.1.1 Simulation results

In order to test the performance of the proposed algorithm, a simple experiment is carried out in a multi-band scenario. The total bandwidth is set to 12 KHz, which is divided into

two subchannels of bandwidth 6 KHz. The sampling frequency is 24 KHz. The remaining parameters are the same as the ones exposed initially in Section 2.2.3. For comparison purposes, the random algorithm is considered.

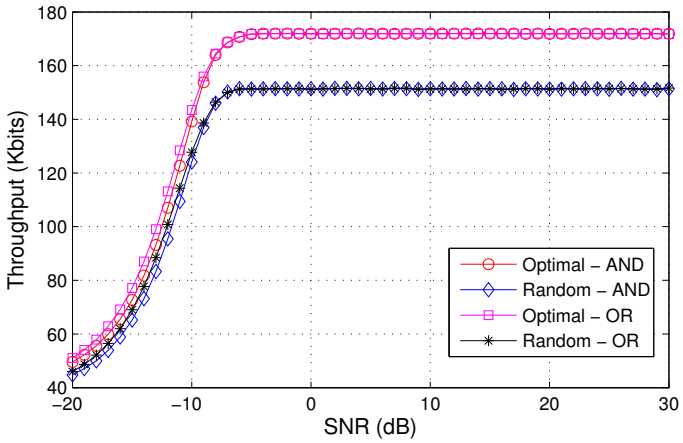

Figure 2.17: Throughput of the SUs versus the SNR of the PU in a multi-band non-sharing frequencies scenario.

Fig. 2.17 shows the SU throughput for different values of the SNR. It shows that the optimal power allocation policy outperforms the random one. For high SNR values, both fusion rules behave identically; however, for SNR values lower than -9 dB, again we observe a slightly better performance when the OR fusion rule is applied. Fig. 2.18 depicts the allocated power to both SUs when the $SNR = 0$ dB. As it was previously observed for the single-frequency band scenario, although the random power allocation algorithm sometimes assigns a higher transmission power, the optimal scheme achieves better performance given that it should be jointly optimized with the detection threshold.

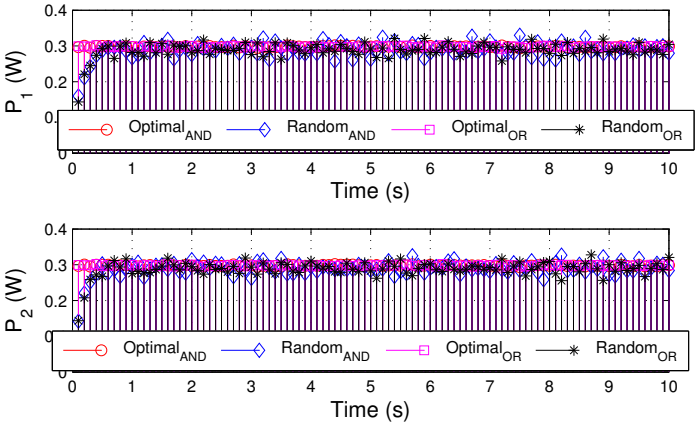

Figure 2.18: Allocated transmission power to the SUs for SNR=0 dB under both fusion rules in a multi-band non-sharing frequencies scenario.

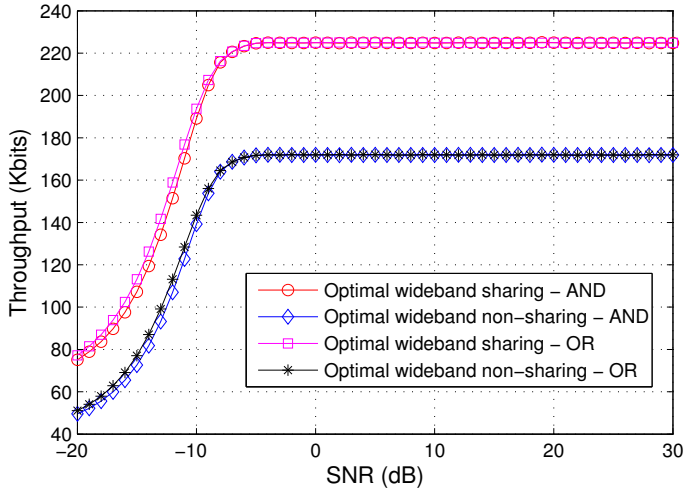

Figure 2.19: Throughput of the SUs versus the SNR of the PU for the two multi-band power allocation strategies and fusion rules in a weak interference environment.

2.3.2 Optimal power allocation in a multi-band sharing frequency bands scenario

In the second scenario, the two SUs share the empty bands, allocating the same transmission power to each band. As empty bands are shared, interference between SUs cannot be ignored. Clearly, this scenario is similar to the one exposed in Section 2.2, so the optimal power allocation and detection threshold detailed in Algorithm 1 can be applied to each empty band of the multi-band scenario.

Finally, we analyze and compare the performance of the sharing and non-sharing frequency band schemes in a multi-band scenario under different channel environments. First, a weak interference scenario is considered. The channel coefficients are set as follows: $h_{11} = h_{22} = -10$ dB and $h_{12} = h_{21} = -20$ dB. The remaining parameters are those detailed in Section 2.3.1.1.

Fig. 2.19 shows the total throughput for different values of the SNR and for the two strategies and fusion rules. It can be observed that the strategy where the SUs share all the frequency bands benefits significantly from a better use of the bandwidth usage and achieves a higher throughput. Not surprisingly, the use of the OR rule improves slightly the performance for SNR values lower than -10 dB. Over this value, both rules perform similar.

On the other hand, we consider a strong interference scenario, where coefficient values are set to $h_{11} = h_{22} = -10$ dB and $h_{12} = h_{21} = 0$ dB (see Fig. 2.20). For this setup, there are no differences between the sharing and non-sharing strategies; and regarding different fusion rules, the results are very close. As it was highlighted in the single-frequency band scenario, the optimal transmission strategy applied to each band follows a TDMA scheme, assigning at every time slot all the transmission power to only one of the SUs.

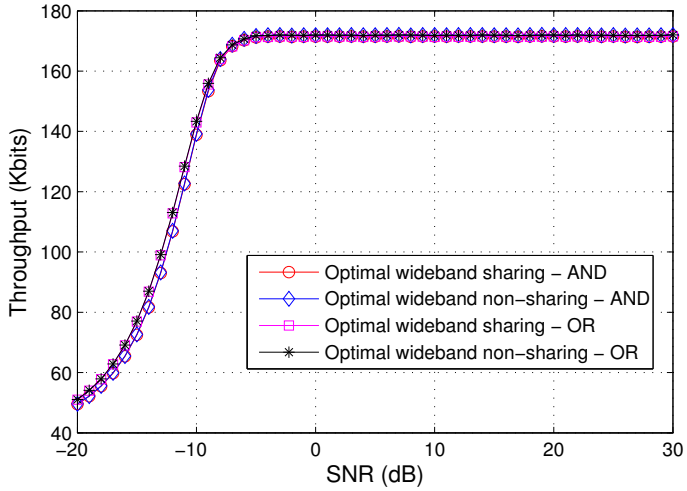

Figure 2.20: Throughput of the SUs versus the SNR of the PU for the two multi-band power allocation strategies and fusion rules in a strong interference environment.

2.4 Discussion about the overflow control constraint

In this section, we open a discussion about the necessity of the overflow control constraint. In practice, we can never have an ideal battery with infinite capacity. Thus, when the left space of the battery is not large enough to accommodate the incoming harvested energy, the excess of energy will be discarded.

In this thesis, we include the overflow control constraint based on the following two aspects.

a) From the channel capacity point of view, the overflow leads to energy inefficiency because the energy could have been consumed before the overflow situation happens in order to achieve a higher channel capacity. This idea has been summarized as a lemma and proved in [50]. This lemma has been applied to achieve the optimal power policies for energy-harvesting networks in [19, 49]. Besides, several works also try to avoid the energy overflow in order to find a optimal transmission strategy [51, 60, 61]. The authors of [60] have showed that the optimal scheduling algorithm should avoid energy overflow to get more system reward. And in [61], the authors designed an algorithm that speeds up the task execution (i.e., the data transmission rate) when overflow is predicted. Also, the work in [51] designs an offline optimal data transmission scheme in order to minimize the transmission time when the overflow constraint is considered.

b) From a practical point of view, energy overflow is not desirable because the line voltage should be limited within certain boundaries [62]. When the peak overflow is too high, it may even destroy the system. To solve this problem, the energy-harvesting device can be shut down, the electrical energy can be converted to other energy source such as thermal energy, a larger storage can be considered or power allocation schemes to avoid overflow can be designed. On the one side, frequent starts and shut down are not desired in most of the energy-harvesting systems for saving reasons [63]. For example, the windmills do not have automatic shut off in case of overflow, and it would require the human intervention. In

order to let the energy-harvesting system operate in a continuous way, it is better to consider devices that can either convert the harvested electrical energy into another type of energy or provide larger storage space to devices. But the cost of implementing such functionalities is still left to be account and in some cases, it is even not possible. Therefore, the most efficient way to avoid the overflow is the use of power allocation schemes.

However, if we only consider the channel capacity, algorithms that avoid overflow may turn to be suboptimal in some scenarios, such as the strong interference environment. In an interference channel, with the increase of the transmission power of one user, the interference to other users increases. Thus the total channel capacity may decrease with the increase of user transmission power. When the battery is limited and the cross-channel gain is very strong, the energy overflow control constraint will force all users to exhaust the residual battery energy, which causes undesirable interference. In this case, the power allocation algorithms that consider the energy-overflow constraint may become sub-optimal approaches, so that the aforementioned lemma in [50] does not hold anymore.

Thus, the transmission power is only constrained by the energy causality constraint and the maximum battery capacity as follows

$$\mathcal{P}\left(\mathcal{A}\right) P_{j,i}\tau_t - P_{\mathrm{s}}\tau_s \leq \min\left(\sum_{k=1}^{i} E_{j,k} - \sum_{k=1}^{i-1} \mathcal{P}\left(\mathcal{A}\right) P_{j,k}\tau_t - \left(i-1\right) P_{\mathrm{s}}\tau_s, E_{j,\max},\right) \quad (2.34)$$

Equation (2.34) reflects that if the harvested energy at time slot i overflows, then the available energy is fixed to the maximum battery capacity $E_{j,max}$. Also, the energy expected spent should not excess the current energy of the battery.

In the following, we perform optimal power allocation in the value range bounded by constraint (2.34). Then, we apply the resulting optimal power allocation algorithm to a scenario where CRs have a very low maximum battery capacity (i.e., $E_{j,max} = 24\text{mJ} \approx E_{j,i}$) and we compare the results with those obtained by the optimal algorithm that considers the overflow control in two different channel environments: a) a weak interference environment, where $h_{11} = h_{22} = -10\text{dB}, h_{12} = h_{21} = -20\text{dB}$; b) a strong interference environment where $h_{11} = h_{22} = h_{12} = h_{21} = -10\text{dB}$. Fig. 2.21 shows how the throughput varies with the PU's SNR for algorithms allowing (and not) the overflow under AND and OR fusion rules. In the weak interference environment, both optimal approaches perform similarly. Even more, the performance of the random power allocation scheme considering the overflow control constraint approximate the optimal solutions. As expected, the random power allocation solution not considering overflow control constraint performs significantly worse than the other solutions. Fig. 2.22 shows the allocated power to SU_1 and SU_2 for the different power allocation schemes for both fusion rules. It can be observed that the transmission power level is much lower in the random power allocation scheme not considering overflow control constraint than in the other power allocation schemes. Therefore, for the weak interference channel scenario we may indicate that the energy overflow constraint (overflow not allowable) is a necessary constraint that should be satisfied.

In Fig. 2.23, we observe the throughput with regard to the SNR of PU in a strong interference environment for the same power allocation algorithms analyzed in the previous scenarios under the AND and OR fusion rules. It is observed that the optimal power allocation scheme not considering overflow control constraint outperforms the optimal power allocation scheme. When the SNR of PU is under about -10 dB, even the random power

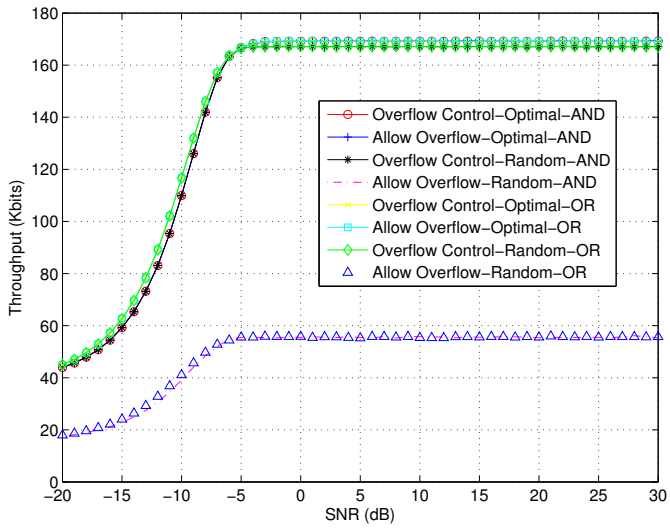

Figure 2.21: Throughput of the SUs versus the SNR of the PU for the power allocation strategies controlling overflow and allowing overflow in a weak interference environment with a very limited battery capacity, $E_{1,max} = E_{2,max} = 24$ mJ.

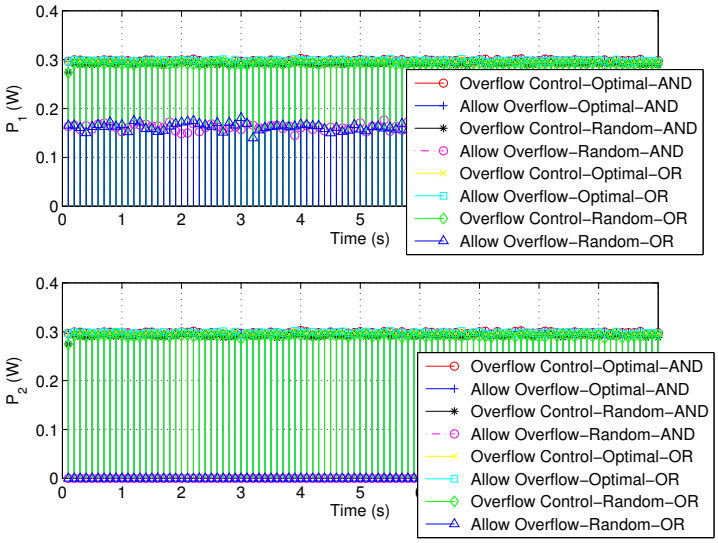

Figure 2.22: Allocated transmission power to the SUs for SNR=0 dB for the power allocation strategies controlling overflow and allowing overflow in a weak interference environment with a very limited battery capacity, $E_{1,max} = E_{2,max} = 24$ mJ.

allocation algorithm not considering overflow control constraint performs better than the two power allocation algorithms considering overflow control constraint. Checking Fig. 2.24, although less power allocated to SUs decreases in the optimal power allocation scheme allowing overflow, the throughput increases because less interference in total. While in the

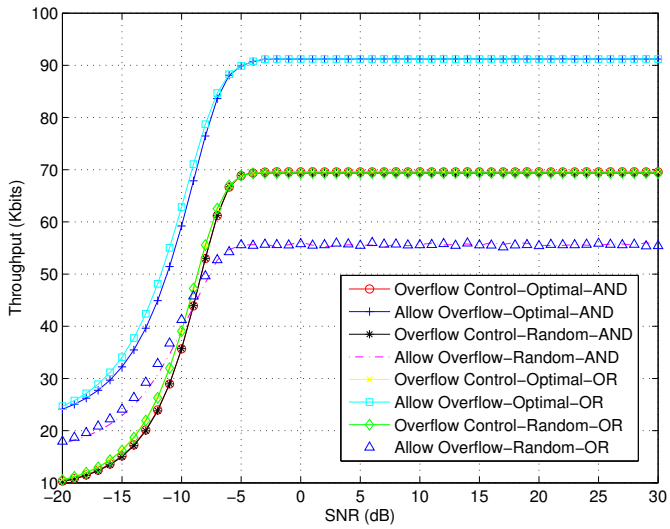

Figure 2.23: Throughput of the SUs versus the SNR of the PU for the power allocation strategies controlling overflow and allowing overflow in a strong interference environment with a very limited battery capacity, $E_{1,max} = E_{2,max} = 24$ mJ.

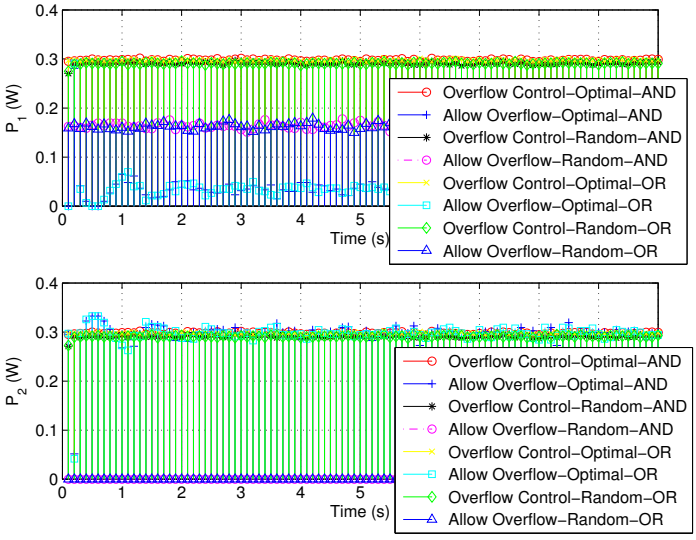

Figure 2.24: Allocated transmission power to the SUs for SNR=0 dB for the power allocation strategies controlling overflow and allowing overflow in a strong interference environment with a very limited battery capacity, $E_{1,max} = E_{2,max} = 24$ mJ.

power allocation schemes considering overflow control constraint, residual battery energy is forced to spend in order to avoid overflow, which will cause more interference resulting in the decrease of throughput. Recall the throughput versus SNR of PU in Fig. 2.13, where the interference is even stronger, but the throughput is even larger comparing with Fig. 2.23.

Fig. 2.14 shows that the optimal power allocation solution that considers the overflow control constraint avoid severe interference by applying a TDMA strategy when the battery capacity is large enough to store the current energy package to next time slot. And in this case, all the harvested energy can contribute to the system and also avoid too much interference. Therefore, we can intuitively indicate that energy overflow will cause the lost of throughput anyway. However, the overflow control constraint should not force the optimal solution degrading to a sub-optimal one. The best solution to solve this problem is to set the lowest bound for the battery capacity so that the overflow constraint won't degrade the optimal solution.

In this work and for simulation purposes, we consider a solar-energy harvesting CR network. In practice, the battery capacity is generally larger than the energy-harvesting rate according to the considered simulation environment. For that reason, the harvested energy would not originate energy overflow. Hence, the optimal power allocation scheme showed in this thesis is practically the optimal one.

Power allocation and detection threshold set for multiple-user energy-harvesting CR networks

3

The previous chapter introduced a joint design of a power allocation and detection threshold strategy for a sharing single-frequency band and a multi-band scenarios in two-user energy-harvesting cognitive radio networks. However, the main limitation of the previous approach is the number of cognitive radio users. Usually, cognitive networks are composed of multiple users. Hence, in this chapter we generalize the previous model to energy-harvesting cognitive radio networks composed of more than two users.

In this scenario, the cognitive radio network is composed of K secondary users that opportunistically use the frequency bands licensed to a PU, as it is shown in Fig. 3.1. Similar to the two-user scenario, the SUs first sense the spectrum and transmit their individual sensing results to the fusion center, which makes the final decision about the presence or absence of the PU according to a fusion rule. Due to the higher mathematical complexity of some fusion rules, such as the k out of N rule, we consider again the AND and OR fusion rules. Whenever the spectrum is deemed to be free, SUs can access the spectrum and transmit their data.

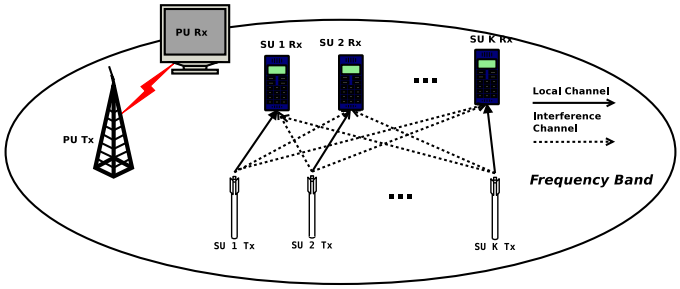

Figure 3.1: Multi-user cognitive radio network

Assuming finite and rechargeable batteries for SUs and a time-slotted operation model as in the previous chapter, the aim is to optimally allocate the transmission power corresponding to each secondary user and select the detection threshold taking into account the interference with the PU and the energy constraints (imposed by the use of energy-harvesting devices) while the network throughput is maximized. However, we should keep in mind that the increase of users will increase exponentially the computation complexity and the difficulty of power allocation [47].

Following the scheme of the previous chapter, the problem is analyzed in two scenarios: a) a single-frequency band case, and b) a multi-band case. In the first scenario, all cognitive users share the empty frequency band, so they will interfere with each other if no interference cancellation (IC) technique is used. On the other hand, in the multi-band case users can

access independently without interference to the different frequency bands of the spectrum.

3.1 Optimal power allocation for a single-frequency-band scenario

In the single-frequency band case, all SUs transmit their data when the spectrum is deemed to be free. Fig. 3.2 shows the channel model for a multi-user cognitive radio network, where h_{jk} $(j,k \in \{1,2,...,K\})$ are the channel coefficients: h_{jk} for $j = k$ are the channel gains and h_{jk} for $j \neq k$ are the interference coefficients between SU transmitter j and SU receiver k. As SUs share the same communication channel, interference between SUs should be considered.

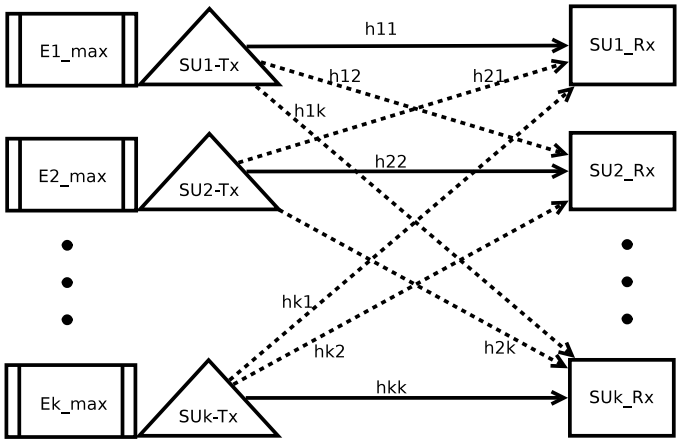

Figure 3.2: Channel model for a multi-user cognitive radio network

Denoting $P_{j,i}$ as the transmission power of SU j at time slot i, and $N_{0,j}$ as the AWGN channel noise for SU j, the channel capacity at time slot i, C_i, is given by

$$C_i = \sum_{j=1}^{K} W \log_2 \left(1 + \frac{|h_{jj}|^2 P_{j,i}}{N_{0,j} + \sum_{k \neq j}^{K} |h_{kj}|^2 P_{k,i}} \right), \tag{3.1}$$

where W is the empty spectrum bandwidth.

Following the same procedure as the one used for the two-user case, our goal is to maximize the network throughput during N time slots, which is defined as

$$R_T = \sum_{n=1}^{N} \pi_0 \mathcal{P}\left(\mathcal{A}|\mathcal{H}_0, \varepsilon_i\right) \tau_t C_i, \tag{3.2}$$

where π_0 is the probability that the PU is absent in the spectrum, τ_t is the transmission time in a time slot and $\mathcal{P}\left(\mathcal{A}|\mathcal{H}_0, \varepsilon_i\right)$ is the probability of accessing the spectrum under hypothesis $\mathcal{H}_0$ for a given detection threshold ε_i.

Note that since the probability of reaching a successful transmission is approximately 0 upon miss detection of the PU, the throughput due to miss detection is approximately zero and thus, it is not taken into account. Also, we include the QoS (2.10) and the power management conditions (2.11)(2.12) as constraints.

Thus, the optimal detection threshold and transmission power allocation at each time slot is obtained by solving the following constrained maximization problem:

$$\underset{\varepsilon_i, P_{j,i}}{\text{maximize}} \quad R_T \tag{3.3a}$$

$$\text{subject to} \quad P_{j,i} \geq 0 \quad j \in \left\{1, 2, ..., K\right\}, i = 1, 2, \cdots, N \tag{3.3b}$$

$$Q_{\mathrm{D}} \geq \alpha \tag{3.3c}$$

$$\sum_{k=1}^{i} E_{j,k} - \sum_{k=1}^{i} \mathcal{P}\left(\mathcal{A}\right) P_{j,k}\tau_t - iP_{\mathrm{s}}\tau_s \geq 0 \tag{3.3d}$$

$$\sum_{k=1}^{i+1} E_{j,k} - \sum_{k=1}^{i} \mathcal{P}\left(\mathcal{A}\right) P_{j,k}\tau_t - iP_{\mathrm{s}}\tau_s \leq E_{j,\max} \tag{3.3e}$$

3.1.1 Multi-user cognitive network with interference

In this setup, we try to solve the problem formulated in (3.3) using the Sequential Quadratic Programming (SQP) method. Again, a two-step strategy is implemented to solve the offline optimization problem. In the first step, the optimal transmission power is considered assuming that the detection threshold is given. Since the interference control constraint (3.3c) is not considered because it only affects the detection threshold, and taking into account that the terms π_0, $\mathcal{P}\left(\mathcal{A}|\mathcal{H}_0, \varepsilon_i\right)$, and τ_t in the throughput (3.2) are constant, the optimization problem is reduced to

$$\underset{P_{j,i}}{\text{maximize}} \quad \sum_{j=1}^{K} \log_2\left(1 + \frac{\left|h_{jj}\right|^2 P_{j,i}}{N_{0,j} + \sum_{k\neq j}^{K} \left|h_{kj}\right|^2 P_{k,i}}\right) \tag{3.4a}$$

$$\text{subject to} \quad P_{j,i} \leq U_{j,i}, \quad j \in \left\{1, 2, ..., K\right\}; i = 1, 2, \cdots, N \tag{3.4b}$$

$$P_{j,i} \geq L_{j,i}^{+} \tag{3.4c}$$

where $U_{j,i} = \frac{\sum_{k=1}^{i} E_{j,k} - \sum_{k=1}^{i-1} \mathcal{P}(\mathcal{A}|\varepsilon_k) P_{j,k}\tau_t - iP_{\mathrm{s}}\tau_s}{\mathcal{P}(\mathcal{A}|\varepsilon_i)\tau_t}$ and $L_{j,i} = \frac{\sum_{k=1}^{i+1} E_{j,k} - \sum_{k=1}^{i-1} \mathcal{P}(\mathcal{A}|\varepsilon_k) P_{j,k}\tau_t - iP_{\mathrm{s}}\tau_s - E_{j,\max}}{\mathcal{P}(\mathcal{A}|\varepsilon_i)\tau_t}$ are the upper and lower bounds for the transmission powers, respectively. Remark that (3.3b) is already included in (3.4c) since $L_{j,i}^{+} = \max\{L_{j,i}, 0\}$.

Let $\mathbf{p}_i = \begin{bmatrix} P_{1,i} & P_{2,i} & \cdots & P_{K,i} \end{bmatrix}^\top$ denote the transmission power vector, and $\mathbf{h}_j = \begin{bmatrix} \left|h_{1,j}\right|^2 & \left|h_{2,j}\right|^2 & \cdots & \left|h_{K,j}\right|^2 \end{bmatrix}^\top$ the channel coefficient vector associated to SU receiver j. Also, let $\mathbf{O}_j = \begin{bmatrix} 1 & 0 & \cdots & 0 & 0 & 0 & 0 \\ 0 & 1 & \cdots & 0 & 0 & 0 & 0 \\ \vdots & \vdots & \ddots & \vdots & \vdots & \vdots & \vdots \\ & & & 0_j & & & \\ & & & & 1 & & \\ \vdots & \vdots & & \vdots & & \ddots & \vdots \\ 0 & 0 & \cdots & 0 & \cdots & & 1 \end{bmatrix}$ be the $K \times K$ cancellation matrix, which cancels the local channel gain in order to compute the interference with other users. Thus, the previous optimization problem is expressed in matrix form as follows

$$\underset{\mathbf{p}_i}{\text{minimize}} \qquad f(\mathbf{p}_i) = -\sum_{j=1}^{K} \log_2 \frac{N_{0,j} + \mathbf{h}_j^{\top}\mathbf{p}_i}{N_{0,j} + \mathbf{h}_j{}^{\top}\mathbf{O}_j\mathbf{p}_i} \tag{3.5a}$$

$$\text{subject to} \qquad \mathbf{l}_i^{+} - \mathbf{p}_i \leq 0 \tag{3.5b}$$

$$\mathbf{p}_i - \mathbf{u}_i \leq 0, \tag{3.5c}$$

where $\mathbf{u}_i = \left[U_{1,i}\ U_{2,i}\ \cdots\ U_{K,i}\right]^{\top}$ and $\mathbf{l}_i^{+} = \left[L_{1,i}{}^{+}\ L_{2,i}{}^{+}\ \cdots\ L_{K,i}{}^{+}\right]^{\top}$.

3.1.1.1 SQP method

Given the non-linear objective function (3.5a), and the linear constraints (3.5b)(3.5c), we propose an algorithm based on the SQP method, which is effective for solving constrained optimization problems with smooth non-linear functions in both, the objective and constraint functions [69].

The basic idea of the SQP algorithm is to model the original optimization problem as a sub-quadratic problem and get our approximation solution. Then the solution of this sub-quadratic problem is used to construct a better approximation of the optimal value in the next iterate [70]. The standard formulation of the SQP algorithm is based on a equality constrained problem. First, let us introduce one nonnegative $2K \times 1$ slack variable vector, denoted by $\mathbf{z}$ ($\mathbf{z} \geq \mathbf{0}$), in order to convert the inequality constraints to equality constraints. Hence, the optimization problem can be formulated as

$$\underset{\mathbf{P}_i}{\text{minimize}} \qquad f(\mathbf{P}_i) \tag{3.6a}$$

$$\text{subject to} \qquad g(\mathbf{P}_i) + \mathbf{z} = \mathbf{0}, \tag{3.6b}$$

where $g(\mathbf{p}_i) = \begin{bmatrix}\mathbf{I}\\ -\mathbf{I}\end{bmatrix}\mathbf{p}_i - \begin{bmatrix}\mathbf{u}_i\\ -\mathbf{l}_i\end{bmatrix}$ ($\mathbf{I}$ is a $K \times K$ identity matrix), and $\mathbf{0}$ is $2K \times 1$ vector composed of zeros.

Being $\boldsymbol{\lambda}_i \geq \mathbf{0}$ ($2K \times 1$) the Lagrange multipliers associated with constraint in (3.6b), the Lagrangian function of problem (3.6) is

$$\mathcal{L}(\mathbf{p}_i, \boldsymbol{\lambda}_i) = f(\mathbf{p}_i) + \boldsymbol{\lambda}_i^{\top}\left(g(\mathbf{p}_i) - \mathbf{z}\right). \tag{3.7}$$

In this constrained optimization problem, , the local optimal solution $\mathbf{P}_i^*$ and the optimal multiplier vector $\boldsymbol{\lambda}_i^*$should satisfy the first order necessary condition that the gradient of (3.7) depending on $\mathbf{p}_i$ equals

$$\nabla\mathcal{L}(\mathbf{p}_i^*, \boldsymbol{\lambda}_i^*) = \mathbf{0} \tag{3.8}$$

We approximate the Lagrangian objective function at the optimal values $(\mathbf{P}_i^*, \boldsymbol{\lambda}_i^*)$. In order to construct a quadratic problem, we approximate the Lagrangian function by means of Taylor series, which at iteration n is given by

$$\begin{aligned}\mathcal{L}(\mathbf{p}_i^*, \boldsymbol{\lambda}_i^*) =& \mathcal{L}(\mathbf{p}_i^n, \boldsymbol{\lambda}_i^*) + \nabla\left(\mathcal{L}(\mathbf{p}_i^n, \boldsymbol{\lambda}_i^*)\right)(\mathbf{p}_i^* - \mathbf{p}_i^n)\\ &+ \frac{1}{2}(\mathbf{p}_i^* - \mathbf{p}_i^n)^{\top} H\left(\mathcal{L}(\mathbf{p}_i^n, \boldsymbol{\lambda}_i^*)\right)(\mathbf{p}_i^* - \mathbf{p}_i^n).\end{aligned} \tag{3.9}$$

The motivation to use this approximation for the Lagrangian as the objective function of optimization problem is due to the fact that it not only iterates to achieve the local minimum of (3.5a), but also includes the first order necessary condition (3.8) and the constraints (3.6b). It means that the resulting algorithm will have good local convergence property [71]. Following the same reasoning for the constraint (3.6b),

$$g\left(\mathbf{p}_i^n\right) + \nabla g\left(\mathbf{p}_i^n\right)\left(\mathbf{p}_i^* - \mathbf{p}_i^n\right) - \mathbf{z} = \mathbf{0}. \tag{3.10}$$

Then, the optimization problem is transferred to minimize (3.9) subject to (3.10).

Observing that $\mathcal{L}\left({\mathbf{P}_i}^n, \boldsymbol{\lambda}_i^*\right)$ is known at iteration n (3.9), we want to update the step size, denoted as $d\mathbf{P}_i$, from the present power vector $\mathbf{p}_i^n$ to the optimal power vector $\mathbf{P}_i^*$ (i.e. $d\mathbf{P}_i := {\mathbf{P}_i}^* - {\mathbf{P}_i}^n$).

Thus, we can formulate the quadratic programming (QP) subproblem at n iteration as

$$\underset{d\mathbf{p}_i}{\text{minimize}} \quad \nabla\left(\mathcal{L}\left(\mathbf{p}_i^n, \boldsymbol{\lambda}_i^*\right)\right) d\mathbf{p}_i + \frac{1}{2} {d\mathbf{p}_i}^\top H\mathcal{L}\left(\mathbf{p}_i^n, \boldsymbol{\lambda}_i^*\right) d\mathbf{p}_i \tag{3.11a}$$

$$\text{subject to} \quad g\left(\mathbf{p}_i^n\right) + \nabla g\left(\mathbf{p}_i^n\right) d\mathbf{p}_i + \mathbf{z} = \mathbf{0} \tag{3.11b}$$

Note that $\mathcal{L}\left(\mathbf{p}_i^n, \boldsymbol{\lambda}_i\right)$ is constant, the solution of $d\mathbf{p}_i$ can be used to generate a new iterate $\mathbf{p}_i^{n+1}$ by forward a step from $\mathbf{p}_i^n$ in the direction of $d\mathbf{p}_i$. As the first order necessary condition (3.8) should hold, we compute its expression for problem (3.11) with regard to variable $d\mathbf{p}_i$,

$$\begin{aligned} &\nabla\left(\mathcal{L}\left(\mathbf{p}_i^n, \boldsymbol{\lambda}_i^*\right)\right) + H\left(\mathcal{L}\left(\mathbf{p}_i^n, {\boldsymbol{\lambda}_i}^*\right)\right) d\mathbf{p}_i = \nabla f\left(\mathbf{p}_i^n\right) + \nabla g\left(\mathbf{p}_i^n\right)^\top \boldsymbol{\lambda}_i^* + H\mathcal{L}\left(\mathbf{p}_i^n, {\boldsymbol{\lambda}_i}^n\right) d\mathbf{p}_i = \mathbf{0} \\ &\Rightarrow \nabla f\left(\mathbf{p}_i^n\right) + \nabla g\left(\mathbf{p}_i^n\right)^\top \boldsymbol{\lambda}_i^n + \nabla g\left(\mathbf{p}_i^n\right)^\top \left(\boldsymbol{\lambda}_i^* - \boldsymbol{\lambda}_i^n\right) + H\mathcal{L}\left(\mathbf{p}_i^n, \boldsymbol{\lambda}_i^n\right) d\mathbf{p}_i = \mathbf{0} \end{aligned} \tag{3.12}$$

Thus, let us denote the step size for the Lagrange multiplier as $d\boldsymbol{\lambda}_i = \boldsymbol{\lambda}_i^* - \boldsymbol{\lambda}_i^n$. The first order KKT conditions for problem (3.11) are

$$\begin{bmatrix} H\mathcal{L}\left(\mathbf{p}_i^n, \boldsymbol{\lambda}_i^n\right) & \nabla g\left(\mathbf{p}_i^n\right)^\top \\ \nabla g\left(\mathbf{p}_i^n\right) & \mathbf{0}^{2K\times 2K} \end{bmatrix} \begin{bmatrix} d\mathbf{p}_i \\ d\boldsymbol{\lambda}_i \end{bmatrix} = \begin{bmatrix} -\nabla\mathcal{L}\left(\mathbf{p}_i^n, \boldsymbol{\lambda}_i^n\right) \\ -g\left(\mathbf{p}_i^n\right) - \mathbf{z} \end{bmatrix} \tag{3.13}$$

Based on (3.13), and in order to obtain a better approximation to the optimal value in the next iteration, new estimate for the multiplier are needed. We can update the step size vectors $(d\mathbf{p}_i, d\boldsymbol{\lambda}_i)$ as

$${\mathbf{p}_i}^{n+1} = {\mathbf{p}_i}^n + \alpha d\mathbf{p}_i \tag{3.14}$$

$${\boldsymbol{\lambda}_i}^{n+1} = {\boldsymbol{\lambda}_i}^n + \alpha d\boldsymbol{\lambda}_i, \tag{3.15}$$

for a step size parameter α.

Hereby, step length parameter α is introduced to ensure the convergence of the algorithm. We define the merit function $\boldsymbol{\phi}$ to measure the progress of the algorithm convergence as

$$\boldsymbol{\phi} = f\left(\mathbf{p}_i\right), \tag{3.16}$$

and for every iteration, if condition $\boldsymbol{\phi}\left({\mathbf{p}_i}^n + \alpha d\mathbf{p}_i\right) < \boldsymbol{\phi}\left({\mathbf{p}_i}^n\right)$ holds, then the algorithm converges. So that step size parameter α should be adjusted to satisfy the previous condition.

Besides, there is one slack variable variable $\mathbf{z}$ that needs to be determined. It can be noticed that the change of $\mathbf{z}$ only affects constraints (3.11b)

$$g\left(\mathbf{p}_i^n\right) + \nabla g\left(\mathbf{p}_i^n\right) d\mathbf{p}_i + \mathbf{z}^n + d\mathbf{z} = \mathbf{0}. \tag{3.17}$$

Noting that $\mathbf{z}$ is a nonnegative slack variable, we can derive step size for $\mathbf{z}$ from (3.17) and then update

$$\mathbf{z}^{n+1} = \max\left(\mathbf{z}^n + \alpha d\mathbf{z}, \mathbf{0}\right). \tag{3.18}$$

Moreover, to guarantee $\mathbf{P}_i^*$ to be an isolated local minimum of problem (3.6), the strong second order sufficient conditions should also be satisfied: a) the update matrix $\begin{bmatrix} H\mathcal{L}\left(\mathbf{p}_i^n, \boldsymbol{\lambda}_i^n\right) & \nabla g\left(\mathbf{p}_i^n\right)^\top \\ \nabla g\left(\mathbf{p}_i^n\right) & \mathbf{0}^{2K\times 2K} \end{bmatrix}$ (3.13) has full row rank; [70] b) the Hessian of Lagrangian function is positive definite on the tangent space of the constraint [71], i.e.,

$$\mathbf{d}^\top H\mathcal{L}\mathbf{d} > 0, \text{ for all } \mathbf{d} \neq \mathbf{0} \text{ such that } g\left(\mathbf{p}_i\right)^\top \mathbf{d} = \mathbf{0}. \tag{3.19}$$

We compute the Jacobian and Hessian of the Lagrange function (3.7) to check whether the strong second order sufficient condition is satisfied. From the expression of $f\left(\mathbf{P}_i\right)$ in (3.5a), we derive the Jacobian

$$\begin{aligned} \nabla f\left(\mathbf{p}_i\right) &= \sum_{j=1}^{K} \nabla\left[-\log_2\left(N_{0,j} + \mathbf{h}_j{}^\top \mathbf{p}_i\right) + \log_2\left(N_{0,j} + \mathbf{h}_j{}^\top \mathbf{O}_j \mathbf{p}_i\right)\right] \\ &= \sum_{j=1}^{K} \frac{1}{\ln 2}\left(-\frac{\mathbf{h}_j}{N_{0,j} + \mathbf{h}_j{}^\top \mathbf{p}_i} + \frac{\mathbf{O}_j{}^\top \mathbf{h}_j}{N_{0,j} + \mathbf{h}_j{}^\top \mathbf{O}_j \mathbf{p}_i}\right), \end{aligned} \tag{3.20}$$

and the Hessian of the objective function is

$$\nabla^2 f\left(\mathbf{p}_i\right) = \sum_{j=1}^{K} \frac{1}{\ln 2}\left[\frac{\mathbf{h}_j \mathbf{h}_j^\top}{\left(N_{0,j} + \mathbf{h}_j{}^\top \mathbf{p}_i\right)^2} - \frac{\mathbf{O}_j{}^\top \mathbf{h}_j \mathbf{h}_j{}^\top \mathbf{O}_j}{\left(N_{0,j} + \mathbf{h}_j{}^\top \mathbf{O}_j \mathbf{p}_i\right)^2}\right]. \tag{3.21}$$

Thus, the Jacobian of the Lagrange function (3.7) is given by

$$\nabla\mathcal{L}\left(\mathbf{p}_i\right) = \nabla f\left(\mathbf{p}_i\right) + \begin{bmatrix} \mathbf{I}^{K\times K} \\ -\mathbf{I}^{K\times K} \end{bmatrix}^\top \boldsymbol{\lambda}_i, \tag{3.22}$$

and the Hessian of Lagrange function is

$$H\mathcal{L}\left((p)_i\right) = \nabla^2 f\left(\mathbf{p}_i\right). \tag{3.23}$$

Here, $H\mathcal{L}$ is a full rank $K \times K$ matrix, and $\nabla g\left(\mathbf{p}_i\right) = \begin{bmatrix} \mathbf{I}^{K\times K} \\ -\mathbf{I}^{K\times K} \end{bmatrix}$, so the update matrix $\begin{bmatrix} H\mathcal{L}\left(\mathbf{p}_i^n, \boldsymbol{\lambda}_i^n\right) & \nabla g\left(\mathbf{p}_i^n\right)^\top \\ \nabla g\left(\mathbf{p}_i^n\right) & \mathbf{0}^{2K\times 2K} \end{bmatrix}$ has full row rank.

Besides, because it is hard to ensure $H\mathcal{L}$ to be positive definite on the tangent space of the constraint, we approximate the Hession of Lagrange to be positive definite using Broyden-Fletcher-Goldfarb-Shanno (BFGS) method in implementation [71],

$$\begin{aligned} &H\mathcal{L}^{n+1} = H\mathcal{L}^n + \frac{\mathbf{q}_n \mathbf{q}_n{}^\top}{\mathbf{q}_n{}^\top d\mathbf{p}_i} - \frac{H\mathcal{L}^n d\mathbf{p}_i d\mathbf{p}_i{}^\top H\mathcal{L}^{n\top}}{d\mathbf{p}_i{}^\top H\mathcal{L}^n d\mathbf{p}_i}, \\ &\text{where } \mathbf{q}_n = \left(\nabla\mathcal{L}\left(\mathbf{p}_i^{n+1}\right) + \nabla g\left(\mathbf{p}_i^{n+1}\right)^\top \boldsymbol{\lambda}_i^{n+1}\right) - \left(\nabla\mathcal{L}\left(\mathbf{p}_i^n\right) + \nabla g\left(\mathbf{P}_i^n\right)^\top \boldsymbol{\lambda}_i^n\right) \end{aligned} \tag{3.24}$$

After assigning the optimal transmission power, we need to find the optimal detection threshold ε_i. Recall the conclusion we get in subsubsection 2.2.2.1: that with the increase of ε_i, $\mathcal{P}(\mathcal{A}|H_0)$ and $\mathcal{P}(\mathcal{A})$ increases, yet the bounds of the transmission power $\left(\mathbf{l}_i^+, \mathbf{u}_i\right)$ decrease. This means that by increasing the detection threshold, although the opportunities to access the spectrum increase, the power that can be assigned decreases for one transmission. This fact calls for the search of the optimal detection threshold search follows the same procedure that we used in subsubsection 2.2.2.1. Thus the whole algorithm is summarized in Algorithm 5

Algorithm 5 SQP Power Allocation for Multi-User Interference Case

Require: $E_{j,max} \geq E_{j,i}$, for $j = 1, 2, \cdots, K$ and $i = 1, 2, \cdots, N$

Initialize $Q_{D,1} = \alpha$
for $p = 1, 2, \cdots, P; P = \frac{Q_{D,max} - \alpha}{\Delta Q_D}$ **do**
  $Q_{D,p} = Q_{D,0} + (p)\,\Delta Q_D$
  for $i = 1$ to N **do**
    $\varepsilon_n \leftarrow \varepsilon_0, \varepsilon_0 = Q_{D,p}^{-1}$,
    for $j = 1, 2, \cdots, K$ **do**
      Compute $U_{j,i} = \frac{\sum_{k=1}^{i} E_{j,k} - \sum_{k=1}^{i-1} \mathcal{P}(\mathcal{A}|\varepsilon_k) P_{j,k} \tau_t - i P_s \tau_s}{\mathcal{P}(\mathcal{A}|\varepsilon_i)\tau_t}$, and $L_{j,i} = \frac{\sum_{k=1}^{i+1} E_{j,k} - \sum_{k=1}^{i-1} \mathcal{P}(\mathcal{A}|\varepsilon_k) P_{j,k} \tau_t - i P_s \tau_s - E_{j,\max}}{\mathcal{P}(\mathcal{A}|\varepsilon_i)\tau_t}$
    end for
    if $U_{j,i} \geq 0$ for all j **then**
      Initialize $\mathbf{P}_i^0$, $\boldsymbol{\lambda}_i^0$,$\mathbf{z}^0$ set merit function $\boldsymbol{\phi}$
      for Interation n **do**
        Form and solve (3.11) to obtain $d\mathbf{p}_i$ $d\boldsymbol{\lambda}_i$ (3.13) and $d\mathbf{z}$ (3.17),
        Choose step length parameter α so that $\boldsymbol{\phi}\left({\mathbf{p}_i}^n + \alpha d\mathbf{p}_i\right) < \boldsymbol{\phi}\left({\mathbf{p}_i}^n\right)$
        Update $\mathbf{p}_i^{n+1}$, ${\boldsymbol{\lambda}_i}^{n+1}$ (3.14) and $\mathbf{z}^{n+1}$ (3.18)
        Stop if converged (i.e. $\mathbf{p}_i^{n+1} - \mathbf{p}_i^n < \varepsilon$, ε is a small value)
      end for
      Record $\mathbf{p}_{i,p} = \mathbf{p}_i^{n+1}$
    else
      $P_{j,i,p} = 0$
    end if
  end for
  Choose $\mathbf{p}_i = \arg\max R_T$, $\mathbf{p}_i \in \left\{\mathbf{p}_{i,1}, \mathbf{p}_{i,2}, \cdots, \mathbf{p}_{i,P}\right\}$.
end for

3.1.1.2 Simulation Results

We first apply Algorithm 5 to a 2-user scenario to test its performance as we can compare them with those obtained in the previous chapter and then apply it to a 3-user case. For the two scenarios, we set two different channel environments: weak interference environment, $h_{jj} = -10dB$, $h_{kj} = -20dB, k \neq j$; and a strong interference environment, $h_{jj} = h_{kj} = -10dB, k \neq j$. We also consider a total time period of $T = 1$ s; and the SNR of the PU signals measured at SU varies in the interval [-20, 10] dB. The other parameter settings are

the same as those selected in subsection 2.2.3. All results are averaged over 200 simulation results and compared to the random power allocation and detection threshold scheme 3.

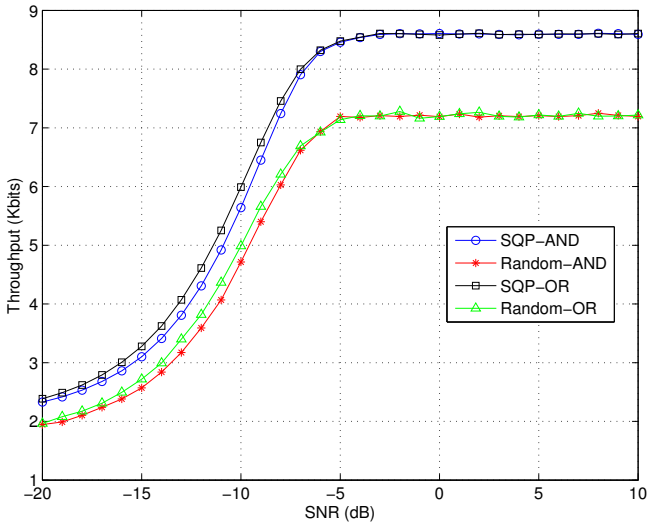

Figure 3.3: Throughput of SUs versus SNR of the PU for a 2-user scenario in a weak interference environment

Fig. 3.3 and Fig. 3.5 present how the throughput varies with measured SNR of PU for weak interference and strong interference scenario. Although they show that Algorithm 5 outperforms the random allocation algorithm, the improvement is limited comparing with the optimal solution proposed in subsubsection 2.2.2.1 as in Fig. 2.5 and Fig 2.13. Espe-

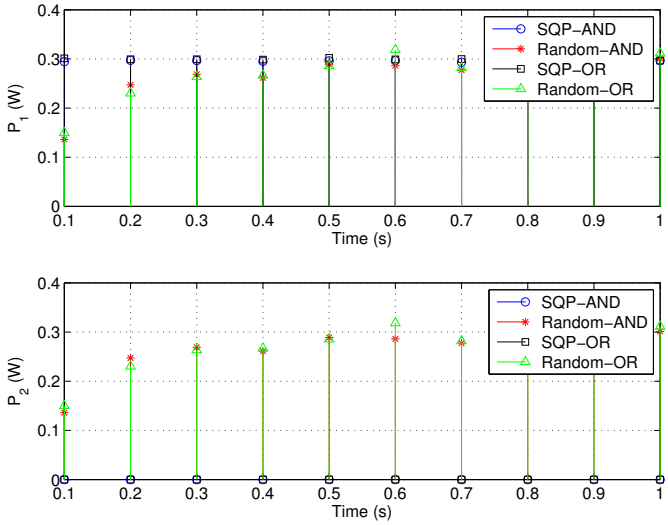

Figure 3.4: Allocated transmission power to SUs for a 2-user scenario in a weak interference environment when SNR=-5 dB

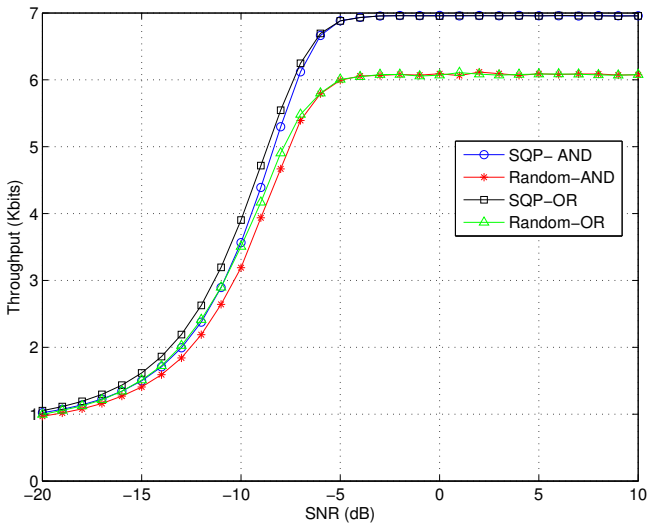

Figure 3.5: Throughput of SUs versus SNR of the PU for a 2-user scenario in a strong interference environment

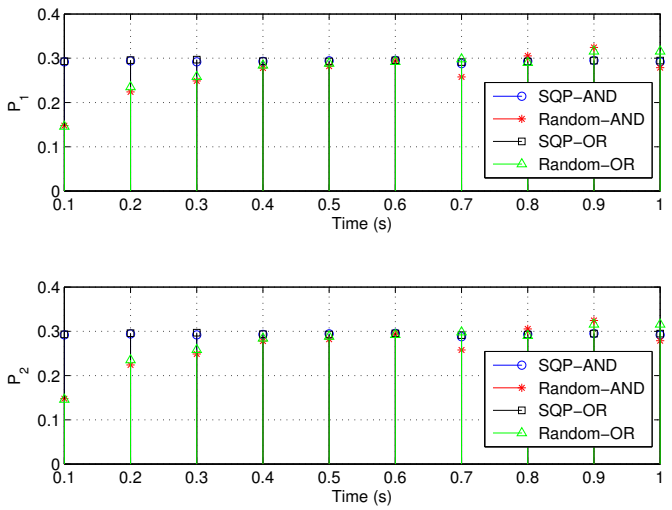

Figure 3.6: Allocated transmission power to SUs for a 2-user scenario in a strong interference environment when SNR=-5 dB

cially in the strong interference environment, when PU's SNR is under -5 dB, the random power allocation scheme performs approximately as SQP based power allocation scheme. Comparing power allocation details in Fig. 3.4 with Fig. 2.6, we can find that the SQP power allocation scheme assigns maximal power only to SU1, while the optimal power allocation scheme assigns power to both SUs. In Fig. 3.6, the SQP algorithm assigns power to both users while the optimal one behaves as TDMA strategy (i.e. one time slot only one SU transmits) in Fig. 2.14 and 3.6. Recall the capacity function shape shows in Fig. 2.3,

the allocated power pair either in Fig. 3.4 or in Fig. 3.6 is only a local optimum where the optimal algorithm will choose from the set given by equation (2.21).

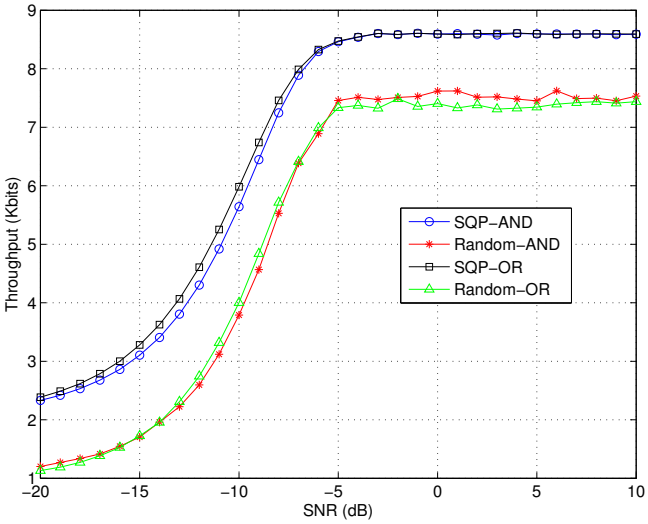

Figure 3.7: Throughput of SUs versus SNR of the PU for a 3-user scenario in a weak interference environment

The performance of this algorithm follows a similar trend when the CR network is composed of 3 users. In the weak interference environment, the SQP power allocation scheme still outperforms the random allocation scheme as it can be seen in Fig. 3.7 shows. In the strong interference environment, the advantage of using the SQP power allocation scheme

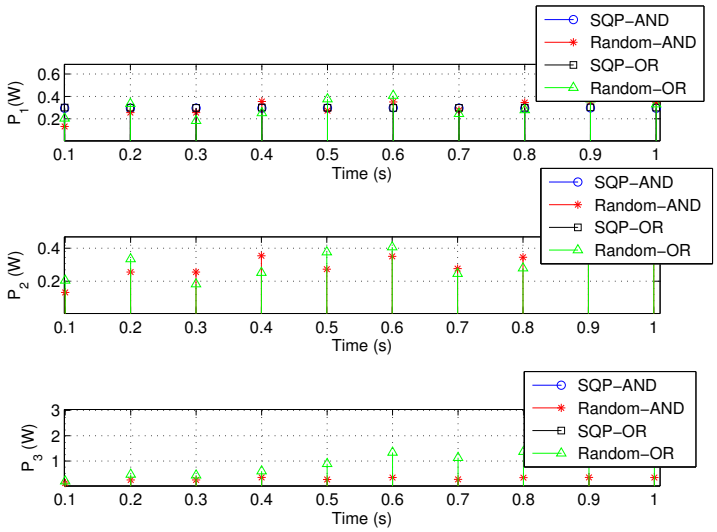

Figure 3.8: Allocated transmission power to SUs for a 3-user scenario in a weak interference environment when SNR=-5 dB

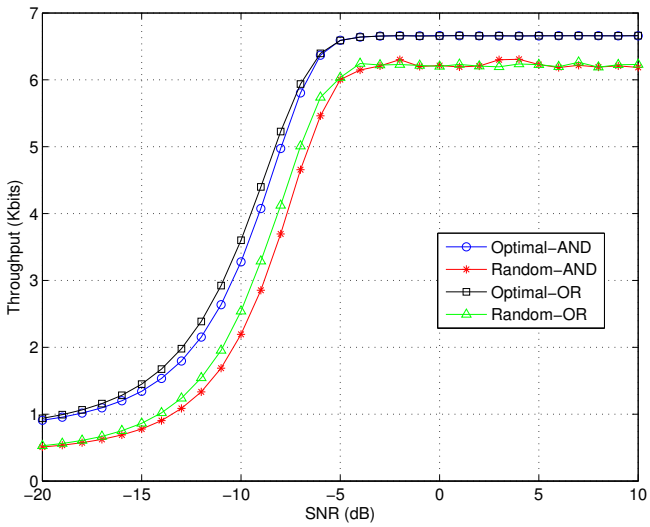

Figure 3.9: Throughput of SUs versus SNR of the PU for a 3-user scenario in a strong interference environment

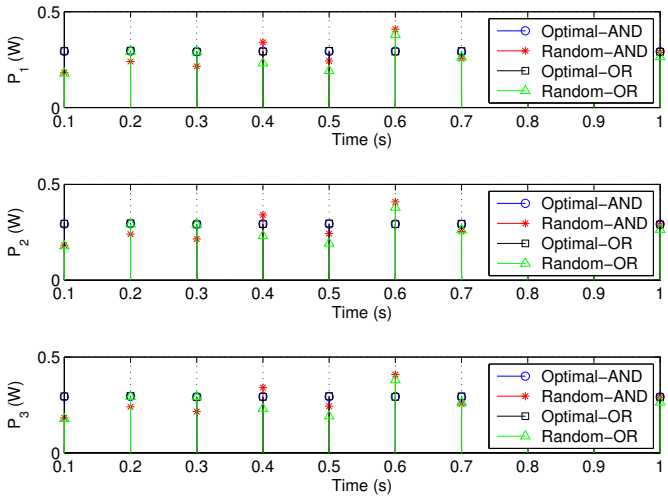

Figure 3.10: Allocated transmission power to SUs for a 3-user scenario in a strong interference environment when SNR=-5 dB

reduces as shown in Fig. 3.9. In the environment that interference is extremely strong ($h_{jj} = -10$ dB, $h_{kj} = 0$ dB, $k \neq j$), the SQP power allocation algorithm gets better performance for low SNR, however, the random power allocation scheme performs approximately as good as the SQP scheme when SNR is above -5 dB. Fig. 3.12 shows the power allocation behavior of SQP scheme for 3-user case in the extreme interference environment. In this case, the power is only assigned to SU1 and SU2 while SU3 does not transmit. It is worth remembering that (3.1) is a non-convex function, and the SQP-based power allocation

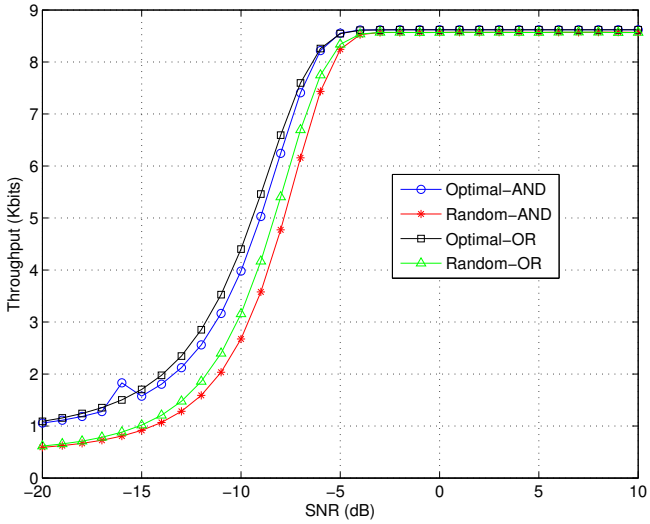

Figure 3.11: Throughput of SUs versus SNR of the PU for a 3-user scenario in a extremely strong interference environment

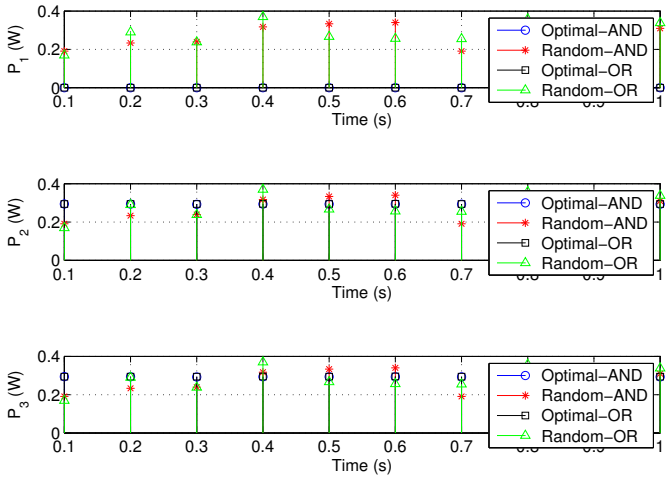

Figure 3.12: Allocated transmission power to SUs for a 3-user scenario in a extremely strong interference environment when SNR=-5 dB

algorithm may only find a local optimum. As a result, its performance of algorithm depends mainly on the initial point. To find the global optimum, we can apply the outer approximation method [66] by searching all the boundaries of the value set. However, this method remains plausible only for small-to-medium problems [67].

3.1.2 Multi-user CR network with interference cancelation (IC) technique

In this subsection, we consider a multi-user CR network where SUs apply IC technique, such as filter-based approaches, transform-domain approaches or spatial processing [68]. Because of the use of IC techniques, interference between SUs can be ignored. Thus the channel capacity at i th time slot is given by

$$C_i^{IC} = \sum_{j=1}^{K} W \log_2 \left(1 + \frac{|h_{jj}|^2 P_{j.n}}{N_{0,j}} \right). \tag{3.25}$$

Note that the capacity function (3.25) has the same expression as the capacity function for the multi-band case (2.25) in the previous chapter. As a result, the optimization problem is a convex one, so we can solve the problem by applying the KKT conditions as we did before. It is apparent that we get the same optimal power allocation scheme as in subsection 2.3.1.

To test its behavior, we apply algorithm 4 to 3-user case. We set $h_{jj} = -10dB$, and the other parameters are the same of those chosen in subsubsection 3.1.1.2. Figure 3.13 shows

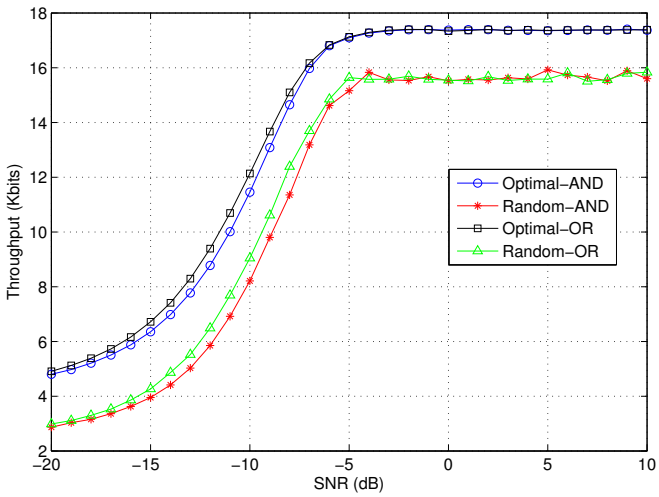

Figure 3.13: Throughput of SUs versus SNR of the PU for a 3-user scenario using IC technique in a weak interference environment

the throughput versus SNR of the PU using optimal and random power allocation scheme under AND and OR fusion rule in the weak interference environment for the 3-user case when each user applies IC technique. It is clearly observed that optimal algorithm performs better than the random one. As expected, the OR rule performs better for low SNR value. Fig. Figure 3.14 shows the transmission power allocation to different users when the SNR of the PU is -5 dB for different schemes. Although at some time slots, the random power allocation scheme assigns more power to the users, however the network performance of the SQP approach is better.

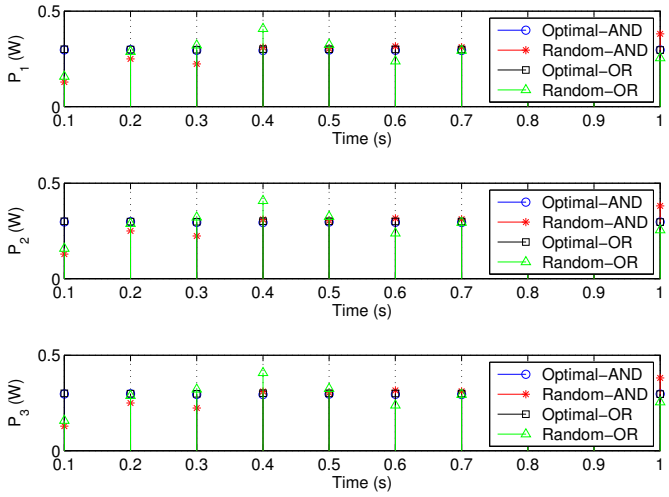

Figure 3.14: Allocated transmission power to SUs for a 3-user scenario using IC technique in a weak interference environment when SNR=-5 dB

3.2 Optimal power allocation in multi-frequency-band case

In this section we analyze the transmission power allocation in a multi-frequency-band scenario. As it was mentioned in section 2.3 we can access the spectrum under two strategies: a) applying FDMA; b) or allowing limited number of users to share each narrowband. In the FDMA case, the algorithm 4 which was obtained for the 2-user CR network follows the power allocation algorithm in 2-user widenand case. For the sub-band sharing case, we apply SQP-based power allocation scheme 5 to each sub-channel, assigning the same transmission power to each band.

We simulate a multi-band scenario for the weak interference and the strong interference environment. Parameter settings follows subsubsection 3.1.1.2. In the sub-band sharing case, we allow up to 3 users to share each equally divided sub-band (2 KHz, the total bandwidth is 6 KHz) for the SQP-based and random power allocation schemes. And in the FDMA case, each SU accesses one sub-band, so the interference between SUs can be ignored.

In the weak interference environment, the sub-band sharing strategy outperforms the FDMA scheme 3.15. Although for SNR values are lower than -10 dB, the FDMA scheme performs better than random allocation scheme even if the improvement is small, the SQP scheme always gets a higher throughput. However, the opposite behavior is observed for the strong interference scenario, see Fig. 3.16. FDMA algorithm outperforms the SQP-based one in regards of throughput. However, both get better performance than the random one.

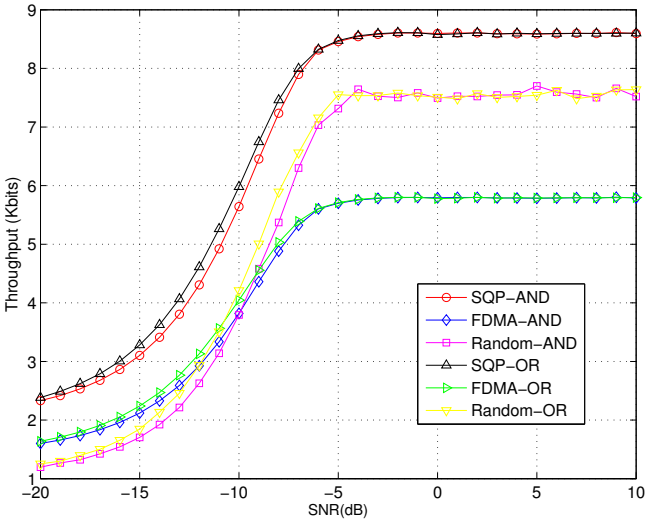

Figure 3.15: Throughput of the SUs versus the SNR of the PU for the 3-user scenario of the two multi-band power allocation strategies and fusion rules in a weak interference environment.

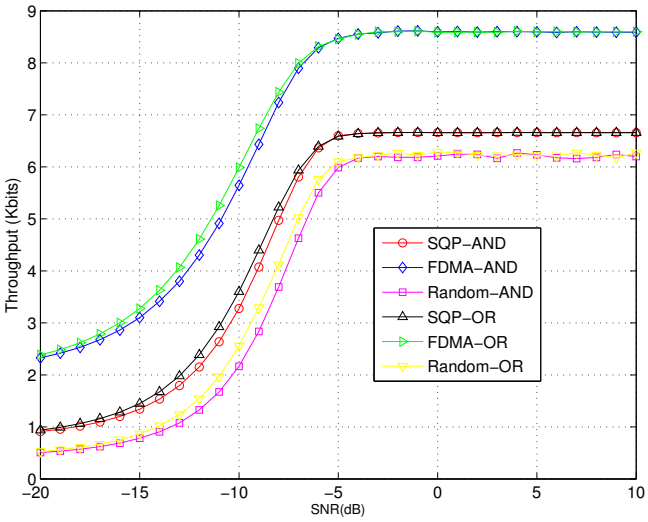

Figure 3.16: Throughput of the SUs versus the SNR of the PU for the 3-user scenario of the two multi-band power allocation strategies and fusion rules in a strong interference environment.

4 Conclusions and future work

In this chapter, we summarize the work of the thesis and derive the final conclusions. Future research directions are drawn at the end.

4.1 Conclusions

This thesis designed offline short-term optimal power allocation and spectrum sensing strategies for multi-user energy-harvesting cognitive radio networks which perform cooperative spectrum sensing in different scenarios.

In chapter 2, we proposed an algorithm for allocating the transmission power and setting the detection threshold for energy-harvesting CR networks which consists of 2 secondary users and one primary user. The optimal transmission powers, and the detection threshold were obtained in a two-step procedure for the AND and OR hard fusion rules under a time slotted energy model and considering different scenarios where at most two available bands were accessed at the same time : a) the empty frequency bands were shared by the cognitive users (so that interference between users played a key role), and b) the frequency bands were accessed independently so that cross channel interference was avoided. First, we analyzed the channel capacity function shape to look for the optimal transmission power. As the optimization function was quasi-convex, the maximum channel capacity was achieved at the vertices of the power value set for the 2-user interference channel. Second, we discovered that with the increase of detection threshold, the probability to access the idle spectrum increase, while the available power can be assigned in each access decreases that leads to the decrease of the channel capacity. So we set the optimal detection threshold by a through-search approach. We compared via simulation the results of applying the optimal algorithm with a benchmark algorithm. The simulation results showed that the network throughput is improved by applying the optimal algorithm under different energy-harvesting and channel scenarios. A suboptimal scheme that needed less computational requirements was also proposed for the single-frequency band case. Interestingly, results showed that the suboptimal algorithm performed nearly as the optimal one under different setups. In general, the AND and OR fusion rules performed almost evenly in terms of the throughput; however, a slightly better performance of the OR rule was observed when the SNR is considerably low. Further, results also evidenced the advantages of SUs sharing all the available bands instead of each SU accessing a different empty frequency band.

Chapter 3 investigated the power allocation and detection threshold problem for multi-user (including more than 2 SUs) energy-harvesting CR networks in single-band and multi-band scenario. We followed an SQP formulation in order to optimally allocate the transmission power and later, we used the same detection threshold search procedure followed in the two-user case. Although the simulation results showed that this algorithm can only achieve a local minimum for the non-convex power allocation problem, it still outperformed the ran-

dom allocation algorithm, even in the extremely strong interference case for a 3-user scenario when the SNR of PU is low. We also extended the power allocation problem to CR networks which use interference cancellation techniques and we showed that the the algorithm developed for the 2-user CR network scenario can be applied to the multi-band sharing power allocation case. Finally, we found out that the scenario where all SUs share all the available bands obtained better performance than the case where SUs access different idle frequency bands for the weak interference environment. On the other hand, making SUs access the different bands is wiser for scenarios with strong interference.

In short, the conclusions are summarized below:

- **The offline short-term optimal/ sub-optimal power allocation and detection threshold shall improve the energy-harvesting CR network throughput significantly.**
  The offline power allocation and detection threshold algorithm is proposed for a short-time period under the assumptions of predicting the energy-harvesting behavior and being the channel environment approximately static. This algorithm provides insights for designing energy-harvesting CR networks which operate in short-term periods, i.e., the optimal transmission power adjusting to the predicted energy-harvesting process and the the spectrum sensing detection threshold can be determined before the CR network starts to work in finite time period. Simulation results showed that the optimal/ sub-optimal solution outperforms the benchmark solution in different environments for different CR network sizes.

- **The total CR network throughput can be improved by assigning higher transmission power when the chances to access the spectrum decrease.**
  This conclusion is derived based on the mathematical analysis of detection threshold influence and observation of Fig. 2.4. Given the allowable detection threshold range, it is possible to elect a optimal detection threshold that provides higher detection probability and also can achieve larger network throughput by allocating more transmission power for one access.

- **The OR hard fusion rule outperforms the AND fusion rule when the SNR of the PU is low.**
  This conclusion is corroborated via simulations for different environments and different CR network sizes. By applying power allocation schemes using OR fusion rule, the network throughput is slightly bigger then the AND fusion rule when SNR is considerably low.

- **Allowing CR users to share the same single frequency band by applying optimal/ sub-optimal power allocation algorithm can gain more throughput when the interference between them is considerable weak in the multi-band spectrum**
  In Fig. 2.19 and Fig. 3.15, we can observe that the throughput is much higher by allowing finite CR users share the same single frequency band than simply applying FDMA scheme that only one user access one single band in the multi-band scenario when the interference between SUs is weak (cross channel gain smaller than the local channel gain).

4.2 Future works

As mentioned before, this offline short-term optimal power allocation algorithm and detection threshold strategy is proposed under some idealistic assumptions. Although it was an initial approach to the power allocation problem in energy-harvesting CR networks which allow us to gain some insights into the problem, better approaches can be proposed which deal with unpredictable energy-harvesting resources and more dynamic channel.

Hereby, we propose several interesting research lines:

- **Define a time-dynamic decision-making framework to solve the power allocation problem in energy-harvesting CR networks.**
  In practice, it is hard to predict the long-term energy-harvesting behavior, the primary users' activity and the channel environment. Thus, the short-term optimal power allocation scheme cannot be adjusted to the long-term dynamic nature of the energy-harvesting CR networks. Therefore, a more realistic time-dynamic decision-making framework is desired in order to form a more accurate on-line power allocation and detection threshold scheme.

- **Investigate the interference channel capacity function for the multi-user CR network in order to find the global optimal solution for the non-convex power allocation problem.**
  The SQP-based sub-optimal power allocation scheme is shown to be a local minimizer for the power allocation problem in chapter 3. However, to find the global optimal solution is still left to be a strong NP-hard problem. And the global optimum maybe be achieved by outer approximation method searching all the boundary values. Thus, a more efficient algorithm that can find a global optimum is strongly expected. Inspired by the optimal power allocation solution for 2-user energy-harvesting CR network, we expect to solve this optimization problem by analyzing the function shape of the interference channel capacity in order to gain analytically accurate results.

- **Explore different band-sharing strategies for multi-band case and find the optimal band-sharing strategy.**
  In this thesis, we only considering two band-sharing strategies for SUs in the multi-band case: a) all SUs access the whole frequency band, i.e. SUs transmit data in all sub-bands and they interfere each other; b) each SU access one separate band in one time instant. However, in practice there exist more situations such as 1 SU use one sub-band and the others sharing another sub-band while one other sub-band is occupied by PU. This leads to the frequency-band allocation task that how to allocate SUs to different sub-bands to achieve the optimal performance of the CR network. When this frequency allocation task is considered in the energy-harvesting networks, the problem is more sophisticated because the SUs access depends not only on the PU's activity and the sensing error but also on the dynamic energy-budget.

- **Analyze the detection threshold impact on the power allocation scheme.**
  This thesis has shown that the power allocation scheme depends on the detection threshold. And we optimize the detection threshold by through-search in the optimal power allocation scheme. However, a mathematically analytical analysis is still left to be done.

Bibliography

[1] H. Zhang. Cognitive green communications: When energy meets intelligence. In *Keynote Speech at the IEEE ISCIT 2012 Workshop*, Gold Coast, Australia, Oct 2012.

[2] G. Gür and F. Alagöz. Green wireless communications via cognitive dimension: An overview. *Network, IEEE*, 25(2):50 – 56, March-April 2011.

[3] M. A. McHenry, D. McCloskey, D. Roberson, and J. T. MacDonald. Spectrum occupancy measurements chicago, illinois. Technical report, Shared Spectrum Company and IIT Wireless Interference Lab Illinois Institute of Technology, 1595 Spring Hill Road, Suite 110 Vienna and 3300 South Federal Street Chicago, IL, December 2005.

[4] J. Mitola and J. Gerald Q. Maguire. Cognitive radio: making software radios more personal. *Personal Communications, IEEE*, 6(4):13–18, Aug 1999.

[5] L. Giupponi and C. Ibars. *Cognitive Radio Systems*. In-tech Press, Nov. 2009.

[6] S. Haykin. Cognitive radio: brain-empowered wireless communications. *IEEE Journal on Selected Areas in Communications*, 23(2):201–220, 2005.

[7] G. Ganesan and Y. G. Li. Cooperative spectrum sensing in cognitive radio, part i: Two user networks. *IEEE Transactions on Wireless Communications*, 6(6), June 2007.

[8] W. Zhang, R. K. Mallik, and K. B. Lefaief. Optimization of cooperative spectrum sensing with energy detection in cognitive radio networks. *IEEE Transactions on Wireless Communications*, 8(12), December 2009.

[9] S. Maleki, S. P. Chepuri, and G. Leus. Optimization of hard fusion based spectrum sensing for energy-constrained cognitive radio networks. *Physical Communications*, 9:193–198, December 2013.

[10] S. Maleki, A. Pandharipande, and G. Leus. Energy-efficient distributed spectrum sensing for cognitive sensor networks. *IEEE Sensors Journal*, 11(3):565–573, March 2011.

[11] D.Teguig, B.Scheers, and V. Nir. Data fusion schemes for cooperative spectrum sensing in cognitive radio networks. In *Communications and Information Systems Conference (MCC), 2012 Military*, pages 1–7, Gdansk, Oct 2012. Dept. CISS, R. Mil. Acad., Brussels, Belgium.

[12] M. D. R. A. Valles. *Statistical Models for Energy-Efficient Selective Communications in Sensor Networks*. PhD thesis, Universidad Carlos III de Madrid. Departamento de Teoría de la Señal y Comunicaciones, 2010.

[13] S. Sudevalayam and P. Kulkarni. Energy harvesting sensor nodes: Survery and implications. *Communications Surveys and Tutorials, IEEE*, 13(3), July 2011.

[14] Z. Ding, S. M. Perlaza, I. Esnaola, and H. V. Poor. Power allocation strategies in energy harvesting wireless cooperative networks. *Submitted to IEEE Transactions in Wireless Communications*, 2013.

[15] Y. Pei, Y.-C. Liang, K. C. Teh, and K. H. Li. Energy-efficient design of sequential channel sensing in cognitive radio networks: Optimal sensing strategy, power allocation, and sensing order. *IEEE Journal on Selected Areas in Communications*, 29(8):1648–1659, 2011.

[16] S. Gao, L. Qian, and D. R. Vaman. Distributed energy efficient spectrum access in wireless cognitive radio sensor networks. In *Proc. of IEEE Wireless Communications and Networking Conference (WCNC'08)*, pages 1442–1447, 2008.

[17] R. Deng, J. Chen, C. Yuen, P. Cheng, and Y. Sun. Energy-efficient cooperative spectrum sensing by optimal scheduling in sensor-aided cognitive radio networks. *Vehicular Technology, IEEE Transactions on*, 61(2):716–725, 2012.

[18] A. Kansal, J. Hsu, S. Zahedi, and M. B. Srivastava. Power management in energy harvesting sensor networks. *ACM Transactions on Embedded Computing Systems*, 6(4), September 2007.

[19] K. Tutuncuoglu and A. Yener. Sum-rate optimal power policies for energy harvesting transmitters in an interference channel. *Journal of Communications and Networks*, 14(2), April 2012.

[20] V. Sharma, U. Mukherji, V. Joseph, and S. Gupta. Optimal energy management policies for energy harvesting sensor nodes. *IEEE Transactions on Wireless Communications*, 9(4):1326–1336, 2010.

[21] J. Yang and S. Ulukus. Optimal packet scheduling in an energy harvesting communication system. *IEEE Transactions on Communications*, 60(1):220–230, 2012.

[22] K. Tutuncuoglu and A. Yener. Optimum transmission policies for battery limited energy harvesting nodes. *IEEE Transactions on Wireless Communications*, 11(3):1180–1189, 2012.

[23] N. Michelusi, L. Badia, R. Carli, L. Corradini, and M. Zorzi. Impact of battery degradation on optimal management policies of harvesting-based wireless sensor devices. In *Proceedings of IEEE INFOCOM, 2013*, pages 590–594, 2013.

[24] Y. Chen, Q. Zhao, and A. Swami. Distributed spectrum sensing and access in cognitive radio networks with energy constraint. *IEEE Transactions on Signal Processing*, 57(2):783–797, 2009.

[25] A. Limmanee and S. Dey. Optimal power policy and throughput analysis in cognitive broadcast networks under primary's outage constraint. In *Proc. of Modeling and Optimization in Mobile, Ad Hoc, and Wireless Networks (WiOpt'12)*, pages 391–397, 2012.

[26] X. Kang, R. Zhang, Y.-C. Liang, and H. K. Garg. Optimal power allocation strategies for fading cognitive radio channels with primary user outage constraint. *IEEE Journal on Selected Areas in Communications*, 29(2):374–383, 2011.

[27] L. M. Lopez-Ramos, A. G. Marques, and J. Ramos. Jointly optimal sensing and resource allocation for multiuser overlay cognitive radios. *Submitted to IEEE Journal on Selected Areas in Communications*, 2012.

[28] K. K. Cohen, A. Leshem, and E. Zehavi. Game theoretic aspects of the multi-channel aloha protocol in cognitive radio networks. *IEEE Journal on Selected Areas in Communications*, 31(11):2276–2288, 2013.

[29] A. Sultan. Sensing and transmit energy optimization for an energy harvesting cognitive radio. *IEEE Wireless Communications Letters*, 1(5):500–503, 2012.

[30] A. El-Shafie, T. Khattab, A. El-Keyi, and M. Nafie. Cooperation between a primary terminal and an energy harvesting cognitive radio terminal. *Available at http://arxiv.org/abs/1307.4744*, pages 1–8, 2013.

[31] A. S. A. El-Shafie. Optimal selection of spectrum sensing duration for an energy harvesting cognitive radio. In *Proc. of IEEE Global Vommunication Conference (GLOBECOM'13)*, 2013.

[32] H. Vu-Van and I. Koo. Optimal throughput for cognitive radio with energy harvesting in fading wireless channel. *Scientific World Journal*, Accepted, 2013.

[33] S. Lee, R. Zhang, and K. Huang. Opportunistic wireless energy harvesting in cognitive radio networks. *IEEE Transactions on Wireless Communications*, 12(9):4788–4799, 2013.

[34] s. Park, H. Kim, and D. Hong. Cognitive radio networks with energy harvesting. *Wireless Communications, IEEE Transactions on*, 12(3):1386–1397, 2013.

[35] S. Park and D. Hong. Achievable throughput of energy harvesting cognitive radio networks. *IEEE Transactions on Wireless Communications*, to appear.

[36] S. Park and D. Hong. Optimal spectrum access for energy harvesting cognitive radio networks. *IEEE Transactions on Wireless Communications*, PP(99):1–14, 2013.

[37] Y.-C. Liang, Y. Zeng, E. C. Peh, and A. T. Hoang. Sensing-throughput tradeoff for cognitive radio networks. *IEEE TRANSACTIONS ON WIRELESS COMMUNICATIONS*, 7(4), April 2008.

[38] Y. Zhang and C. Leung. Resource allocation in an ofdm-based cognitive radio system. *IEEE TRANSACTIONS ON COMMUNICATIONS*, 57(7), July 2009.

[39] Z. Hasan, G. Bansal, E. Hossain, and V. K. Bhargava. Energy-efficient power allocation in ofdm-based cognitive radio systems: A risk-return model. *IEEE Transactions on Wireless Communications*, 8(12), December 2009.

[40] S. Wang, Z.-H. Zhou, M. Ge, and C. Wang. Resource allocation for heterogeneous cognitive radio networks with imperfect spectrum sensing. *IEEE Journal on Selected Areas in Communications*, 31(3), March 2013.

[41] G. Bansal, M. J. Hossain, V. K. Bhargava, and T. Le-Ngoc. Subcarrier and power allocation for ofdma-based cognitive radio systems with joint overlay and underlay spectrum access mechanism. *IEEE Transactions on Vehicular Technology*, 62(3), March 2013.

[42] P. Wu, R. Schober, and V. K. Bhargava. Optimal power allocation for wideband cognitive radio networks employing sc-fdma. *IEEE Communication Letters*, 17(4), April 2013.

[43] F. Wang, M. Krunz, and S. Cui. Price-based spectrum management in cognitive radio networks. *IEEE Journal of Selected Topics in Signal Processing*, 2(1), Feb 2008.

[44] A. Baharlouei and B. Jabbari. Dynamic subchannel and power allocation using nash bargaining game for cognitive radio networks with imperfect pu activity sensing. In *2013 8th International Conference on Cognitive Radio Oriented Wiress Network*, 2013.

[45] L. Akter and B. Natarajan. Game theory based distributed approach for power and rate allocation to secondary users in cognitive radio networks. In *Informatics, Electronics and Vision (ICIEV), 2013 International Conference on*, 2013.

[46] F. Wang, M. Krunz, and S. Cui. Spectrum sharing in cognitive radio networks. In *INFOCOM 2008. The 27th Conference on Computer Communications*, pages 1885 – 1893, Phoenix, AZ, April 2008.

[47] Z.-Q. T. Luo and S. Zhang. Dynamic spectrum management: Complexity and duality. *IEEE Journal of Selected Topics in Signal Processing*, 2, Feb 2008.

[48] M. Wei Yu and R. Lui. Dual methods for nonconvex spectrum optimization of multicarrier systems. *IEEE Transactions on Communications*, 54(7), 2006.

[49] O. Ozel, K. Tutuncuoglu, J. Yang, S. Ulukus, and A. Yener. Transmission with energy harvesting nodes in fading wireless channels: Optimal policies. *IEEE Journal on Selected Areas in Communications*, 29(8):1732–1743, Oct 2011.

[50] K. Tutuncuoglu and A. Yener. Optimum transmission policies for battery limited energy harvesting nodes. *IEEE Transactions on Wireless Communications*, 11(3):1180–1189, March 2012.

[51] M. Gregori and M. Payaró. Energy-efficient transmission for wireless energy harvesting nodes. *IEEE Transactions on Wireless Communications*, 12(3):1244–1254, March 2013.

[52] W. Hamlen and J. Tschirhart. Solar energy, public utilities, and economic efficiency. *Southern Economic Journal*, 47(2):348–365, Oct 1980.

[53] Y.-C. Liang, Y. Zeng, E. C. Peh, and A. T. Hoang. Sensing-throughput tradeoff for cognitive radio networks. *IEEE Transactions on Wireless Communications*, April 2008.

[54] S. M. Kay. *Fundamentals of statistical signal processing - Detection theory*. Prentice Hall, February 1998.

[55] K. Tutuncuoglu and A. Yener. Communicating with energy harvesting transmitters and receivers. *Information Theory Workshop (ITW)*, pages 94 – 98, 2012.

[56] E. J. Duarte-Melo and M. Liu. Analysis of energy consumption and lifetime heterogeneous wireless sensor networks. In *Global Telecommunications Conference IEEE*, volume 1, pages 21 – 25, 2002.

[57] M. G. C. Torres. Energy consumption in wireless sensor networks using gsp. Master's thesis, University of Pittsburgh, July 2006.

[58] V. Raghunathan, A. Kansal, J. Hsu, J. Friedman, and M. Srivastava. Design considerations for solar energy harvesting wireless embedded systems. In *Information Processing in Sensor Networks, Fourth International Symposium on*, April 2005.

[59] O. Ozel, K. Tutuncuoglu, J. Yang, S. Ulukus, and A. Yener. Resource management for fading wireless channels with energy harvesting nodes. Shanghai, April 2011.

[60] C. Moser, J.-J. Chen, and L. Thiele. Reward maximization for embedded systems with renewable energies. In *Embedded and Real-Time Computing Systems and Applications, 2008. RTCSA '08. 14th IEEE International Conference on*, pages 247–256, Kaohsung, Aug 2008.

[61] S. Liu, J. Lu, QingWu, and Q. Qiu. Harvesting-aware power management for real-time systems with renewable energy. *Very Large Scale Integration (VLSI) Systems, IEEE Transactions on*, 20(8):1473–1486, Aug 2012.

[62] I. Roasto, T. Lehtla, T. Moller, and A. Rosin. Control of ultracapacitors energy exchange. In *Power Electronics and Motion Control Conference, 2006. EPE-PEMC 2006. 12th International*, pages 1401–1406, Portoroz, September 2006.

[63] J. McGowan, J. Manwell, and S. Connors. Wind/diesel energy systems: Review of design options and recent developments. *Solar Energy*, 41(6):561–575, 1988.

[64] K. Meah, S. Fletcher, and S. Ula. Solar photovoltaic water pumping for remote locations. *Renewable and Sustainable Energy Reviews*, 12(2):472–482, Feb 2008.

[65] P. E. Gill, W. Murray, and M. A. Saunders. Snopt: An sqp algorithm for large-scale constrained optimization. *SIAM REVIEW*, 47(1):99–131, 2005.

[66] T. Kuno, Y. Yajima, and H. Konno. An outer approximation method for minimizing the product of several convex functions on a convex set. *Journal of Global Optimization*, 3(3):325–335, September 1993.

[67] C. W. Tan, S. Friedland, and S. H. Low. Spectrum management in multiuser cognitive wireless networks: Optimality and algorithm. *IEEE Journal on Selected Areas in Communications*, 29(2), Feb 2011.

[68] X. Hong, Z. Chen, C.-X. Wang, S. A. Vorobyov, and J. S. Thompson. Interference cancelation and management techniques. In *IEEE Vehicular Technology Magazine I*. December 2009.

[69] P. E. Gill, W. Murray, and M. A. Saunders. Snopt: An sqp algorithm for large-scale constrained optimization. *Sian Review*, 47(1):99–131, 2005.

[70] J. Nocedal and S. J. Wright. *Numerical Optimization*. Springer, 2 edition, 2006.

[71] P. T. Boggsa and J. W. Tolle. Sequential quadratic programming. *Acta Numerica*, 4:1–51, January 1995.